MASTER OF SCIENCE IN ELECTRICAL AND ELECTRONIC ENGINEERING

Control and Stability Study of Grid-connected Doubly-fed Induction Generator

By

Muhammad Waleed

Department of Electrical and Electronic Engineering

Islamic University of Technology (IUT)

June 2015

CERTIFICATE OF APPROVAL

The thesis entitled "**Control and Stability Study of Grid-connected Doubly-fed Induction Generator**" submitted by **Muhammad Waleed**, Student No. **122614** of Academic Year 2012-2013 has been found as satisfactory and accepted as partial fulfillment of the requirement for the Degree of MASTER OF SCIENCE IN ELECTRICAL AND ELECTRONIC ENGINEERING on 05 June 2015.

BOARD OF EXAMINERS:

1. _____
   Dr. Md. Shahid Ullah (Supervisor) — Chairman
   Professor
   EEE Dept., IUT, Board Bazar, Gazipur-1704.
2. _____
   Dr. Md. Shahid Ullah — Member
   Professor and Head — (Ex-Officio)
   EEE Dept., IUT, Board Bazar, Gazipur-1704.
3. _____
   Dr. Kazi Khairul Islam — Member
   Professor
   EEE Dept., IUT, Board Bazar, Gazipur-1704.
4. _____
   Dr. Md. Ashraful Hoque — Member
   Professor
   EEE Dept., IUT, Board Bazar, Gazipur-1704.
5. _____
   Dr. Muhammad Fayyaz Khan — Member
   Professor — (External)
   EEE Dept., UIU, Dhaka.

DECLARATION OF CANDIDATE

It is hereby declared that this thesis or any part of it has not been submitted elsewhere for the award of any degree or diploma.

(Signature of the Supervisor)

Prof. Dr. Md. Shahid Ullah

Designation: Professor

Address: EEE Dept., IUT,

Board Bazar, Gazipur-1704

(Signature of Candidate)

Muhammad Waleed

Student No.:122614

Academic Year: 2012-2013

DEDICATION

I would like to dedicate this work to the memory of my Baba and Mum, who gave me life, taught me about life, gave me support, believed in and encouraged me all these years. Also I would like to dedicate this work to my beloved countries Afghanistan and Bangladesh.

TABLE OF CONTENTS

TOPICS **Page**

LIST OF FIGURES

LIST OF TABLES

ACKNOWLEDGEMENTS

First and foremost, I thank Allah (SWT) for letting me live to see this thesis.

This thesis is a result of research of more than one and a half year and this is by far the most significant scientific accomplishment in my life. This thesis would not have been possible without the guidance and the help of several individuals who in one way or another contributed and extended their valuable assistance in the preparing and completion this study.

First of all I would like to extend my gratitude and sincere thanks my supervisor and head of EEE department Prof. Dr. Md. Shahid Ullah for his unwavering support, encouragement and patience through entire process of my thesis. I truly appreciate and value his guidance and encouragement from the beginning to the end of this thesis. I am indebted to him for all the help he has provided me, the experience he has helped me gain by working in this thesis under his supervision, the precious time he spent in editing my many mistakes and making sure my thesis is always on track. I thanking him so much!

I am very fortunate and grateful to honor Mr. Ashik Ahmed , Asstt. Proff, EEE department, IUT. For always keeping an eye on the progress of my work, and guided me in critical phases of my thesis and the programming experience that he showed with me. His thoughtfully and timely comments gratefully influenced my understanding to deeply insight into my thesis work and helped me to achieve desired results. Ashik Sir is truly an outstanding person and an able educator, and I thank him from the bottom of my heart.

I would like to express my sincerely appreciation to Prof. Dr. Md. Ashraful Hoque for valuable knowledge that he shared with me throughout my bachelor and master program. I have learned valuable lessons from his wisdom, carefulness, and visions. Without his erudite and wholehearted assistance, it would have been impossible for me to complete my master.

I would like to extend my appreciation to my course teachers in IUT, staff members and also all fellow graduate students.

Special thanks to Mr. Golam Sarowar who helped me come up with the thesis topic and guided me over almost a year of development. And during the most difficult times when writing thesis, he gave me the moral support and the freedom I need to move on.

I also wish to gratefully acknowledge the financial and moral supports of the vice principle of Turkish hope School Mr Erkam Çarpan.

I expand my thanks to my roommates Kamalluddin Shirzai and Zheer khan for their brotherly love towards me. They are really amazing friends. They always made me feel rejuvenated when my spirt was down.

I wish to express my gratitude to my parents, whose love and encouragement have a great support throughout my education.my sisters, little brothers , uncles, aunties and cousins deserve my whole hearted thanks as well.

Last but not the least a big thanks to all people of Bangladesh.

ABSTRACT

The availability of electrical energy is a precondition for the functioning of modern societies. It is used to provide the energy needed for operating information and communication technology, transportation, lighting, food processing and storage as well as a great variety of industrial processes, all of which are characteristics of a modern society. The present fossil energy reserves is declining significantly, so it is time to investigate new sources of energy. Globally, experts are working hard to find out how renewable sources of energy can be used to better fulfill our energy needs. Renewable energy is generally defined as energy that comes from resources which are naturally replenished on a human timescale such as sunlight, wind, rain, tides, waves and geothermal heat.

In this thesis work, focuses have been given on the utilization of wind energy to generate electricity by wind turbine. Doubly Fed Induction Generator (DFIG) coupled with the wind turbine has been chosen in this research. Mathematical formulation of full order nonlinear dynamic model of DFIG connected to grid is done as basic part of the research. A critical assessment of a parameters variation of a DFIG-based wind turbine led to the identification of the critical variables that affect most the frequency and damping ratio of the dominant oscillation modes is also accomplished. A better understanding of the dynamic performance of the DFIG based wind turbine has been achieved by implementation of the genetic algorithm optimization of closed loop PI controller. The obtained result is compared with the PI controller performance without optimization. The optimized results with genetic algorithm showed that the system presents far better performance than classical PI controller without GA. It can be expected that this work may be helpful in feeding the grid with wind generated power for a stable operation.

CHAPTER 1

Introduction

Modern life cannot go without electricity. Electricity is mainly generated from fossil fuel like petroleum, natural gas, etc. Because of tremendous demand of electric power, fossil energy is being diminished very quickly. Also in recent years, the environmental pollution has become a major concern in daily life and a possible energy crisis has led to develop new technologies for generating clean and sustainable energy. Therefore, renewable energy is becoming a viable alternative to meet the crisis. Renewable energy is generally defined as energy that comes from resources which are naturally replenished on a human timescale such as sunlight, wind, rain, tides, waves and geothermal heat.

1.1 Electricity Supply

The availability of electrical energy is a precondition for the functioning of modern societies. It is used to provide the energy needed for operating information and communication technology, transportation, lighting, food processing and storage as well as a great variety of industrial processes, all of which are characteristics of a modern society. Because the energy for many of the technologies, systems and possibilities that are a property of the developed world is provided as electricity, it can be presumed that there is a link between the level of penetration and consumption of electricity on the one hand and various properties of a society on the other.

Research has indeed shown that there is a significant relation between economic growth and even societal development in general, measured by indicators such as illiteracy and life expectancy, and electricity consumption [1, 2].

The relation between economic and societal development and electricity consumption is bidirectional. The availability of electricity greatly facilitates industrialization, because electricity is a convenient way to replace human power by other sources of energy, which are converted into electricity for transmission, distribution and consumption. Further, the availability of electricity enables the application of modern technologies, such as information and communication technology (ICT). All of this leads to large improvements in productivity and thus to an increase in economic welfare. This increase in welfare in turn enables people to pay their electricity bill and to buy goods that consume electricity, such as televisions, computers and fridges, which leads to an increased electricity consumption. Hence, electricity consumption is both a precondition to and a consequence of economic development and growth. Electricity is an energy carrier. It is generated in power plants, in which a primary energy source is converted into electrical power. Examples of widely used primary energy sources are fossil fuels, falling or flowing water and nuclear fission. An important drawback of generating electricity from fossil fuels and nuclear fission, currently worldwide the most applied primary energy sources for electricity generation, are the adverse environmental impacts, such as the greenhouse effect caused by the increase of the CO_2 concentration in the earth's atmosphere and the nuclear waste problem. Further, fossil fuel and uranium reserves are principally finite. An additional disadvantage of using uranium and fossil fuels to generate electricity, particularly for those countries which themselves do not have supplies of these primary energy sources, is the dependence on other countries for supplying a critically important resource. Countries with large primary energy supplies that are exporting to other countries could use their control over the export as a means to exert pressure on other countries that are dependent on these exports, e.g. to carry out or to stop certain activities or to support or reject certain views.

Large scale hydro power plants that convert the energy in flowing or falling water into electricity comprise a valuable alternative for thermal and nuclear power generation, because they do not have the drawbacks of finite primary energy source supplies and emissions and nuclear waste. Nevertheless, it is difficult to supply the world's electricity demand completely with large scale hydro plants. In developed countries, the available hydro power potential has been utilized for a large part. In order to increase the share of hydro power in the electricity generation in these countries, it would be necessary to construct hydro power plants at distant locations, which are often difficult to access. Further, the transport of the electrical power to the load becomes increasingly difficult, both because the cost and complexity of the transmission system increases due to the long distances to be covered and because in some cases, politically unstable regions must be crossed, in which the risk of sabotage of the electricity transmission system exists. Finally, the construction of dams and basins for hydro power generation causes the flooding of large areas and thus destroys local ecosystems and sometimes forces many people to move. Thus, although it's primary energy supplies are infinite and it does not cause emissions or nuclear waste, large scale hydro power has its own complications and negative environmental impacts.

There exist other electricity generation technologies using renewable primary energy sources that do hence not involve the disadvantages of nuclear and thermal generation. Examples are wave and tidal power, solar power and wind power. In wave and tidal power plants, energy is extracted from the waves and from the water flows caused by the tide. In solar power plants, consisting of solar panels, sunlight is converted into electricity, whereas in wind turbines, the energy contained in flowing air is converted into electricity. Up to this moment, the contribution of these technologies to the demand for electricity is rather modest. This is caused by two important drawbacks of these technologies. The first is that the electricity they generate tends to be more expensive than that

generated by the conventional technologies mentioned above. The second is that in many cases, they are far less flexible than conventional power generation, because the primary energy source from which they generate electricity cannot be controlled.

1.2 Promoting Renewable Energy

As can be concluded from the last section, the main advantages of conventional thermal, nuclear and hydro power generation are the price of the generated electricity and the controllability and flexibility of their output. On the other hand, the main advantages of renewable power generation are the usage of an infinitely available primary energy source (such as sunlight, wind or biomass) and the less severe environmental consequences. Worldwide, many governments tend to value the advantages of renewable power generation more than those of conventional power generation. Hence, they support the expansion of the renewable energy generation capacity in various ways, which basically aim at reducing both disadvantages of most technologies for renewable energy generation: cost and lack of controllability.

The cost of the equipments which are used for producing renewable energy in most cases are reduced by socializing the burden by some form of cross subsidy. An example is forcing power companies to buy the power from renewable sources at a guaranteed price which is not based on the actual value of this power, but which is calculated such that the renewable energy project becomes ‘profitable’ for the developer. Unless the power companies are able to sell this power as ‘green power’ at a premium price, arrangements like this will lead to a general increase in the electricity price, as a result of which all consumers pay for the additional cost of electricity generated from renewable sources. Another example is subsidy that is given to the developers of renewable energy projects, which spread the burden associated with renewable energy overall tax payers. One more approach towards reducing the cost disadvantage of renewable electricity is to

impose taxes on electricity from conventional plants, thus raising the cost of this electricity and making it easier to compete for renewable energy.

The controllability disadvantage is counteracted by accepting renewable sources from contributing to maintaining the system balance. All generators that want to connect to a network must meet the so-called connection requirements of the grid company. These contain requirements that refer to the interaction between the generator and the grid. In order to be able to keep the generation and consumption balanced, which is necessary for correct functioning of a power system, among other things the controllability of generators is addressed in these connection requirements. However, renewable sources are often exempted to a certain extent or even completely from the requirements that concern the controllability of the generated power. In this way, the drawback of uncontrollability is cancelled, at least seen from the point of view of the project developer, who is now allowed to connect to the system without the need to take additional measures to improve the controllability of the renewable sources, e.g. by using a storage system or backup generator. In reality, the problem is of course transferred to the operators of controllable generators, because the technical precondition that a balance between demand and supply must exist is not affected by administratively changing the connection requirements.

1.3 Wind

Wind is a renewable energy resource and there is no fuel costs. No harmful polluting gases are produced. On the other hand, wind farms are noisy and may spoil the view for people living near them. The amount of electricity generated depends on the strength of the wind - if there is no wind, there is no electricity.

1.3.1 Wind Power

The power of the wind has been utilized for at least three thousand years. Until the early twentieth century, wind power was used to provide mechanical power to pump water or to grind grain. At the beginning of modern industrialization, the use of the fluctuating wind energy resource was substituted by fossil fuel-fired engines or the electrical grid, which provided a more consistent power source.

In the early 1970s, with the first oil price shock, interest in the power of the wind re-emerged. This time, however, the main focus was on wind power providing electrical energy instead of mechanical energy. This way, it became possible to provide a reliable and consistent power source by using other energy technologies -via the electrical grid – as a back-up. The first wind turbines for electricity generation had already been developed at the beginning of the twentieth century. The technology has improved step by step since the early 1970s. By the end of the 1990s, wind energy had re-emerged as one of the most important sustainable energy resources. During the last decade of the last century, worldwide wind capacity has doubled approximately every three years. Until the start of the new millennium, the cost of electricity from wind power has fallen to about one-sixth since the early 1980s. Ten years later, overall worldwide investment in wind power had reached a record level of EUR 70.4 billion (USD 9 6 billion) in 2010 (GWEC, 2011a) [3]. Wind energy has become a major industry. Wind energy technology itself has also moved very fast towards new dimensions. At the end of 1989, a 300 kW wind turbine with a 30 m rotor diameter was state-of-the-art. Only 10 years later, 2000 kW turbines with a rotor diameter of around 80 m were available from many manufacturers. The first demonstration projects using 3 MW wind turbines with a rotor diameter of 90 m were installed before the turn of the century; 3 to 3.6 MW turbines became commercially available in 2004, and 5 to 6 -MW turbines around 2006 –2008,

7 to 8 MW turbines developed around 2009-2013 and 9-10 MW turbines are underdevelopment since 2014 and onward [3]. The following table1.1 shows the development of wind turbine size between periods of 1985-2014.

Table 1.1: Development of wind turbine size between 1985 and 2014[3]

Year	Capacity (kW)	Rotor diameter (m)
1985	50	15
1989	300	300
1992	500	37
1994	600	46
1998	1500	70
2003	3000-3600	90-104
2004	4500	112
2006	5000	126
2008	6000	126
2010	7500	126
2012	8000	130
2014	10000	130

1.3.2 Wind Turbine

A wind turbine is a revolving machine that convert the kinetic wind energy into electrical energy through squirrel-cage induction generator (SCIG) or doubly fed induction generator (DFIG) and then fed into grid. In a wind turbine two conversion process take place. The kinetic energy is first converted into mechanical energy. Next, that mechanical energy is converted into electrical energy. Wind turbines can be either constant speed or variable speed generator. In this thesis only DFIG will be considered which are generally used for variable speed operation.

1.4 Literature Survey

In this part of the study, a literature review regarding variable speed wind turbine equipped with doubly-fed induction generator will be explained. More specifically the earlier studies and

researches related to the modeling of DFIG, control strategies applied in the rotor side converter of DFIG will be presented.

1.4.1 Modeling of Wind Turbine Equipped With DFIG

Variable speed wind turbines are complex electromechanical devices and incorporate a large number of controls , in order to tackle complexity ,wind turbines can be taught of a as a collection of subsystems which can be modeled individually such as aerodynamic modeling, the drive train system modeling, the DFIG modeling, and the power converter modeling as shown in the Figure 1.1. Hence, this part of the study will only focus on the modeling of the components of wind energy conversation system (WECS) connected to gird.

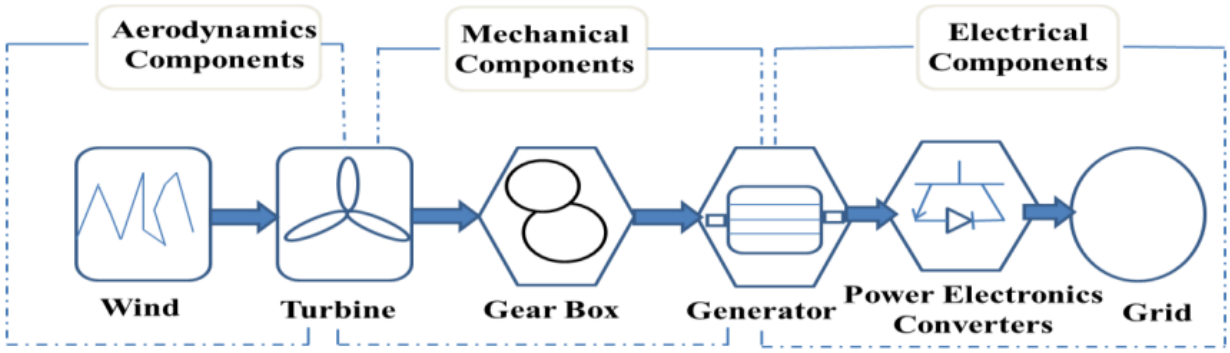

Fig.1.1: Block diagram showing the components of *WECS* connected to grid

1.4.2 Aero Dynamic Modeling

The aerodynamics of a wind turbine is normally described by dimensionless coefficients, which define the wind turbine ability to convert kinetic energy of moving air into mechanical power $\mathbf{C_p}$ or torque $\mathbf{C_q}$ [4], the maximum energy that a wind turbine system can extract from the air system under ideal conditions are explained elaborately by Tao Sun [5].

1.4.3 Drive Train Modeling

It has been reported that for stability of wind turbine generator systems a multi-mass drive train model is needed such as six-mass drive train model, 3-mass drive train and 2-mass drive train model. Many researchers investigated different ways for stability analysis for example in reference [6] the author elaborately explained the multi-mass drive train model and compared a six-mass model with reduced mass model based on transient stability analysis.

In reference [7], the author used a six-mass drive train model to assess the transient stability and small signal stability analysis throughout the fault and other disturbances. In reference [8] the author studied three-mass drive train model, two-mass drive train model and single mass model, and compared their effects on the stability analysis. In addition, the effects of gearbox, shafts bending and elasticity, blade and hub inertias on the transient stabilities of variable speed wind turbines equipped with DFIG are also analyzed. In reference [2, 9], the authors structured three mass model, then after some investigation they realized that the resonance frequency of the gearbox and high speed shafts are much higher, which is not according their interest, thus they derived two mass model from 3 mass model. In references [6] and [10], the authors claimed that a two-mass drive train model (one for the turbine the other for generator) is sufficient for small signal and large signal stability assessment of wind turbine generator system. Generally the two-mass drive train model is widely used by several authors due to its amplification and controller design [11-16]. In some references, such as [17-21] the authors simply concentrated on the generator control and modeling, where the drive train system is expressed by single mass models.

1.4.4 Doubly-Fed Induction Generator (DFIG) Modeling

Along with the mechanical drive train, the electrical system is a fundamental part of a wind turbine. The electrical system comprises the components necessary to convert the mechanical energy into electric power, including electrical auxiliaries and control systems.

The electrical generator is the main component for the mechanical/electrical energy conversion process in a wind turbine. The wind turbine based DFIG model studied in this thesis is illustrated in figure 1.2. In this system the wind turbine is connected to the DFIG through a drive train system, which consist of a low and a high speed shaft with a gearbox in between. The DFIG is a wound rotor induction type generator in which the stator windings are directly connected to the three-phase grid and the rotor windings are fed through three phase back-to-back converters.

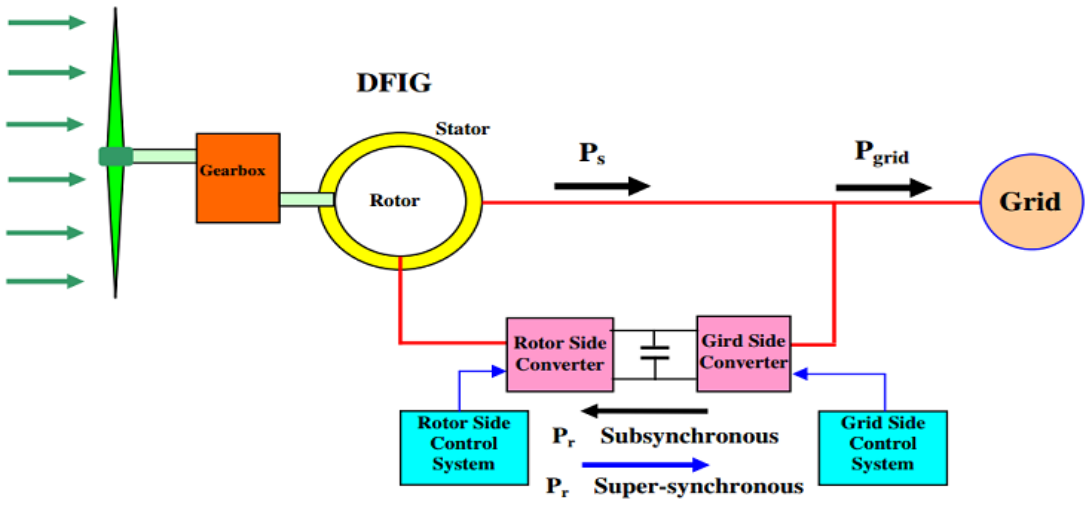

Fig.1.2: Doubly-fed induction generator based VSWT

with the evolution of the control technology the doubly fed induction machine can be sorted into three types: 1) the Doubly Fed Induction Machine (DFIM), which is the conventional wound-rotor doubly fed electric machine with an active winding set on the rotor and stator, respectively, and

flux vector controlled rotor excitation through a multiphase slip-ring assembly; 2) the Brushless Doubly-Fed Induction Machine (BDFIM), which is the burushless doubly-fed induction machine (or reluctance) electric machine with cascaded active winding sets of unlike pole-pairs on the stator assembly of which one is flux vector controlled and a flux focusing rotor assembly; 3) Synchro-Sym electric machine system, which is the only Brushless Doubly-Fed Synchronous Machine (BDFSM). Unlike the doubly-fed electric machine topologies that always rely on slip-induction for operation. The Synchro-Sym electric machine system has a brushless real time control method that eliminates reliance on slip-induction, multiphase slip ring assemblies, or any derivative of rotor flux vector controllers to provide twice synchronous speed for a given frequency of excitation with active rotor and stator winding sets [22]. However only the DFIG is widely used in the wind turbine generator systems. In reference [23] the authors developed the brushless DFIG system by employing two cascaded induction machines to eliminate the brushes and copper rings in the tradition DFIG, and the control strategy for flexible power flow control is developed .The independent control of the active and reactive power flows is achieved by means of a four quadrant power converter under the closed-loop stator flux oriented control scheme. In reference [24] the author proposed a direct power control strategy for cascaded brushless doubly fed induction generator (CBDFIG), which eliminates the slip rings and brushes in conventional DFIG wind turbine systems and features quick dynamic response and excellent steady state performance.

The authors investigated the DFIG model in different orders and compared their results, some authors used full order model, some author used fifth order model of DFIG and some others used third order model by neglecting both the stator and rotor transients. In the research of B.C. Pal F. Mei [25] the full order, 5^{th} order and 3^{rd} order model of DFIG is used in the case of small signal stability analysis and the results are compared. In reference [26] the author developed a reduced

order DFIG model that restricts the calculation for the fundamental frequency component. However, the enhanced reduced order model considers the alternating components of the rotor currents, which is necessary for triggering the crowbar operation. In reference [27], the author studied 5^{th} order model, then he developed a new reduced third order model by ignoring the stator resistances and inductances through applying the Laplace transformation, and compared the proposed model with a full order model for transient analysis of rotor current and stator voltage. In reference [28] the author represented a reduced order model for grid connected wind turbines with doubly-fed induction generators. The model is based on the field oriented control of the generator, considering that the rotor is fed by an ideal current regulated voltage source. This assumption makes the order, if the induction machine model to be reduced to three. In reference [29] the author studied the effect of neglecting stator transients in doubly-fed induction generators, and compared the simulation results with the full order model at two operating points: one at sub-synchronous speed and one at supers-synchronous speed during a short circuit fault at the generator terminal. In many other references such as [28, 30-31] the comparison between full-order and reduced-order model of DFIG has been done and their stability analysis are assessed accordingly. In reference [32] the author simulated the transient response of DFIG during voltage sag considering saturation effects and neglecting saturation effects of leakage flux for different order model of DFIG. As we know, the difference between the model of a squirrel-cage induction generator (SCIG) and a DFIG is the rotor input. Hence, the simplified models of squirrel-cage induction generators may be helpful for understanding the reduced order models of DFIGs [33-34].

1.4.5 Converter Model

The converter of the doubly fed induction generator is modelled as a fundamental frequency voltage source. The model is only a low-frequency representation of the converter dynamics, does not include any switching phenomena and is not suitable for investigating high-frequency phenomena associated with power electronics [3]. The back to back HVDC-link converter connected between the DFIG rotor and grid consist of two pulse width modulation (PWM) inverters as shown in figure 1.2. The back-to-back converter is divided into two components: the rotor-side converter (RSC) and the grid-side converter (GSC) with a dc-link capacitor between them in order to keep the voltage variations in the dc-link voltage small. Both of these converters are Voltage-Sourced Converters (VSC) that use forced-commutated power electronic devices (IGBTs) to synthesize an AC voltage from a DC voltage source, which enable a bi-directional power flow [35-36]. The VSC is used to convert the *ac* voltage source into the *dc* voltage source and vice versa.

The three phase voltage source PWM converter can be transformed from abc reference frame into dqo reference frame which, is easy for control purpose of DFIG as discussed in references[37-39]. In reference [40] the author derived the mathematical model of indirect current control for a PWM voltage source converter based on space vector expressed in abc reference frame. The main advantage of this proposed system is to improve power factor and ripple-free DC output voltage waveform are achieved without any current sensor. In reference [41] the author widely described the working principles and control strategies of PWM converters and he also compared the three phase voltage source and current source PWM converters principles.

1.4.6 Control Strategies for a Wind Turbine-Generator System

The main idea behind this thesis is to design and analyze a DFIG control technique for small signal stability analysis and overall system stability under d-q reference frame and conditions. To a great extent the control strategies for a wind turbine generator is classified into three categories 1) pitch angle control, 2) maximum power point tracing control and 3) DFIG control. In this section of thesis different types of control techniques such as traditional techniques and advanced techniques of wind turbine generators are reviewed

I. Pitch Angle Control

The pitch control system is one of the most widely used control techniques to regulate the output power of a wind turbine generator when it exceeds its rated value. The method relies on the variation in the power captured by the turbine as the pitch angle of the blades is changed. The pitch angle control is only activated at the high wind speed. In references [42-48] the authors proposed different techniques to control and regulate pitch angel during high wind speed. In references [42-44] the authors used PI controllers' technique to regulate the conventional pitch angle of wind turbine speed. However, numerous advanced pitch control strategies are investigated by several researchers. A new approach for the pitch control of wind turbine blades, which is well suited in noisy and unstable wind conditions, proposed in reference [45]. In reference [49] the author proposed a fuzzy logic pitch angle control strategy for a variable speed pitch-controlled wind turbine generation scheme for the supply of an autonomous system with no energy storage units. In reference [48] the author presented a learning adaptive controller in the form of a self-tuning regulator (STR).The STR incorporates a hybrid controller of a linear quadratic Gaussian (LQG), neuro-controller and a linear parameter estimator (LPE) to develop the pitch angle controller of wind turbine.in order to regulate the relationship between rotational speed and wind speed by

controlling the generator torque and further, the rotational speed. A pitch actuator ensures system operation geared toward maintaining output at rated power. In reference [46], the author developed a fuzzy logic pitch angle controller, in which it does not need well known about the system and the mean wind speed is used to compensate the nonlinear sensitivity. In reference [47] the author presented a control strategy based on average wind speed, standard division of wind speed and pitch angle control using a generalized predictive control for output power leveling of wind turbine generator in all operating region.

II. Maximum Power Point Tracking Control

Maximum power point tracking (MPPT) is a technique that grid connected inverters and similar devices used to get the maximum possible power from one or more aerodynamic modules of wind turbine. Sometimes due to the sudden changes in wind, which cannot be predicted and controlled, it is necessary to control the WECS through its power interface, to achieve satisfactory results. So in order to extract the maximum power available, three main control methods used are: hill-climb search (HSC) control, tip speed ratio (TSR) control and power signal feedback (PSF) control.

Generally the maximum power point tracking control (MPPTC) is divided in to two schemes, which are conventional control schemes and intelligent control schemes.

a) Conventional Control Schemes

In conventional control schemes the authors generally focus on the current-mode control and speed-mode control of wind turbine generator systems. This kind of controller mainly depends on the setting of reference values. In the research works of several authors the electromagnetic torque and active power is used as a reference values for current mode control [50-53] and rotational speed is used as reference value for speed mode control [54-55]. In reference [56] the author

presented current mode control and speed mode control to assess transient dynamic of the system, and concluded that the system dynamics characteristics under speed-mode control are superior compared to the dynamic characteristics under current-mode control in the process of maximum power point tracking. In reference [57] the author used several control strategies of maximum power capture for DFIG in wind turbine and discussed the limitations of current mode control and speed mode control. Sometime during the high speed wind, the anemometer cannot precisely measure the wind due to some complexity such as flow distortion, vibrations in wind tower and etc. In order to avoid these drawbacks in reference [58] a novel of wind energy tracking control strategy based on variable-speed constant-frequent (VSCF) wind turbine with DFIG is proposed. In which, wind velocity, rotating-speed and power signals are all adopted in fuzzy logical system for DFIG optimal rotating-speed control. In some other references such as [59, 60, 61] the authors presented the maximum power point tracking (MPPT) of wind by DFIG without needing a tachometer or an anemometer for measuring wind power speed.

b) Intelligent Control

Intelligent control is a class of control techniques that use various artificial intelligence (AI) computing approaches like neural networks, Bayesian probability, fuzzy logic, machine learning, evolutionary computation and genetic algorithms Hill-climbing search.

For the maximum power pint tracking of wind power the hill-climbing control and fuzzy logic control strategies are widely used. In reference [62], the author used a fixed-step speed disturbance optimal control method based on hill-climbing control strategy to determine the speed, perturbation size and direction according to the changes in the power before and after sampling. However, this control method is usually slow in speed because the step disturbance is fixed.

Therefore, some improved hill-climbing control methods are proposed. For example, a method of using variable-step wind energy perturbation method to control the captured wind power is analyzed in [57]. In reference [63] the author developed advanced hill-climb searching algorithm to take into account the wind turbine inertia and the same author also described the intelligent memory method with an on-line training process to control the inverter for maximum wind power extraction, without the need for either knowledge of wind turbine characteristics or the measurements of mechanical quantities such as wind speed and turbine rotor speed.

In reference [64], the author developed a complete control system of fuzzy logic with vector control in the inner loops. First fuzzy controller tracks the generator speed with the wind velocity to extract the maximum power. A second fuzzy controller programs the machine flux for light load efficiency improvement, and a third fuzzy controller gives robust speed control against wind gust and turbine oscillatory torque.

III. Doubly-fed Induction Generator Control

The doubly-fed induction generator (DFIG) control is to day one of the most popular schemes for variable-speed wind turbines regulations which has been introduced to replace the fixed-speed, squirrel-cage induction generators control. This variable speed technology offers advantages such as four quadrant power capabilities, maximum aero dynamic efficiency, reduced mechanical stress and a relatively small converter size. But Control of the DFIGs is more complicated than the control of a squirrel-cage induction generator, because the DFIGs can operate at sub-synchronous speed and super-synchronous speed by regulating the rotor terminal voltages. The DFIG control capabilities have been investigated by several researchers and it has been shown that wind power can increase the damping of inter-area oscillations and that advanced controls may be used to

enhance even further their damping performance. Where the advanced control strategy of DFIGs are presented such as direct torque/power control, field oriented control, predictive control, sensor-less control, slide mode control and nonlinear control.

a) Field Oriented Control of DFIG

Field-oriented control (FOC) also called Vector control is a traditional control.

It is a variable-frequency drive (VFD) control method where the stator currents of a three-phase AC electric motor are identified as two orthogonal components that can be visualized with a vector. In Field Oriented Control, motor currents and voltages are manipulated in the d-q reference frame of the rotor. This means that measured motor currents must be mathematically transformed from the three-phase static reference frame of the stator windings to the two axis rotating d-q reference frame, prior to processing by the PI controllers. Similarly, the voltages to be applied to the motor are mathematically transformed from the d-q frame of the rotor to the three phase reference frame of the stator before they can be used for PWM output. Field oriented control is widely used by several researchers in variable speed wind turbine DFIG due to its ability of controlling the motor speed and electrical torque more efficiently, and it is less expensive to build a field oriented control system. Another goodness of FOC is that, it has the ability of separately controlling the active and reactive power of generator. The commonly used orientation frames for a DFIG system are the stator-voltage and stator-flux frames. In most of the traditional strategies, the control of DFIG real and reactive powers is achieved through a nested power and current-loop controller in stator flux oriented frame [65]. In several research studies, the stator flux oriented control is widely used in the DFIG control designs, in which the q-axis current component is used for active power control and the d-axis is used for reactive power control [55, 59, 66]. While for the stator voltage oriented

control, the situation is opposite, the d-axis component is used for active power control and the q-axis current component is used for reactive power control [67-68]. In reference [69] the author compared real and reactive power control for a DFIG based wind turbine system using stator voltage and stator flux oriented frame. And comparisons are made to evaluate the theoretical difference of the DIFG using stator-voltage and stator-flux oriented frame.

b) Direct Power /Torque Control of DFIG

It is a new technique for controlling the torque and active/reactive power of DFIG.

Direct torque/power control techniques do not require coordinate transformations, current regulators, current control loops and specific modulations. Thus the direct torque control has the ability to control directly the rotor flux magnitude and electrical torque. Through properly selecting the inverter switching states [70]. The direct torque control is first developed by Toshihiko Noguchi in references [71-72]. Based on the principle of direct torque control on electrical machine the direct power control is presented in [73]. In reference [74] the author proposed a new direct power control (DPC) strategy for a doubly fed induction generator (DFIG)-based wind turbine system. The required rotor control voltage, which eliminates active and reactive power errors within each fixed time period, is directly calculated based on stator flux, rotor position, and active and reactive powers and their corresponding errors. No extra power or current control loops are required, simplifying the system design, and improving transient performance. In reference [75] the author presented a grid-connection control strategy of doubly fed induction generator wind system based on the direct control of both a virtual torque and rotor flux of the generator. This control is achieved with no proportional-integral regulator and requires the measurement of only grid voltages, rotor currents, and rotor position. In reference [76] the author contributed for a

detailed comparison between the field oriented controls (FOC) and direct torque control techniques, and emphasized the advantages and disadvantages. The performance of the two control scheme is evaluated in terms of torque and current ripple, and transient response of step variation of the torque commands. In the result it shows that, unlike field oriented control (FOC), DTC does not require any current regulator and PWM signal generator; as a consequence, timers are not required. In spite of its simplicity, DTC allows obtaining a good torque control in steady state and transient operating conditions. In addition, this controller is very little sensible to parameters detuning in comparison with FOC. The problem with DTC, the flux is conventionally obtained from the stator voltage model, using the measured stator voltages and currents. This method, utilizing open loop pure integration, suffers from increased noise on voltage and current and quantization errors in the digital system. In reference [77] the author presented direct torque control of induction machines using space vector modulation to estimate the synchronous speed and the voltage behind the transient reactance. And space vector PWM is used to define the inverter switching state and to reduce the torque error during the entire switching interval.

In reference[78] the author presented a direct torque control for a doubly-fed induction generator of variable speed wind turbine, operating above the rated power nonlinear state-feedback control law has been used to provide the torque reference so as to reduce the produced electrical power tracking error. And improve the produced electrical power quality and increase the robustness against the different perturbations causing structural stress. In reference [79] the author presented a direct torque control of doubly-fed induction generators with a space vector modulation scheme for wind energy conversion. The scheme is to independently control the torque and reactive power flow of the doubly-fed induction generator and directly compute the voltage acting on the rotor winding from the differences between reference values and feedback quantities as the proposed

algorithm is more robust and has less harmonic distortion than the hysteresis direct torque control method. In reference [75] the author presented a grid connection control strategy of doubly fed induction generator wind speed base, on the direct control of both a virtual torque and rotor flux of the generator. This control is achieved with no proportional-integral (PI) regulator and requires the measurement of only grid voltages, rotor currents, and rotor position. The same switching table is used for grid synchronization and for running process. In reference [80], the author proposed a novel direct torque control of doubly-fed wound rotor induction machines and applied to variable speed wind power generation systems. The proposed control strategy is developed based on the control of the rotor power factor. By keeping the rotor power factor equal to one, a switching-table-based hysteresis direct torque control system is built and the corresponding rotor voltage vector table is obtained. The validity of the proposed method is examined using the simulation of the variable speed winding power generation. Promising results were obtained and attractive advantages of the proposed control idea were illustrated including simple structure of the control system, low capacity of the inverter, reduced harmonic pollution to the power grids as well as the other advantages.

In reference [81] the author presented the comparison of three different strategies for the control of a doubly fed induction generator (DFIG) in wind energy conversion systems (WECS).namely, vector control, direct torque control, and direct power control. The above control methods are reviewed and their performances analyzed and compared on the basis of simulations and experimental results. The results showed that the direct power control has the merits of being simple, requiring fewer sensors, having low computational complexity, fast transient response and low machine model dependency compared with DTC. In reference [82], the author presented comparison between field oriented control and direct power control for a PWM rectifier, and the

simulation results showed that the virtual-flux-based direct power control was superior to the voltage-based direct power control and field oriented control. In recent years numerous techniques based on direct power control has been applied in DFIG-based wind turbine generator. For example in reference [83] the author proposed direct power control of grid-connected wound rotor induction machine without rotor position sensors, which gave an excellent dynamic performance. In reference [84-85] the authors studied the behavior of a doubly fed induction generator (DFIG) under unbalanced grid voltage conditions. It is shown that if no special control efforts are employed, the behavior of the generator is deteriorated, basically due to two reasons: (I) electromagnetic torque oscillations and (II) nonsinusoidal current exchange with the grid. These phenomena are first analyzed theoretically as a function of the stator active and reactive instantaneous power exchange by the stator of the DFIG and the grid-side converter (GSC). This analysis provides the main ideas for generation of the active and reactive power references for the rotor-side converter (RSC) and the GSC, controlled by means of direct power control techniques under unbalanced grid voltage. In reference [86] the author proposed a new direct power control strategy for doubly fed induction generator system, the strategy is based on the direct control of stator active and reactive power by selecting appropriate voltage vectors on the rotor side. It is found that the initial rotor flux has no impact on the change of stator active and reactive power. The proposed method only utilizes the estimated stator flux so as to remove the difficulties associated with rotor flux estimation. The only machine parameter required by the proposed DPC method is the stator resistance whose impact on the system performance is found to be negligible.

c) Predictive Control of DFIG

Predictive control (PC) is an advanced method of process control that has been in use in the process industries in chemical plants and oil refineries since the 1980s. In recent years it has also

been used in power system balancing models. Some of the researchers used it in DIFG connected to grid. In order to control the rotor and grid side converter of DFIG. The main advantages of this method are no need of linear controllers, coordinates transformations or modulators for converter and inverter. Several predictive direct power control strategies is studied and compared for a back-to -back converters in reference [87].

d) Sensor Less Control of DFIG

Sensor-less vector control is a variable frequency drive (VFD) control strategy that improves motor performance by regulating the VFD output based on a mathematical determination of motor characteristics and operating conditions. Operating conditions are estimated from measurements of electrical parameters. Sensor-less vector control is called "sensor-less" to distinguish it from vector control with encoder feedback which optimizes motor performance by regulating the VFD output based on motor shaft speed and position feedback from an encoder.

So in the case of sensor-less control there is no need for any encoder feedback, to adjust the rotor position. The rotor position is estimated from measuring of electrical parameters. There are several researchers investigated about sensor-less control strategies of DFIGs [89-91]. In reference [91], the author developed a simple sensor-less method for the detection of mechanical rotor position of the DFIG. This method is based on the phase comparison of the actual and estimated rotor currents, using the classical model of the machine. In this method the author used a hysteresis comparator instead of PI controller to detect the rotor position. In this way, the method does not need parameter determination for the controllers and shows a considerable independence of parameter uncertainties. Moreover, direct torque/power control strategies can be considered as "sensor-less

type" control techniques because direct torque/power control could obtain a good dynamic control of the torque/power without any mechanical transducers on the machine shaft [76].

e) Sliding Mode Control(SMC) of DFIG

Sliding mode control is a nonlinear control. SMC concept consists of moving state trajectory of the system towards and maintains it around the sliding surface with an appropriate logic commutation, the latter gives birth to a specific behavior of the state trajectory in a neighborhood of the sliding surfaces known as sliding regimes [92, 93]. SMC emerges as a particularly suitable option to deal with electronically controlled variable speed operating WECS, owing to its potential to eliminate the undesirable effects of parameter variations with minimum complexity of implementation [94, 95].

1.5 Objectives and Approach of the Thesis

The main objective of this thesis is to design and analyze controllers at the rotor side of the DFIG for small signal stability study. Controller's parameters need to be tuned efficiently to ensure proper operation for varying operating condition.

In order to design and optimize controller, a model of DFIG at the most detail level will be presented, namely full-order model. VSC of the rotor is not modeled with details in full-order as the switching frequency is far above the dynamics under study [25].

In order to control the dynamic behavior of DFIG connected to single machine infinite bus (SMIB), a generic closed PI controller is better option for controlling rotor speed, reactive power and pitch angle[25], The control schemes for the rotor side converter involves two PI control loops i.e. outer loop and inner loop. The outer loop will work as speed regulator control loop and the inner loop

will work as current control loop. In this thesis, PI controller will be used and genetic algorithm will be applied for the optimization of controller parameters to improve the small signal stability.

The specific objectives of the research can be outlined as follows.

I. Study of full-order nonlinear dynamic model of doubly fed induction generator (DFIG).
II. Study of full order nonlinear dynamic model of DFIG connected to grid.
III. Design and performance comparison of open loop and closed loop controllers for grid connected DFIG.
IV. Design of efficient PI controller to study the small signal stability of the DFIG connected grid.
V. Use of efficient parameter optimization algorithm for proper tuning of the controller gains.

1.6 Thesis Organization

The thesis is organized in six chapters as follows:

Chapter 1: A background of the research study is represented in this chapter. It includes renewable energy , electricity supply , promoting renewable energy , wind turbine, literature survey about variable speed wind turbine DFIG model and different type of controllers in used in wind turbine generator system. Objective of the thesis is presented here.

Chapter 2: Presents a review of general power system stability, classification of stability and category of stability and provides current definitions of transient stability and small signal stability. Furthermore, the eigenvalue characteristics and participation factors are discussed elaborately.

Chapter 3: presents a review of the state of the art in wind turbines. It includes basic component of wind turbine, general survey of wind turbine topology such as fixed speed and variable speed wind turbine. Furthermore, model of variable speed wind turbines with DFIG is presented. More specifically, the aerodynamic model, two-mass drive train model, the detailed doubly-fed induction generator model expressed in abc reference frame and then transformed to dqo reference frame via park transformation theory. The brief explanation of back-to-back converter also given.

Chapter 4: The small signal stability of single machine infinite bus without the controller in rotor side converter is analyzed in this chapter. The computer simulation results are presented to show the eigenvalue and state of the modes for small signal analysis.

Chapter 5: presents a review of the state of the art in optimization technique. It includes background of optimization, objective of optimization, techniques of optimization, genetic algorithm, and background of genetic algorithm. Furthermore, it presents optimization of PI controller gains using genetic algorithm. Chapter 5 also contains the complete design of rotor side controller of DFIG. The simulation performances of the DFIG with and without genetic algorithm are also presented in this chapter.

Chapter 6: Presents the conclusions of results, together with suggestions for the further study in this area.

CHAPTER 2

General Stability Analysis of a DFIG Connected To Grid

As usual the demand for electricity is remarkable in all over the world, especially in developing countries like Afghanistan, Bangladesh and Pakistan etc., this sustainable demand is leading to operation of the power system at its limit. Despite this the need for reliable, stable and quality power is also on the rise due to electric power sensitive industries such as electronics, communication, information technology etc.

In this situation, dealing the electric power demand is not the only criteria, in the meanwhile it is the responsibility of the power system engineers to provide a reliable and stable quality power to the consumer's and these issues highlight the necessity of understanding the power system stability.

In this chapter, we will study how to assess the stability of a power system, how to improve the stability and how to protect our system from moving to unstable system. In order to do these issues, the present chapter includes a review of general concepts relating to power system stability in order to contextualize this research. The classification of stability problems in power grid along with the methods that have been proposed for its analysis are also summarized.

2.1 Basic Concepts and Definitions of Power System Stability

Wind power generation has been developed very quickly during the past few years. At present the capacity of the installed wind power in the world is more than 45GW. With the growing penetration of wind energy into power grids the impact of wind turbines (WTs) on power system stability is of increasing concern, and the dynamics of wind turbines should be carefully considered in power system stability analysis.

Over the years, several definitions of power systems stability have been formulated aiming at clarifying technical and physical aspects of the problem from the system theory perspective. The stability concert more consistent with the emphasis placed in this research work is the one relating to the system's ability to ride-through disturbances arising the system itself and its capacity to settle down to a new stable operating state after the effects of such disturbance disappears. A formal definition of power system stability is provided by [96-98].

"Power system stability is the ability of an electric power system, for a given initial operating condition, to regain a state of operating equilibrium after being subjected to a physical disturbance, with most system variables bounded so that practically the entire system remains intact."

The definition applies to an interconnected power system as a whole. Often, however, the stability of a particular generator or group of generators is also of interest. A remote generator may lose *stability* (synchronism) without cascading instability of the main system. Similarly, stability of particular loads or load areas may be of interest; motors may lose *stability* (run down and stall) without cascading instability of the main system.

The power system is a highly nonlinear system that operates in a constantly changing environment; loads, generator outputs and key operating parameters change continually. When subjected to a disturbance, the stability of the system depends on the initial operating condition as well as the nature of the disturbance.

The stability of a power system is determined mainly by the generators. In most power systems, conventional directly grid-coupled synchronous generators are the dominant generation technology. The behavior of the grid-coupled synchronous generator under various circumstances

has been studied for decades and much of what is to be known is known. However, although this generator type used to be applied in wind turbines in the past, this is no longer the case. Instead, wind turbines use other types of generators, such as squirrel-cage induction generators or generators that are grid-coupled via power electronic converters which is called doubly-fed induction generators (DFIGs) [142]. Since most modern wind turbines are of Variable Speed with Partial -Scale Frequency Converter and Variable Speed with Full-Scale Frequency Converter

[3-99], the analyses completed in this chapter will mainly focus on dynamic models based on these wind turbine models. Fixed Speed wind turbine will still be discussed and studied, as they are still in service within power systems; however, most modern wind farms utilize variable speed wind turbines [2]. The interaction of these generator types with the power system is different from that of a conventional synchronous generator. As a consequence, wind turbines affect the dynamic behavior of the power system in a way that might be different from synchronous generators. Further, there are also differences in the interaction with the power system between the various wind turbines types presently applied, so that the various wind turbine types must be treated separately. This chapter will address each stability issue individually and provide results and discussion based on how stability might be impacted by large penetrations (larger than 30%) of wind generators [142]. For the purposes of system analysis, power system stability is divided into two broad classes [100-101] as large and small system stability.

2.2 Classification of Power System Stability

Power system stability is traditionally classified as a single problem; however, there are several types of instability that may influence the power system and, as such, must be studied individually. Essentially, power system stability can be broken down into three distinct areas [97-98, 3]:

- **Rotor angle stability**
- **Voltage stability**
- **Frequency stability**

These three areas of power system stability require various simulation techniques and can be classified into more detailed areas of study. This chapter will briefly assess how wind generation, in large (above 30%) penetrations, in modern power systems may influence power system stability across the three areas which is well discussed by Kundur et al 2004[98].The stability of the system will depend on the physical conditions, the type of disturbance and the current operating conditions of the power system. The response of the power system to a disturbance may involve much of the equipment. For instance, a fault on a critical element followed by its isolation by protective relays will cause variations in power flows, network bus voltages, and machine rotor speeds; the voltage variations will actuate both generator and transmission network voltage regulators; the generator speed variations will actuate prime mover governors; and the voltage and frequency variations will affect the system loads to varying degrees depending on their individual characteristics. Further, devices used to protect individual equipment may respond to variations in system variables and cause tripping of the equipment, thereby weakening the system and possibly leading to system instability.

2.2.1 Categories of Stability

The classification of power system stability proposed here is based on the following considerations [98]:

- The physical nature of the resulting mode of instability as indicated by the main system variable in which instability can be observed.

- The size of the disturbance considered, which influences the method of calculation and prediction of stability.
- The devices, processes, and the time span that must be taken into consideration in order to assess stability.

Figure (1) gives the overall picture of the power system stability problem, identifying its categories and subcategories. The following are descriptions of the corresponding forms of stability phenomena.

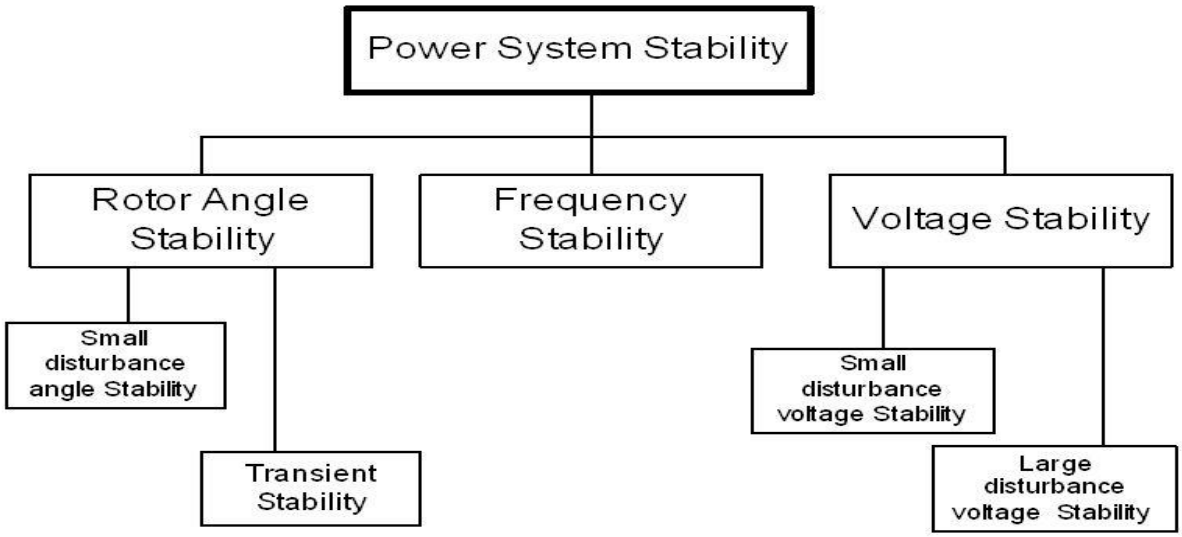

Fig 2.1: Classification of the power system stability

2.2.2 Rotor Angle Stability

Rotor angle stability is the ability of the synchronous machines of an interconnected power system to maintain synchronism following a disturbance [97, 3]. Rotor angle synchronism depends on a variety of physical factors in the power system, mainly the synchronizing torque component and the damping torque component. As wind power is introduced into power systems, conventional generation will be displaced in order to accommodate the rising penetration levels of wind

generation. Conventional synchronous generation provides inertia to the systems, and this in turn supplies the synchronizing torque and damping torque to the system. The lack of the synchronizing torque results in aperiodic or non-oscillatory instability, while the lack of damping torque results in oscillatory instability (Kundur et al., 2004), [98,3,102-103].

Rotor angle stability can be further broken down into two subcategories:

- Small-disturbance rotor angle stability or small-signal stability;
- Large-disturbance rotor angle stability or transient stability

The classification of rotor angle stability into small-signal stability and transient stability requires different analytical approaches that both utilize the dynamic and steady-state components of the power system. Small-signal stability assesses system stability by linearizing around a signal operating point, while transient stability assesses system states through time-domain analysis. This chapter will provide discussion and examples of both types of rotor angle stability.

It should be emphasized that transient stability is a function of both, the signal operating condition and the time-domain analysis, whereas small-signal stability is a function only the signal operating condition.

2.2.3 Voltage Stability

The second aspect of power system stability is the voltage stability of the power system under high (larger than 30%) penetrations of wind generation like rotor angle stability. It is the ability of the system to maintain steady state voltages at all the system buses when subjected to a disturbance. If the disturbance is large then it is called as large-disturbance voltage stability and if the disturbance is small it is called as small-disturbance voltage stability [3]. Unlike angle stability, voltage stability can also be a long term phenomenon. In case voltage fluctuations occur due to

fast acting devices like induction motors, power electronic drive, HVDC etc. then the time frame for understanding the stability is in the range of 10-20 s and hence can be treated as short term phenomenon. On the other hand if voltage variations are due to slow change in load, over loading of lines, generators hitting reactive power limits, tap changing transformers etc. then time frame for voltage stability can stretch from 1 minute to several minutes [104-107]. The main difference between voltage stability and angle stability is that voltage stability depends on the balance of reactive power demand and generation in the system where as the angle stability mainly depends on the balance between real power generation and demand.

2.2.4 Frequency Stability

Frequency stability is a phenomenon that involves the whole system. Frequency stability is the ability of a power system to maintain steady-state frequency following a severe system upset resulting in a significant imbalance between generation and load' (Kundur et al., 2004) [98].

The disturbance here reduces the total active power output and the system goes to an imbalance condition, which may lead to frequency sewing and result in further tripping of generation or load.

Although, the penetration level of wind generation is increasing in huge amount in interconnected power systems, the presence of wind generation may result in very little impact in frequency-division events that arise in the system [108-109].

In the wind power system frequency stability depends on system stiffness level rather than active power lost in the system. Therefore a small level of stiffness suggests that the system frequency is less sensitive to change active power. While a large level of stiffness suggests the system frequency is very sensitive to change the active power [3].

In general, apart from insufficient generation reserve, frequency stability problems concerns deficiencies in equipment responses, poor control coordination and protection equipment [97].

Though, stability is classified into rotor angle, voltage and frequency stability they need not be independent isolated events. A voltage collapse at a bus can lead to large excursions in rotor angle and frequency. Similarly, large frequency deviations can lead to large changes in voltage magnitude. Each component of the power system i.e. prime mover, generator rotor, generator stator, transformers, transmission lines, load, controlling devices and protection systems should be mathematically represented to assess the rotor angle, voltage and frequency stability through appropriate analysis tools. In fact entire power system can be represented by a set of Differential Algebraic Equations (DAE) through which system stability can be analyzed. Solution of the differential equations representing the system will yield at least one positive real root, or one pair of complex roots with real parts. In cases of small disturbances, this class of stability can be assessed by analyzing the roots of the linearized system, whilst in cases of large disturbances, because of the non-linearity involved, the difference between the torque components (synchronizing and damping torque) can only be estimated from the nature of the trajectories.

In the next few Chapters we will be concentrating on variable speed wind turbine modeling for stability analysis.

2.3 General Category of Stability

To a greater or lesser extent, all power system disturbance which has mentioned above subjected into two categories: small and large signal disturbances of the power system.

2.3.1 Transient Stability

Transient stability is concerned with the system's ability to maintain synchronism following a large or severe disturbance. Unlike small-signal stability, transient stability is analyzed by studying and simulating how the system responds in the time domain. The transient stability of the system depends on both the initial operating conditions of the system and the severity of the disturbance, in general the transient stability is defined as, the capability of a power system to return to a stable operating point after the occurrence of a disturbance that changes its topology.

Examples of changes of the topology of a power system are:

- The sudden change of a load, including a load trip, which is equivalent to the change of load to zero.
- The occurrence of a fault, i.e. a short circuit, which is equivalent to switching on an impedance of very low value and
- The tripping of a generator or a line.

If one of the above disturbances occurs, the system is no longer in steady state. Various quantities in the system, such as rotor speeds and node voltages, start to change and to deviate from their steady state values. If the fluctuations of the system's quantities damp out and the system settles at a stable operating point, it is considered stable, whereas when the deviation of the various quantities becomes ever larger, the system is unstable and will eventually collapse, leading to a blackout [97, 110].

In the case of wind generation, particularly based on variable seeped wind turbines, the lack of synchronizing torque or appropriate voltage support may result in decreased levels of system security and a higher probability of instability. This is due to the fact that, by adding the speed

control capability to variable speed wind turbines, the rotational speed of wind turbines is independent from system frequency. Most of the dynamic models available address this issue and present a decoupled structure for the power electronics of variable speed wind turbines. Xu and Cartwright, 2006[86] modelled the decoupled structure and presented a model that represents the unbalanced nature of the wind turbines. The model developed by Lei et al., 2006[18] further developed the power electronic controls to simulate the turbine as a voltage source that controls the rotor current of the machine. Finally, Erlich et al., 2007[26] presented a simplified simulation model that allows for multiple modes of operation for the reactive power control of the turbines. Each of these models demonstrates how variable speed wind turbines can effectively contribute in the electrical side of the power system by providing reactive power, but remain decoupled from the mechanical aspects of the system due to the implementation of the control. This means that the oscillations that influence rotor angle stability of the system will not originate from the wind generators in the power system, but from the conventional synchronous generation units themselves and how they are electrically impacted by the wind power generation.

But in case of more wind penetration in wind turbine the damping of rotor speed oscillation will be increased due to damper winding, the exciter and the rest of the power system. The above definition of transient stability specifies that the system's electrical topology must change. This point is the main distinction between transient stability and small signal stability.

The latter refers to the response to disturbances that do not change the system's topology, but only the values of the state variables, like generator load angle, rotor speed and exciter voltage and the state variables of generator controllers. The impact of wind power on the small signal stability of power systems is the topic of this chapter.

2.3.2 Small Signal Stability

Small signal stability is defined as the capability of the power system to return to a stable operating point after the occurrence of a disturbance that leads to an incremental change in one or more of the state variables of the power system.

Whereas the definition of small signal stability refers to the system's response to a small change in one or more of its state variables. The disturbances are considered to be sufficiently small that linearization of system equations is permissible for purposes of analysis [97-98, 2, 111].

Examples of state variables of a power system are:

- synchronous and asynchronous machine rotor speeds
- synchronous machine load angles
- magnetic flux linkages
- controller state variables

If a disturbance causes a change in the value of one or more of these state variables, the system is driven from the equilibrium. If thereafter the system returns to its steady state, it is stable, whereas if the initial deviation from the steady state becomes ever larger, it is unstable. A further difference between transient stability and small signal stability is that if a steady state is reached after a disturbance leading to a transient phenomenon, i.e. a change in the system's topology, the new steady state can be different from the initial one. In contrast, if a system returns to a steady state after an incremental change in a state variable, this steady state is identical to the initial steady state, because no change in the network's topology has occurred.

2.3.2.1 Characteristics of the Small Signal Stability Problems

Small signal stability problems may be either local or global in nature. Local problems involve a small part of the power system, and are usually associated with rotor angle oscillations of a single power plant against the rest of the power system. Such oscillations are called local plant mode oscillations. Stability (damping) of these oscillations depends on the strength of the transmission system as seen by the power plant, generator excitation control systems and plant output [97-98, 112].

Global problems are caused by interactions among large groups of generators and have widespread effects. They involve oscillations of a group of generators in one area swinging against a group of generators in another area. Such oscillations are called inter-area mode oscillations. Their characteristics are very complex and significantly differ from those of local plant mode oscillations. Load characteristics, in particular, have a major effect on the stability of inter-area modes [97- 98].

The time frame of interest in small-disturbance stability studies is on the order of 10 to 20 seconds following a disturbance.

2.3.2.2 Eigenvalues and Small Signal Stability

The main goal of this section is to figure out the correspondence between the eigenvalues of an electrical power system and its dynamic characteristics. First the linearization of the state equations of the power system will be discussed. After that, the correspondence between the eigenvalues of the state matrix which is the crucial part of the linearized description, and the time domain will be pointed out.

2.3.2.4 Linearization of State Equations for DFIG

Modal Analysis

In this thesis the focus will be on modeling of wind turbine connected to DFIG, which can be described by a set of n First-order non-linear, ordinary algebraic-differential equations (DEA) of the following form [98, 112-113]:

$$\frac{dx_i}{dt} = f_i\left(x_1, x_2, ..., x_n; z_1, z_2, ..., z_m; u_1, u_2, ..., u_r\right) \quad (2.1)$$

$$0 = g_i\left(x_1, x_2, ..., x_n; z_1, z_2, ..., z_m; u_1, u_2, ..., u_r\right) \quad (2.2)$$

The mathematical model of a power system can be written as a set of DAE

$$\dot{x} = f\left(x, z, u\right) \quad (2.3)$$

$$y = g\left(x, z, u\right) \quad (2.4)$$

With

$$\mathbf{x} = \begin{bmatrix} x_1 \\ x_2 \\ \vdots \\ x_n \end{bmatrix} \quad \mathbf{z} = \begin{bmatrix} z_1 \\ z_2 \\ \vdots \\ z_m \end{bmatrix} \quad \mathbf{u} = \begin{bmatrix} u_1 \\ u_2 \\ \vdots \\ u_r \end{bmatrix} \quad \mathbf{f} = \begin{bmatrix} f_1 \\ f_2 \\ \vdots \\ f_n \end{bmatrix} \quad \mathbf{g} = \begin{bmatrix} g_1 \\ g_2 \\ \vdots \\ g_n \end{bmatrix} \quad (2.5)$$

Where

$\mathbf{f}$ is a vector containing n first-order non-linear differential equations

$\mathbf{x}$ is a vector containing n state variables

u is a vector containing r input variables

g is a vector containing n non-linear algebraic equations

z is a vector containing m algebraic variables

y is a vector containing m output variables

By assuming that the system in equation 2.3 is time invariant, i.e. the time derivatives of the state variables are not explicit functions of the time, t can be excluded from equation 2.3. In small-signal analysis, equations 2.3and 2.4 can be linearized by a Taylor series expansion around an operating point (x_0,z_0,u_0) and the resulting linearized description of the system can be used to investigate its response to small variations in the input or state variables, starting at an equilibrium point [98, 114-115].Neglecting the terms of order two and above and eliminating the algebraic variables **z** just taking into account first-order terms ,the system state matrix is obtained from derivations given below.

A procedure for small perturbations is established for ith component of vector **x** .

$$\dot{x}_i = \dot{x}_{i0} + \Delta\dot{x}_i = f_i\left[\left(x_0 + \Delta x_0\right),\left(u_0 + \Delta u_0\right)\right] \tag{2.6}$$

$$= f_i\left(x_0, u_0\right) + \frac{\partial f_i}{\partial u_i}\Delta x_i + \ldots + \frac{\partial f_i}{\partial u_n}\Delta x_n + \frac{\partial f_i}{\partial u_1}\Delta u_1 + \ldots + \frac{\partial f_i}{\partial u_r}\Delta u_r \tag{2.7}$$

From equation (2.3) it follows that

$$\dot{x}_{i0} = f_i\left(x_0, u_0\right) \tag{2.8}$$

And therefore (2.7) can be written as

$$\Delta\dot{x}_i = \frac{\partial f_i}{\partial x_i}\Delta x_i + ... + \frac{\partial f_i}{\partial x_n}\Delta x_n + \frac{\partial f_i}{\partial u_1}\Delta u_1 + ... + \frac{\partial f_i}{\partial u_r}\Delta u_r \qquad (2.9)$$

With $i = 1, 2, ..., n$

The same can be done for the jth component of y, with reference to (2.4),

$$\Delta\dot{y}_j = \frac{\partial g_j}{\partial x_1}\Delta x_1 + ... + \frac{\partial g_j}{\partial x_n}\Delta x_n + \frac{\partial g_g}{\partial u_1}\Delta u_1 + ... + \frac{\partial j_j}{\partial u_r}\Delta u_r \qquad (2.10)$$

With $j = 1, 2, ..., n$

The prefix Δ denotes a small deviation, thus

$$\Delta x = x - x_0 \qquad \Delta y = y - y_0 \qquad \Delta u = u - u_0$$

Doing this for all components of the vectors x and y gives the following linearized set of state and output equations

$$\Delta\dot{\mathbf{x}} = \mathbf{A}\Delta\mathbf{x} + \mathbf{B}\Delta\mathbf{u} \qquad (2.11)$$

$$\Delta\mathbf{y} = \mathbf{C}\Delta\mathbf{x} + \mathbf{D}\Delta\mathbf{u} \qquad (2.12)$$

With

$$\mathbf{A}=\begin{pmatrix} \frac{\partial f_1}{\partial x_1} & \cdots & \frac{\partial f_1}{\partial x_n} \\ \vdots & \ddots & \vdots \\ \frac{\partial f_n}{\partial x_1} & \cdots & \frac{\partial f_n}{\partial x_n} \end{pmatrix} \quad \mathbf{B}=\begin{pmatrix} \frac{\partial f_1}{\partial u_1} & \cdots & \frac{\partial f_1}{\partial u_r} \\ \vdots & \ddots & \vdots \\ \frac{\partial f_n}{\partial u_1} & \cdots & \frac{\partial f_n}{\partial u_r} \end{pmatrix}$$

$$\mathbf{C}=\begin{pmatrix} \frac{\partial g_1}{\partial x_1} & \cdots & \frac{\partial g_1}{\partial x_n} \\ \vdots & \ddots & \vdots \\ \frac{\partial g_m}{\partial x_1} & \cdots & \frac{\partial g_m}{\partial x_n} \end{pmatrix} \quad \mathbf{D}=\begin{pmatrix} \frac{\partial g_1}{\partial u_1} & \cdots & \frac{\partial g_1}{\partial u_r} \\ \vdots & \ddots & \vdots \\ \frac{\partial g_m}{\partial u_1} & \cdots & \frac{\partial g_m}{\partial u_r} \end{pmatrix} \qquad (2.13)$$

Thus, the matrices **A**, **B**, **C** and **D** contain the partial derivatives of the functions in **f** and **g** to the state variables **x** and the input variables **u**. Matrix **A** is the state matrix of the system. Equations ((2.11) and (2.12)) can be Laplace transformed to obtain the state equations in the frequency domain.

Take the Laplace transform assuming zero initial conditions [2, 113]

$$s\,\Delta x(s)-\Delta x(0)=\mathbf{A}\,\Delta x(s)+\mathbf{B}\,\Delta u(s) \qquad (2.14)$$

$$\Delta\, y(s)=\mathbf{C}\,\Delta x(s)+\mathbf{D}\,\Delta u(s) \qquad (2.15)$$

A solution to the state equations can be obtained by rearranging the upper equation of (2.14) & (2.15) as follows

$$(s\mathbf{I} - \mathbf{A})\Delta x(0) + \mathbf{B}\Delta u(s) \qquad (2.16)$$

$\mathbf{I}$ is the identity matrix and the values of s which satisfy

$$\det(s\mathbf{I} - \mathbf{A}) = 0 \qquad (2.17)$$

Are known as the eigenvalues of matrix A and equation (6.10) is defined as the characteristic equation of matrix **A**.

2.4 Eigenvalues

Eigenvalue is a scalar associated with a given linear transformation of a vector space and having the property that there is some nonzero vector which when multiplied by the scalar is equal to the vector obtained by letting the transformation operate on the vector; *especially* it is the root of the characteristic equation of a matrix.

2.4.1 Properties of Eigenvalues

In Small signal stability analysis the properties of the system equations ((2.11), (2.12)) around operating point (x_0, z_0, y_0), studied through an eigenvalue analysis of the state matrix **A**. the study determine the time domain response of the system to small perturbations, and therefor contain important information's on the dynamic behavior of the system under study condition called mode, which is obtained from **A** matrix**.**

For a system to be stable the real parts of all eigenvalues of the state matrix **A** has to be negative and must lie in the left half-plane of the complex plane. An eigenvalue with a negative real part ensures that oscillations will decay with time and will return to a steady state following a small disturbance. The opposite will occur if an eigenvalue has a positive real part. The amplitude of the modes will increase exponentially and the power system will be unstable at that operating point.

If **A** is real, complex eigenvalue occur in conjugate pairs, and each pair would correspond to an oscillatory mode. Figure (2.2) shows the possible natural modes of a system. The eigenvalues of **A** contain essential information about the mode's frequencies and their damping after a small disturbance. The real part component gives the damping and the imaginary component gives the frequency of oscillation.

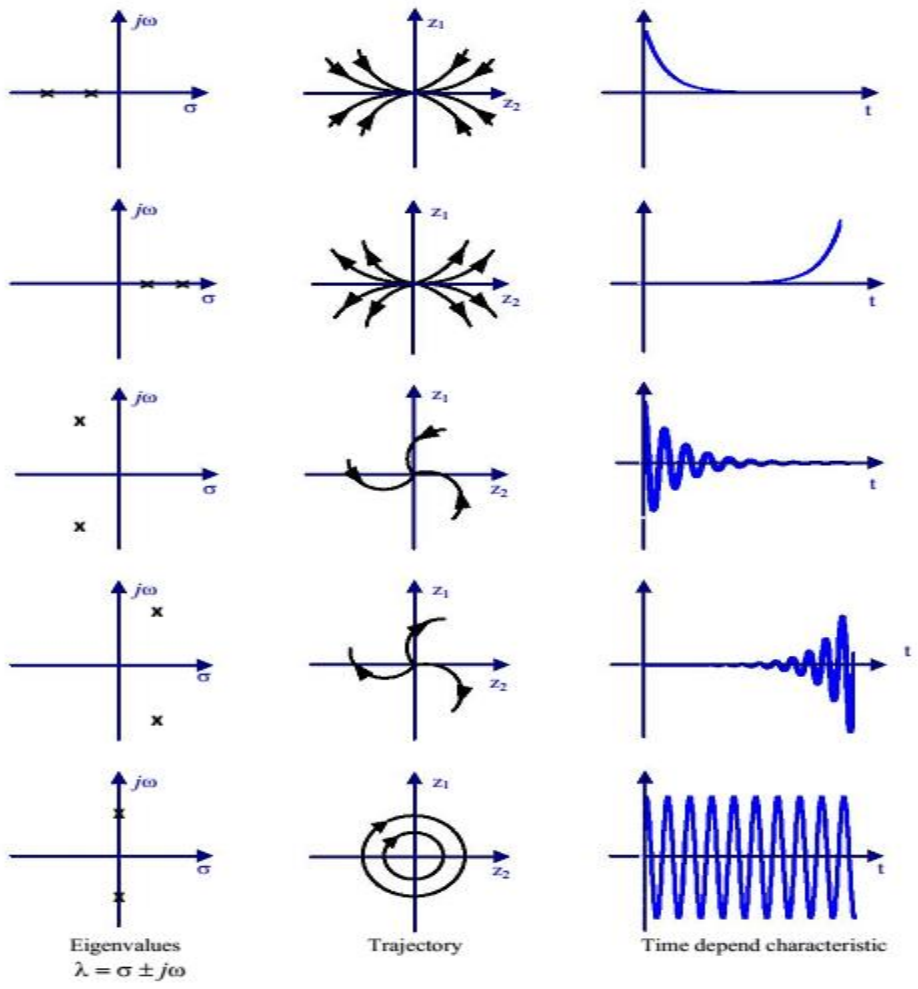

Fig 2.2: Possible combination of eigenvalues pairs (left). Their trajectories (middle) and time responses (right).

2.4.2 Eigenvalues and Eigenvectors Formulation

It can be shown that for any eigenvalue λ, a left and right eigenvector **Ψ** and **Φ** can be calculated, such that

$$\begin{aligned} \mathbf{A}\Phi &= \lambda\Phi \\ \Psi\mathbf{A} &= \lambda\Phi \end{aligned} \qquad (2.18)$$

Φ is a vector with *n* rows and **Ψ** is a vector with *n* columns. According to the upper equation of ((2.11), (2.12)), if no inputs are applied, the system is described by

$$\Delta\dot{x} = \mathbf{A}\Delta x \qquad (2.19)$$

In this equation, the states are coupled, which means that they influence each other. It is hence difficult to draw conclusions with respect to the system behavior. Therefore, the eigenvalues are put onto the diagonal of a matrix Λ, the transposed right eigenvectors are turned into the columns of a matrix **Ψ**, and the left eigenvectors are turned into the columns of a matrix **Φ** [2]**,** after which the following transformation is applied

$$\Delta x = \Phi z \qquad (2.20)$$

Substituting this into equation (2.18) gives

$$\Phi\dot{z} = \mathbf{A}\Phi z \qquad (2.21)$$

When the individual eigenvalues in the upper equation of (2.18) are replaced by the diagonal matrix Λ and both sides of the equations are multiplied the inverse of **Φ**, the following is true

$$\mathbf{A}\Phi = \Phi\Lambda$$
$$\Phi^{-1}\mathbf{A}\Phi = \Lambda \qquad (2.22)$$

Using the second equation together with (2.21), it can be seen that

$$\dot{z} = \mathbf{A}\mathbf{z} \qquad (2.23)$$

Because the matrix Λ is diagonal, it represents *n* uncoupled algebraic equations of the form

$$\dot{z}_i = \lambda_i z_i \qquad (2.24)$$

An equation of this form can be easily transformed back to the time domain, yielding

$$z_i(t) = z_i(o)e^{\lambda_i t} \qquad (2.25)$$

Again using the transformation in equation (2.20) results in

$$\Delta x(t) = \Phi z(t) \qquad (2.26)$$

In which **z** contains the *n* equations as given in (2.25).

This can be written as

$$\Delta x(t) = \sum_{i=1}^{n} \Phi_i z_i(0) e^{\lambda_i t} \qquad (2.27)$$

It can be shown that the inverse of the matrix **Φ**, containing the left eigenvectors as columns, is the matrix **Ψ**, containing the transposed right eigenvectors as columns. Thus, using equation (2.26).

$$z(t) = \Psi \Delta x(t) \qquad (2.28)$$

And with $t = 0$

$$z(0) = \Psi \Delta x(0) \tag{2.29}$$

The scalar product of Ψ_i and $\Delta x(0)$ can be replaced by C_i. With equation (2.28), this results in

$$\Delta x(t) = \sum_{i=1}^{n} \Phi_i C_i e^{\lambda_i t} \tag{2.30}$$

Thus, the time response of the ith state variable is given by

$$\Delta x_i(t) = \Phi_{i1} c_1 e^{\lambda_1 t} + \ldots + \Phi_{in} c_n e^{\lambda_n t} \tag{2.31}$$

And it has been shown that the eigenvalues of the linearized system matrix determine the time domain response of the system to a perturbation, as was the aim of this discussion. If the eigenvalues are complex, in the case of real physical systems they always occur in pairs that are complex conjugates. Therefore, the imaginary parts cancel each other and equation (2.31) is real.

Equation (2.31) clearly illustrates the well-known fact that the real part of an eigenvalue has to be negative for a system to be stable [98].

2.5 Damping Ratio and Oscillation Frequency

For the eigenvalues $\lambda = \sigma \pm j\omega$ of matrix **A** the damping ration ζ is defined as

$$\zeta_i = -\frac{\sigma}{\sqrt{\sigma_i^2 + \omega_i^2}} \tag{2.32}$$

With $\zeta \in [-1,1]$.

The damping ratio ζ determines the rate of decay of the amplitude of the oscillation. The time constant τ of the amplitude decay is $\tau = 1/|\sigma|$ [98, 115].

The mechanical part of a synchronous system is intrinsically prone to weakly damped oscillations, it doesn't affect the rotor speed oscillations. Therefor the damping of rotor speed oscillations come from damper winding, the controllers of the machines and the rest of power system. However, the lower the frequency the less damping is provided by the damper windings. Because power system oscillations have frequencies in the order of few Hz and lower and rather a small amplitude, so hardly any damping is provided by damper windings. Leaving the controllers and the rest of the power system as the main contributors to the damping of the rotor speed oscillations.

Small signal stability is strongly related to the damping of system oscillations, which is discussed by several researchers [116-119].

The oscillation frequency f of the i^{th} mode, in Hz, is defined as:

$$f_i = \frac{\omega}{2\pi} \qquad (2.33)$$

2.6 Participation Factors

Participation factors are non-dimensional scalars that measure the relative contribution of system modes to system states, and of system states to system modes, for linear system.

Participation factors helps us to obtain the influence of state on modes, because then we will know which states machines should be controlled in order to increase damping of a certain problem.

The participation matrix $\mathbf{P_f}$, proposed in [120-121] is defined as:

$$\Psi_{jk}^{T}\Phi_{jk} = \begin{bmatrix} \Psi_{1j} & \Psi_{2j} \dots \Psi_{nj} \end{bmatrix} \begin{bmatrix} \Phi_{j1} \\ \Phi_{j2} \\ \Phi_{j3} \\ \Phi_{j4} \end{bmatrix} \tag{2.34}$$

We may express the above vector product as a summation.

$$\Psi_{jk}^{T}\Phi_{jk} = \sum_{j=1}^{n} \Psi_{kj}\Phi_{jk} \tag{2.35}$$

After some steps [] we will obtain

$$\xi_k = \left[\Psi_{ki}^{T} x_j(0) \right] \left[\sum_{j=1}^{n} \Psi_{kj}\Phi_{jk} \right] e^{\lambda_k t} \tag{2.36}$$

Now we are in a position to make a definition of participation factor

$$p_{jk} = \Psi_{kj}\Phi_{jk} \tag{2.37}$$

Substitution of eq. (2.36) in eq. (2.37) results.

$$\xi_k = \left[\Psi_{ki}^{T} x_j(0) \right] \left[\sum_{j=1}^{n} p_{fjk} \right] e^{\lambda_k t} \tag{2.38}$$

The participation factor P_{fjk} indicates the participation (influence) of the j^{th} state in the k^{th} mode. The participation factor is extremely useful. Consider that through eigenvalue calculation and/or time-domain simulation it is learnt that mode k is a "problem mode," i.e., it is marginally damped or negatively damped. Then one can identify what to do about this is by inspecting the participation

factors for this mode. Before going to do the analysis of DFIG system, it is necessary to build up a model of DFIG. This has been described in chapter 3.

CHAPTER 3

Wind Turbine

A wind turbine is a revolving machine that convert the kinetic wind energy into electrical energy through squirrel-cage induction generator (SCIG) or doubly fed induction generator (DFIG) and then fed into grid. In a wind turbine two conversion process take place. The kinetic energy is first converted into mechanical energy. Next, that mechanical energy is converted into electrical energy. Wind turbines can be either constant speed or variable speed generator. In this thesis only variable speed wind turbines connected to DFIG will be considered.

3.1 Basic Component of Wind Turbine

The main mechanical and electrical components of a wind turbine system are shown in figure 3.1. A typical horizontal axis wind turbine (HAWT) is made up of the following parts: rotor, drive train, nacelle, mainframe, tower and foundation. The rotor is formed by blades and hub and this part is responsible to extract the wind energy and convert it into mechanical energy. For drive train, it is formed by brakes, low-speed shaft, gearbox, electrical generator, and high-speed shaft. This group is using the mechanical energy from the rotor and converts it into electricity through the electrical generator. For nacelle and main-frame, they are formed by housing, bedplate, and yaw system. Also, the transformer and power electronics converters can be added to last group if possible. The yaw system is used to allow the rotor facing the wind direction to extract maximum power [122].

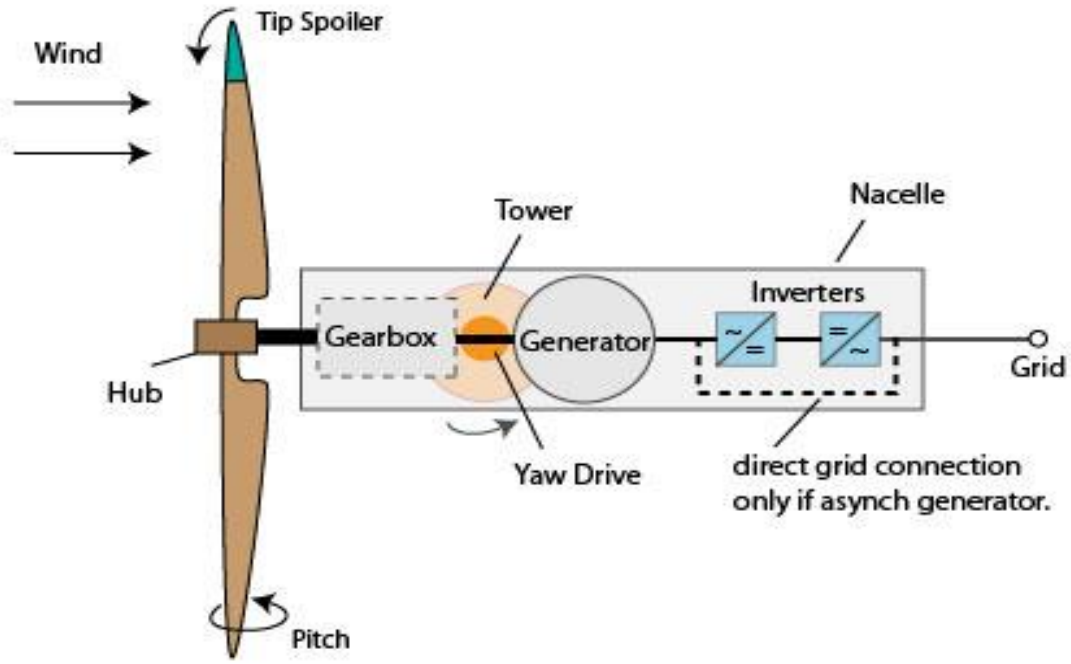

Fig.3.1: Components of a wind turbine-generator system

In this chapter, a general introduction to the wind turbine is given, in which a wind energy conversion is discussed briefly. Second, fixed speed wind turbine connected to SCIG and variable speed wind turbine connected to DFIG are discussed. Third variable speed wind turbine is compensate of complex model, each model is named and derived individually. At last a DFIG expressed in DQO-dqo reference frame, and its state-space model is developed and linearized.

3.2 General Survey of Wind Turbine Topologies

Wind turbines can operate either with a fixed speed or a variable speed. Fixed-speed operation is generally associated with smaller turbines whereas variable speed operation is associated with largest machines.

3.2.1 Fixed Speed Wind Turbine

A fixed-speed wind turbine with a squirrel cage induction generator is the simplest electrical topology in a wind turbine concept. The schematic structure of the fixed speed wind turbine equipped with squirrel cage induction generator (SCIG) is illustrated in Figure 3.2.

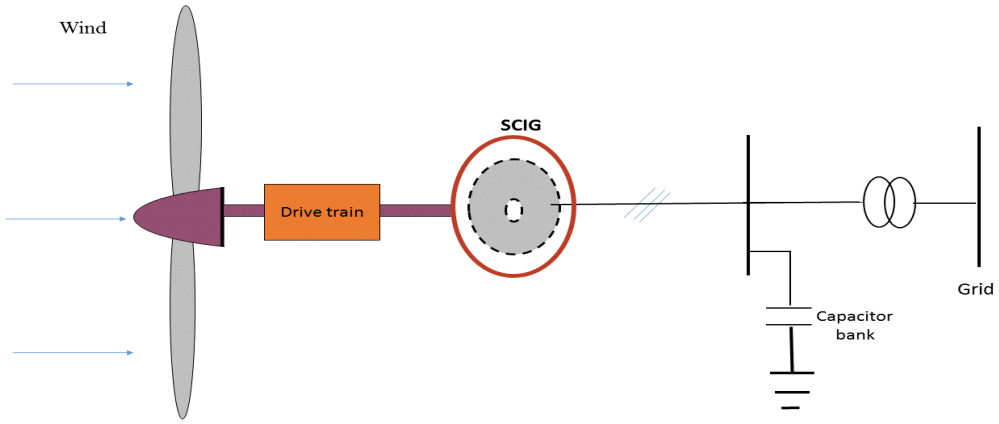

Fig.3.2: Squirrel cage induction generator based wind turbine

As it is shown in figure 3.2, a fixed speed wind turbine is equipped with the SCIG that is directly connected to grid, with a soft-starter and a capacitor bank for reducing reactive power compensation.

They are designed to achieve maximum efficiency at one particular wind speed. In the fixed speed wind turbine the generator slip varies slightly depending on the amount of power generated and so is not entirely constant. The rotor speed variations are in the order of 1 to 2% [2, 123].

Fixed speed wind turbine uses one of the most common machines in power systems. Because of its simple construction, it is cheap, robust and easy to maintain. However it does experience mechanical stresses in its drive train [124], and because of its lack of power electronics, cannot deliver a steady output power to the grid or contribute reactive power which is important for

voltage stability. In this type of turbine the power control is done by stall and pitch control which allow reducing the aerodynamic efficiency of the rotor [125].

3.2.2 Variable-Speed Wind Turbine

During the past few years the variable-speed wind turbine has become the dominant type among the installed wind turbines.

Variable-speed wind turbines are designed to achieve maximum aerodynamic efficiency over a wide range of wind speeds. Within variable-speed operation, it is possible continuously to adapt (accelerate or decelerate) the rotational speed ω of the wind turbine according to the wind speed v. This way, the tip speed ratio λ ($\lambda = \omega R/v$ $\therefore$ R is the radius of the rotor) is kept constant at a predefined value that corresponds to the maximum power coefficient [3]. Contrary to a fixed-speed system, a variable speed system keeps the generator torque fairly constant and the variations in wind are absorbed by changes in the generator speed. The electrical system of a variable-speed wind turbine is more complicated than that of a fixed-speed wind turbine. The configuration of a variable speed wind turbine equipped with a DFIG is given in the figure 3.3.

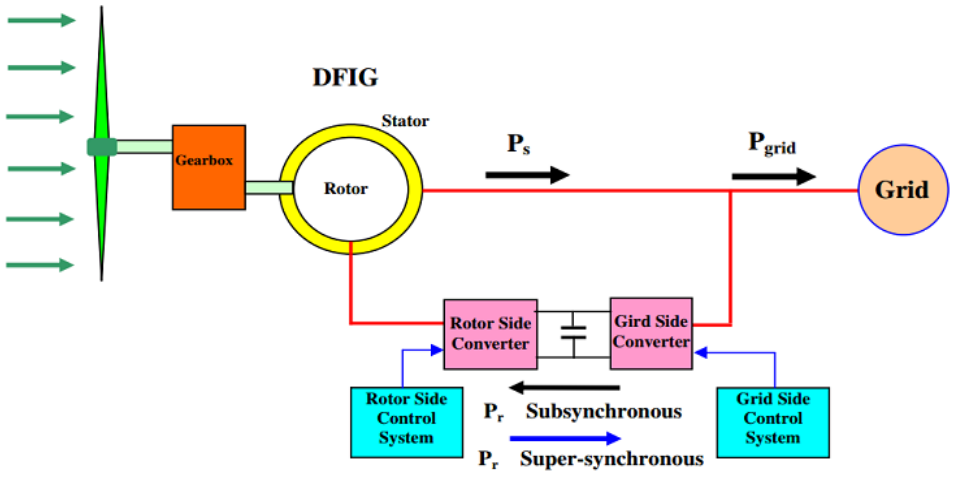

Fig. 3.3: Doubly-fed induction generator connected to grid

The stator phase windings of the doubly-fed induction generator (DFIG) are directly connected to grid, while the rotor phase windings are connected to a bidirectional power converter via slip rings to take current into and out of the rotor. The bidirectional power converter consists of two converters, i.e., grid side converter and rotor side converter, and between the two converters a dc-link capacitor is positioned [2, 123]. The main objective for the grid-side converter is to keep the variation of the dc-link voltage small. With control of the rotor side converter, it is possible to control the torque, the speed of the DFIG as well as its active and reactive power at the stator terminals.

Since the back-to-back power converters could be operated in bi-directional mode, the DFIG could thus be operated either in sub-synchronous speed mode or super synchronous speed mode. Here, the speed range for the DFIG is around ±30% of the synchronous speed [126]. The advantages of variable-speed wind turbines are an increased energy capture, improved power quality and reduced mechanical stress on the wind turbine. The disadvantages are losses in power electronics, the use of more components and the increased cost of equipment because of the power electronics converter.

In this thesis, the model of the variable speed wind turbine with a DFIG is developed in a Matlab coding environment.

3.3 Model Development of Variable Speed Wind Turbine

Variable speed wind turbines are complex electromechanical devices and incorporate a large number of controls. In order to tackle complexity, wind turbines can be thought of as a collection of subsystems which can be modeled individually. The individual subsystem models can then be

assembled into a complete wind turbine model. From a modeling standpoint, variable speed wind turbine consists of the following mechanical and electrical subsystems:

- Aerodynamic model for rotor;
- Mechanical two-mass model for drivetrain;
- Pitch controller;
- Doubly fed induction generator model;
- Rotor-side converter;
- Grid-side inverter;
- Unit transformer and grid representation

The interaction between each of the components listed above determines the variable speed wind turbine models steady-state and dynamic response. Modeling of the aerodynamics and mechanical derive-train is based on the differential and algebraic equations that describe their operation.

3.3.1 Aerodynamic Model

The aerodynamics of a wind turbine is normally described by dimensionless coefficients, which define the wind turbine ability to convert kinetic energy of moving air into mechanical power $\mathbf{C_P}$ or torque $\mathbf{C_q}$ [4] both coefficients $\mathbf{C_P}$ and $\mathbf{C_q}$ depends on the constructive aspects of the VSWT blades and they are nonlinear functions of pitch angle β, yaw angle θ and a parameter known as tip-speed ration λ, which is defined for the ith blade of VSWT

$$\lambda_i = \frac{R\omega_i}{\nu_i} \tag{3.1}$$

Where ω_i is the rotation of the VSWT ith blade admitting that the VSWT is always aligned with

the wind direction (θ=0), the aerodynamic power and torque developed in the wind turbine is given by [127- 130]

$$T_a = \tfrac{1}{2}\rho\pi R^3 \frac{C_P(\lambda_i,\beta)}{\lambda_i} v_i^2 \tag{3.2}$$

The aerodynamic power is calculated by

$$P_a = T_a \omega_i \tag{3.3}$$

By manipulating eq. (3.2) into eq. (3.3) we get the below expression

$$\therefore \quad A = \pi R^2 \qquad\qquad P_a = \tfrac{1}{2}\rho A C_q(\lambda_i,\beta) v_i^3 \tag{3.4}$$

Where ρ is the air density, *A* is the rotor surface, v_i is the wind speed and R is the rotor radius. The power coefficient depends of aerodynamic turbine design and his value never is greater than a theoretical maximum value of 0.593, called Betz limit.

Based on [130] for VSWT, the coefficient $\mathbf{C}_p$ (λ, β) is calculated as shown below.

$$\frac{1}{\lambda_i} = \frac{1}{\lambda + 0.08\beta} - \frac{0.035}{\beta^3 + 1} \tag{3.5}$$

With λ as given by equation 3.2

$$C_P(\lambda,\beta) = c_1\left(\frac{c_2}{\lambda} - c_3\beta - c_4\right)e^{\frac{c_5}{\lambda_i}} + c_6\lambda \tag{3.6}$$

The code of above equations are written under Matlab simulation software help to plot the characteristic of Cp as well as the power generated shown in figure 3.4 and 3.5 respectively.

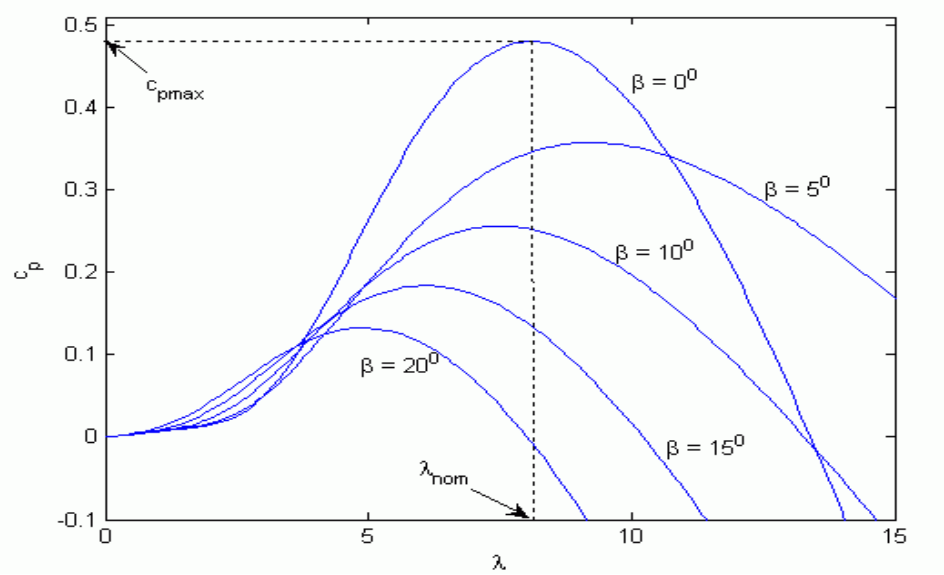

Fig. 3.4: Power coefficients versus tip speed ratio

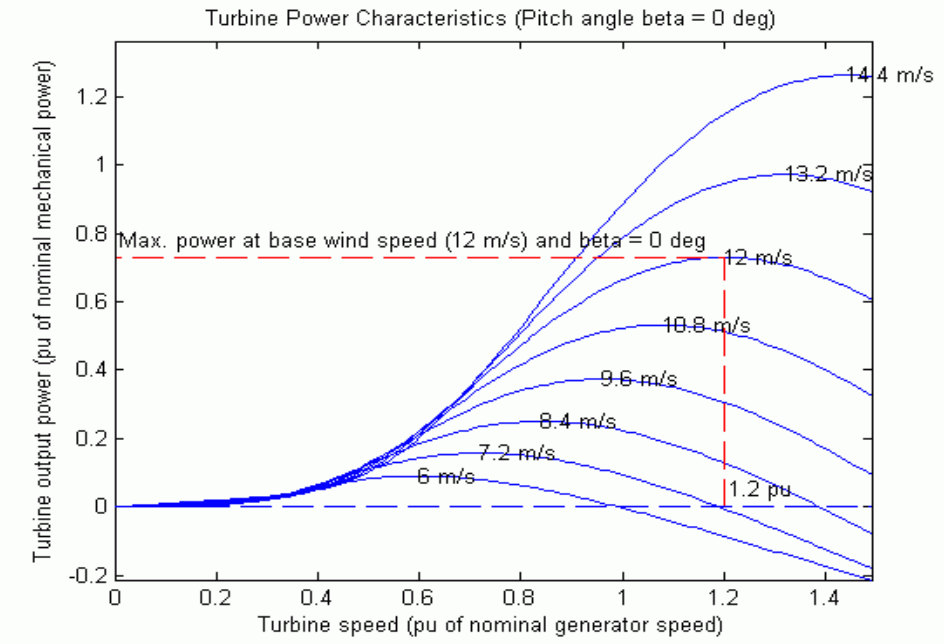

Fig. 3.5: Wind turbine output power vs rotational speed, with wind speed as parameter.

3.4 Drive Train

It has been reported that for stability analysis of WTGSs a multi-mass drive train model is such as six-mass drive train, 3-mass drive train or 2-mass drive train is needed. However, the six-mass drive train model increase the simulation time due to the complex and lengthy mathematical computation with small time-steps, therefore for small signal analysis of variable speed wind turbine with doubly fed induction generator (DFIG) a two-mass model drive train is used for simplicity and controller design[10,131]. The complete structure of two mass model of drive train is consist of turbine, low-speed shaft, gearbox , high-speed shaft and DFIG as it has been shown in the figure 3.6.

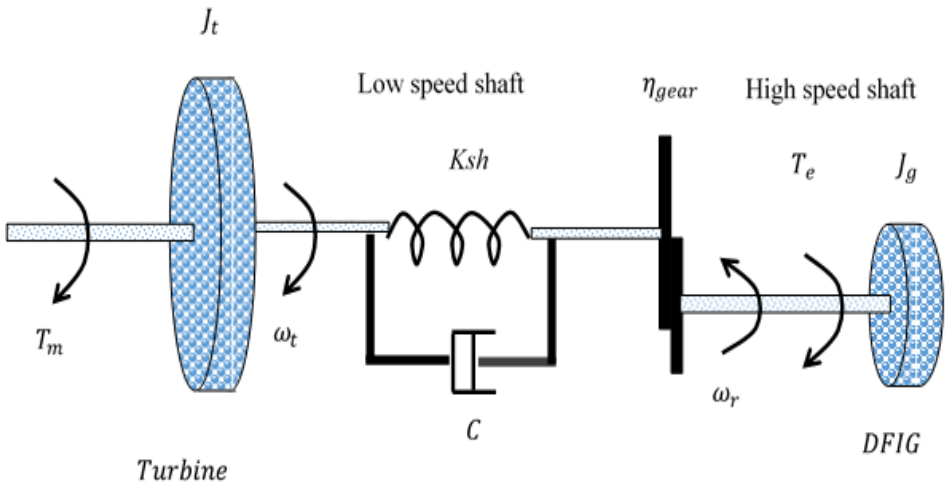

Fig. 3.6: Two mass model drive train with gear

If $K'_{ls} = K_{ls} / n_{gb}^2$ is the low-speed shaft stiffness referred to the high-speed side, the high-speed side can be considered rigid respect to the low-speed shaft, since the gear ratio for machines rated between 300 kW and 2000 kW (with higher rotational speeds between 48 and 17 r.p.m.) is between about 1:31 and 1:88 [132].

Thus, one of the masses is related to the wind turbine (low-speed shaft) representing the lumped-mass of hub and blades, while the second mass represents the equivalent shaft, the high-speed shaft, in which gearbox and generator inertia are lumped together. The shaft stiffness in figure 3.7 is represented by K_{sh} and c is the mutual damping representing balancing dynamics that occur because of different speed between the generator rotor and the turbine shaft. It should be mentioned that the gearbox of the wind turbine represents a low mechanical stiffness K_{sh}, therefore, the two-mass model is used to preserve correctly the drive train dynamics [131].

In the two-mass model of VSWT drive train only the low speed shaft of the turbine needs to be included, because its resonance frequency is about 2 Hz and hence well within the bandwidth of interest, 0.1-10 Hz. The resonance frequencies of the gearbox and high speed shaft are much higher and therefore these are assumed to be infinitely stiff [2-133], thus we can simplify figure 3.7 into simple form of two-mass model figure 3.7.

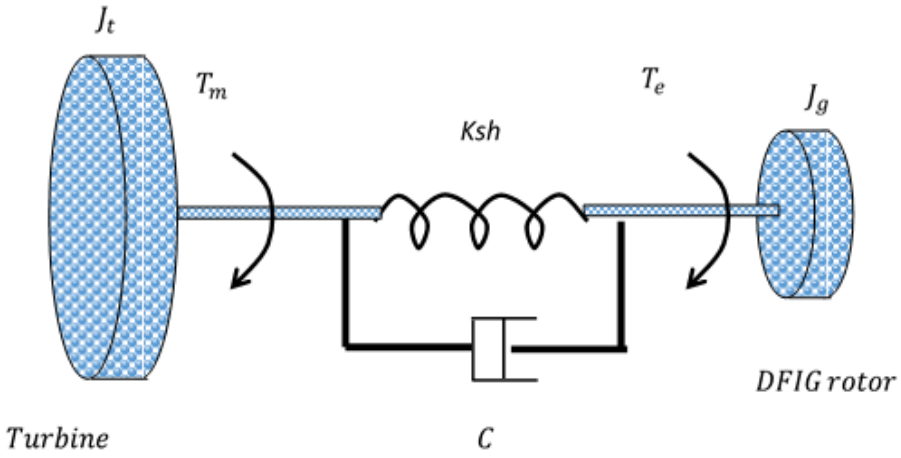

Fig. 3.7: Simple form of two mass model

The dynamics equations for the shaft system can be obtained from Newton's equations of motion for each mass (rotational speed) and shaft (torsion or twist angle) [2,115]

$$J_t \frac{d\omega_t'}{dt} = \left(T_t' - T_{sh}\right) \tag{3.7}$$

$$J_g \frac{d\omega_t'}{dt} = \left(T_{sh} - T_e\right) \tag{3.8}$$

$$\frac{d\theta_{wt}}{dt} = \omega_{eleB}\left(\omega_t' - \omega_g\right) \tag{3.9}$$

Where J_t and J_g are the inertia of the turbine and generator; ω_r and ω_t are the turbine and generator speed; T_t and T_e are the torques of the turbine and generator; θ_{tw} is the shaft torsional angle. All turbine variables (angular speed and torque) are referred to the generator side of the gearbox are denoted by a single prime.

3.4.1 Per Unit System

Per unit (pu) systems are commonly and traditionally used in many power system simulation programs. Therefore, one is bound to encounter pu systems sooner or later when working with simulation programs for electrical power systems.

Experience shows that the questions relating to pu systems and data interpretation, especially for the mechanical part of the system, are a source of many serious misunderstandings, problems and errors – e.g. when an (electrical) engineer must convert manufacturer (mechanical) information into valid data in a simulation program. For that reason we will describe this in more detail here, even though it, theoretically, seems to be basic knowledge. This way, we hope to raise awareness of this issue in order to avoid, or at least reduce, pu-related problems.

At first glance, the pu concept may be rather confusing. However, it is nothing more than a definition of a new set of – conveniently and carefully chosen – basic measuring units for the physical quantities that are under consideration. This means that, for example, instead of measuring the power from a wind turbine in watts, kilowatts or megawatts the power may be measured as the percentage of the rated power from the wind turbine. In fact, the power can be measured as the percentage of any other constant power that is suitable to be used for a comparison in a given context. Likewise, all voltages at the same voltage level as the wind turbine generator can be measured as the percentage of the nominal voltage of the wind turbine. These basic 'measuring units' are the base values of the pu system.

Once the most fundamental base values for electrical quantities such as power and voltage have been chosen, it is possible to derive base values for other electrical quantities such as current, resistance and reactance on each voltage level in the system. Power is an invariant quantity at all voltage levels, so it is only possible to choose one base value for power. For voltage, it is possible and necessary to define a base value for each voltage level in the system [98].The per unit value is given by the ratio between the actual value and the base value [98, 3].

$$per\,unit\,value = \frac{actual\,value}{base\,value} \tag{3.10}$$

Now, if the pu system is to be extended to the rotating mechanical system. It becomes necessary to define additional base values, in our case the base speed and base torque are defined to express the drive train system in per unit values.

$$\omega_{tB} = \frac{\omega_{rB}}{\eta_{gb}} \tag{3.11}$$

$$T_{tB} = T_{eB}\eta_{gb} \tag{3.12}$$

Where $\omega_{rB} = \omega_{elB}/\eta_{PP}$ is the base speed of the generator with ω_{elB} the electrical speed equal to $2\pi f$, and η_{PP} the generator's pole-pair number, $T_{eB} = P_{rated}/\omega_{rB}$ is the base of the generator electrical torque and, η_{gb} is the gearbox ratio. With the turbine speed inertia and torque referred to the high-speed shaft by $\omega_t' = \eta_{gb}\omega_t$ $J_t' = J_t/\eta_{gb}^2$ and $T_t' = T_t/\eta_{gb}$ respectively, and the turbine bases. (ω_{tB}, T_{tB}), equation 3.7 in per unit can be written as.

$$\frac{J_t}{n_{gb}^2}\omega_{rB}\frac{\omega_{t_{pu}}}{dt} = T_{eB}\left(T_{t_{pu}} - T_{sh_{pu}}\right) \tag{3.13}$$

And together with the inertia constant of the turbine (in seconds),

$$H_t = \tfrac{1}{2}\frac{J_t\omega_{rB}}{\eta_{gb}^2 T_{eB}} \tag{3.14}$$

Yields to the turbine speed equation,

$$\frac{d\omega_{t_{pu}}}{dt} = \frac{1}{2H_t}\left(T_{t_{pu}} - T_{sh_{pu}}\right) \tag{3.15}$$

Similarly, the rotor generator speed equation (3.8) in per unit form is obtained

$$\frac{d\omega_{g_{pu}}}{dt} = \frac{1}{2H_g}\left(T_{sh_{pu}} - T_{e_{pu}}\right) \tag{3.16}$$

Where the electromagnetic torque, T_{sh} and shaft mechanical torque T_e in per unit, are given in the following equations

$$T_{sh} = K_{sh}\theta_{wt} + c\frac{d\theta_{wt}}{dt} \tag{3.17}$$

$$T_e = \left(\frac{e'_{qs}}{\omega_s}\right) i_{qs} + \left(\frac{e'_{ds}}{\omega_s}\right) i_{ds} \tag{3.18}$$

The shaft torque from equation 3.17 can be expressed in per unit by applying the per unit definition with the stiffness base as $K_B = T_{eB}/(1el.rad)$ and the base damping coefficient as $c_B = T_{eB}/(1el.rad/1s)$.

$$T_{sh_{pu}} = k_{sh_{pu}}\theta_{wt} + c_{pu}\frac{d\theta_{wt}}{dt} \tag{3.19}$$

The equation 3.9 for the equivalent twist angle is expressed in actual units (radians). The equations for the drive train system are summarized below. The system model in this document is assumed to be expressed in per unit notation therefore the subscript 'pu' is omitted, from now on

$$2H_t\frac{d\omega_t}{dt} = \frac{p_t}{\omega_t} - T_{sh} \tag{3.20}$$

$$\frac{1}{\omega_{elB}}\frac{d\theta_{tw}}{dt} = \omega_t - \omega_r \tag{3.21}$$

$$2H_g\frac{d\omega_r}{dt} = T_{sh} - T_e \tag{3.22}$$

Where

H_t The inertia constant of the turbine;

H_g The inertia constants of the generator;

P_t The turbine input power;

T_{sh} The shaft torque;

T_e The generator torque;

ω_t The wind turbine angle speed;

3.5 Electrical System of VSWTs Provided With DFIG

Along with the mechanical drive train, the electrical system is a fundamental part of a wind turbine. The electrical system comprises the components necessary to convert the mechanical energy into electric power, including electrical auxiliaries and control systems.

The electrical generator is the main component for the mechanical/electrical energy conversion process in a wind turbine. The wind turbine model studied in this thesis is illustrated in figure 3.3. In this system the wind turbine is connected to the DFIG through a drive train system, which consist of a low and a high speed shaft with a gearbox in between. The DFIG is a wound rotor induction type generator in which the stator windings are directly connected to the three-phase grid and the rotor windings are fed through three phase back-to-back converters. The back-to-back converter consist of three parts: a Rotor Side Converter (RSC), a Grid Side Converter (GSC) and a dc link capacitor placed between the two converters. The controller also consist of three parts: rotor side controller, grid side controller and wind turbine controller. The function of these controllers are to produce smooth electrical power with constant voltage and frequency to the

power grid whenever, the wind system is working at sub-synchronous speed or super-synchronous speed, depending on the velocity of the wind. Here the vector control strategy is employed for the RSC to achieve decoupled control of active and reactive power.

The main features of DFIGs are:

- The range of rotational speed can be −40% up to +30% of the synchronous speed [3].
- The frequency converter is rated at approximately 30% of the rated generator power [3, 134].
- The grid frequency (electrical) and the rotor speed (mechanical) are decoupled [136, 17].
- The power is supplied from the stator to the power network and provided or absorbed from the grid through the rotor circuit.

Likewise, the controllability of the electrical system is an important aspect linked to the energy quality of the power system and plays an important role to ensure its security and stability.

3.5.1 Model of DFIG

For the purpose of better understanding and designing control schemes in VSWTs generator system, it is necessary to know the dynamic model of the machine subjected to control. A model of the electrical machine which is adequate for designing the control system must preferably incorporate all the important dynamic effects occurring during steady state and small signal operation analysis [136]. It should be valid for any arbitrary time variations of the voltages and currents generated by the converters which supplies the machine. In this section, such a model which is valid for any instantaneous variations of the voltages and currents, and can adequately describe the performance of the system under stability of small signal analysis will be developed in dqo reference frame.

3.5.2 D-Q Theory

The d-q theory is also known as reference frame theory. R.H .Park proposed a new theory to overcome the problem of time varying parameters with the ac machine. He built a transformation matrix which is called park's transformation. Its function is to change time varying ac quantities into time independent quantities. Next we will apply parks transformation in DFIG modeling.

3.5.3 Transformation of Three Phase abc To Two Phase dq Axes

Consider a symmetrical three phase induction machine with stationary a-phase, b-phase and c-phase axes are placed at $120°$ angle to each other as shown in figure (3.8). The main target is to transform the three phase stationary frame variables into two phase stationary frame variables (d-q) and transform these to synchronously rotating reference frame variables (d-q).

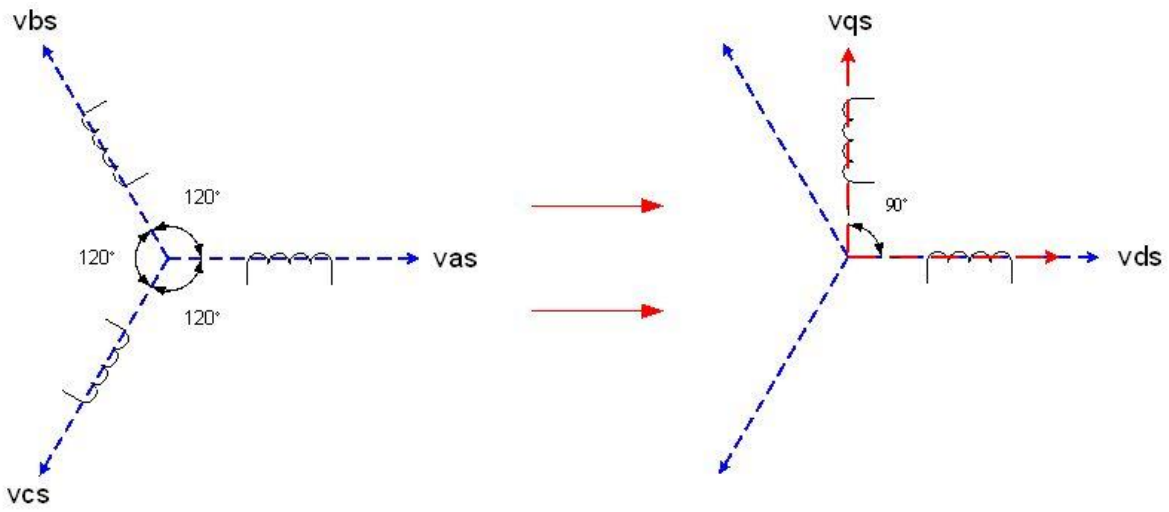

Fig. 3.8: Transformation of three phase ABC to two phase DQ frame

3.6 Stator and Rotor Winding Equations of DFIG in abc Form

As the machine is working in generator mode, positive currents are flowing out of it. The sign of the self-flux linkage produced by current in a circuit is the same as that of the current. The polarity

of the voltage induced by changing flux is so that it results in a current that opposes the change (Lenz's law).for positive current, voltage and flux directions as shown in figure 3.9.

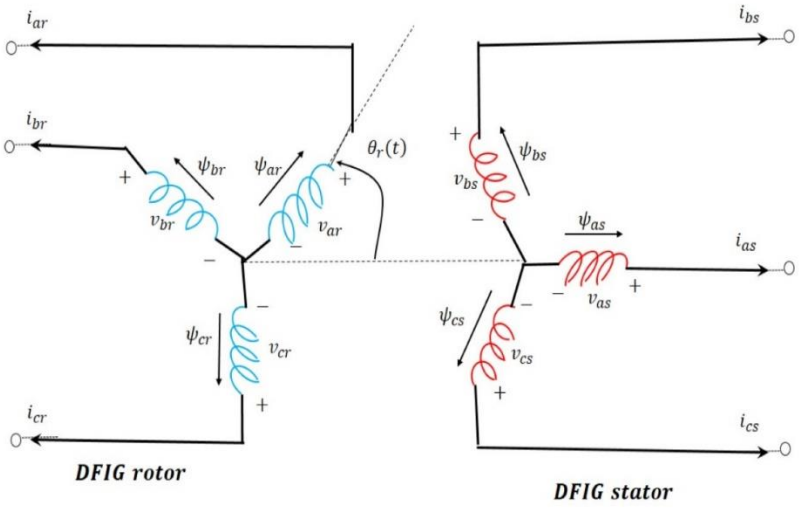

Fig. 3.9: Definition of positive current, voltage and flux directions

Depending on stator and rotor windings, the voltage dynamics of the machine can be described by applying the Kirchhoff voltage law to figure 3.10. It gives:

$$v_{as}(t) = -\frac{d}{dt}\psi_{as}(t) - R_s i_{as}(t) \tag{3.23}$$

$$v_{bs}(t) = -\frac{d}{dt}\psi_{bs}(t) - R_s i_{bs}(t) \tag{3.24}$$

$$v_{cs}(t) = -\frac{d}{dt}\psi_{cs}(t) - R_s i_{cs}(t) \tag{3.25}$$

$$v_{ar}(t) = -\frac{d}{dt}\psi_{ar}(t) - R_r i_{ar}(t) \tag{3.26}$$

$$v_{br}(t) = -\frac{d}{dt}\psi_{br}(t) - R_r i_{br}(t) \tag{3.27}$$

$$v_{cr}(t) = -\frac{d}{dt}\psi_{cr}(t) - R_r i_{cr}(t) \tag{3.28}$$

where $v_{as}(t)$, $v_{bs}(t)$, $v_{cs}(t)$ are the dynamic stator voltages of phases *a*, *b*, *c*; $i_{as}(t)$, $i_{bs}(t)$ $i_{cs}(t)$ are the stator phase currents of phases a, b and c; $\psi_{as}(t)$, $\psi_{bs}(t)$, $\psi_{cs}(t)$ are the stator flux linkages and, R_s is the stator resistance. Similar definitions are applied to the rotor.

Stator and rotor flux linkages are produced by the currents flowing through the windings. By assuming symmetrical stator, and rotor structures and a balanced system $(i_{as} + i_{bs} + i_{cs} = 0)$, the flux linkages are given by

$$\psi_{as} = \left(L_{self,s} + L_{leak,s}\right) i_{as} + L_{mut,s}\left(i_{bs} + i_{cs}\right) + \ldots$$
$$L_{sr}\left(\cos\theta_r i_{ar} + \cos(\theta_r + \frac{2\pi}{3}) i_{br} + \cos(\theta_r - \frac{2\pi}{3}) i_{cr}\right) \tag{3.29}$$

$$\psi_{bs} = \left(L_{self,s} + L_{leak,s}\right) i_{bs} + L_{mut,s}\left(i_{as} + i_{cs}\right) + \ldots$$
$$L_{sr}\left(\cos(\theta_r - \frac{2\pi}{3}) i_{ar} + \cos\theta_r i_{br} + \cos(\theta_r + \frac{2\pi}{3}) i_{cr}\right) \tag{3.30}$$

$$\psi_{cs} = \left(L_{self,s} + L_{leak,s} \right) i_{bs} + L_{mut,s} \left(i_{as} + i_{bs} \right) + \ldots$$
$$L_{sr} \left(\cos(\theta_r + \frac{2\pi}{3}) i_{ar} + \cos(\theta_r - \frac{2\pi}{3}) i_{br} + \cos\theta_r i_{cr} \right) \qquad (3.31)$$

$$\psi_{ar} = \left(L_{self,r} + L_{leak,r} \right) i_{ar} + L_{mut,r} \left(i_{br} + i_{cr} \right) + \ldots$$
$$L_{rs} \left(\cos\theta_s i_{as} + \cos(\theta_s + \frac{2\pi}{3}) i_{bs} + \cos(\theta_s - \frac{2\pi}{3}) i_{cs} \right) \qquad (3.32)$$

$$\psi_{br} = \left(L_{self,r} + L_{leak,r} \right) i_{br} + L_{mut,r} \left(i_{ar} + i_{cr} \right) + \ldots$$
$$L_{rs} \left(\cos(\theta_s - \frac{2\pi}{3}) i_{as} + \cos\theta_s i_{bs} + \cos(\theta_s + \frac{2\pi}{3}) i_{cs} \right) \qquad (3.33)$$

$$\psi_{cr} = \left(L_{self,r} + L_{leak,r} \right) i_{cr} + L_{mut,r} \left(i_{ar} + i_{br} \right) + \ldots$$
$$L_{rs} \left(\cos(\theta_s + \frac{2\pi}{3}) i_{as} + \cos(\theta_s - \frac{2\pi}{3}) i_{bs} + \cos\theta_s i_{cs} \right) \qquad (3.34)$$

where $\theta_r = \theta_r(t)$ is the angle between the stator-axis (stationary) and rotor-axis (rotationary) as shown on figure 3.10; $L_{slef,s}$ and $L_{leak,s}$ are the self- and leakage inductance of a stator winding, $L_{slef,s}$ and $L_{leak,s}$ are the self and leakage inductance of a rotor winding respectively; $L_{mut,s}$ is the mutual inductance between two stator windings, $L_{mut,r}$ is the mutual inductance between two rotor winding and L_{rs}, L_{sr} is the peak value of the mutual inductance between stator and rotor windings.

3.7 Transformation Matrix

For easier control and simulation purposes, the dynamic equation of a three-phase DFIG can be represented in the d-q variables. In matrix notation, we have:

$$v_{qdo} = T_\theta v_{abc} \tag{3.35}$$

Where

$$v_{qdo} = \begin{bmatrix} v_q \\ v_d \\ v_0 \end{bmatrix}, v_{abc} = \begin{bmatrix} v_a \\ v_b \\ v_c \end{bmatrix}$$

$$T_\theta = \sqrt{\frac{2}{3}} \begin{bmatrix} \sin\theta & \sin(\theta - 2\pi/3) & \sin(\theta + 2\pi/3) \\ \cos\theta & \cos(\theta - 2\pi/3) & \cos(\theta + 2\pi/3) \\ 1/\sqrt{2} & 1/\sqrt{2} & 1/\sqrt{2} \end{bmatrix}$$

T_θ is the abc-to-dq transformation matrix. In this thesis, the power invariant transformation is chosen, and the d-axis is leading the q-axis [101]. Figure 3.11 shows the dq-frame with respect to the stator 3-axis frame. It should be noted that v_0 is the zero component of v_{qdo} and during the balanced system v_0 is equal to zero.

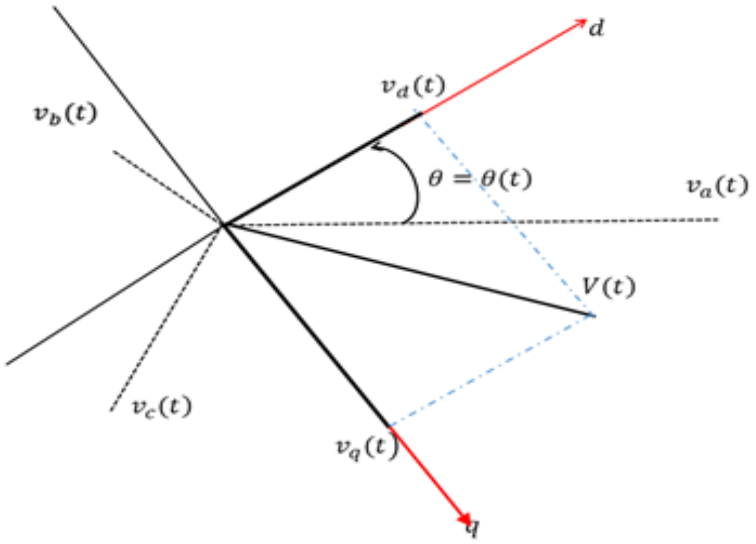

Fig. 3.10. dq-frame with respect to stator abc-frame

3.8 DFIG Equations in dq-Form

By applying the transformation to equations 3.23-3-28 we will get the DFIG dq-model.

$$v_{qs}(t) = -\frac{d}{dt}\psi_{qs}(t) - R_s i_{qs}(t) + \omega\psi_{ds}(t) \tag{3.36}$$

$$v_{ds}(t) = -\frac{d}{dt}\psi_{ds}(t) - R_s i_{ds}(t) - \omega\psi_{qs}(t) \tag{3.37}$$

$$v_{qr}(t) = -\frac{d}{dt}\psi_{qr}(t) - R_r i_{qr}(t) + (\omega - \omega_r)\psi_{dr}(t) \tag{3.38}$$

$$v_{dr}(t) = -\frac{d}{dt}\psi_{dr}(t) - R_r i_{qr}(t) - (\omega - \omega_r)\psi_{qr}(t) \tag{3.39}$$

With rotor and stator dq fluxes given by

$$\psi_{qs}(t) = L_{ss} i_{qs}(t) + L_m i_{qr}(t) \tag{3.40}$$

$$\psi_{ds}(t) = L_{ss} i_{ds}(t) + L_m i_{dr}(t) \tag{3.41}$$

$$\psi_{qr}(t) = L_{rr} i_{qr}(t) + L_m i_{qs}(t) \tag{3.42}$$

$$\psi_{dr}(t) = L_{rr} i_{dr}(t) + L_m i_{ds}(t) \tag{3.43}$$

In equations 3.36 to 39, ω is the rotational speed of the dq-frame, i.e. $\omega = d\theta/dt$ where $\theta = \theta(t)$ is the angle between the d-axis and stator a-axis figure 3.11; and ω_r is the rotational speed of the rotor, i.e. $\omega_r = d\theta_r/dt$ .For the synchronously rotating frame, ω is the synchronous speed. In equation 40-43 $L_{ss} = L_{self,s} + L_{leak,s} - L_{mut,s}$, $L_{rr} = L_{self,r} + L_{leak,r} - L_{mut,r}$ and $L_m = L_{sr}$, respectively.

3.8.1 Per Unit System of DFIG

In order to normalize the electrical system, the power and the voltage are usually chosen as base quantities; that is to say, equal to one per unit under rated condition.

The DFIG model in dq-axis reference frame 36-39 is converted to per unit (pu) values based on nominal voltage, on three phase nominal power of generator and synchronous speed of generator,

$$V_B = \sqrt{3} V_{LLrated} \quad \text{V} \tag{3.44}$$

$$S_B = S_{3\phi,rated} \quad \text{VA} \tag{3.45}$$

$$\omega_B = 2\pi f \quad \frac{el.rad}{\text{sec}} \tag{3.46}$$

Where *f* is the electrical grid frequency in Hz.

Thus, the base current and impedance are defined as

$$I_B = \frac{S_B}{V_B} \ \text{A} \quad , \ Z_B = 3\frac{V_B^2}{S_B} \ \ \Omega$$

The mechanical and electrical speeds are related by the pole-pair number as

$$\omega_{rB} = \frac{\omega_B}{\eta_{pp}} \quad \frac{\text{mech.rad}}{\text{sec}}$$

For the synchronously rotating frame, ω the synchronous speed, thus in [PU] $\omega = \omega_s = 1$ and $(\omega - \omega_r) = (\omega_s - \omega_r) = s\,\omega_s$ where s is slip. With the per-unit definition in equation 3.10, stator and rotor voltage equations of DFIG in *d-q* reference frame equations 3.36-3.39 in per-unit notation can be rewritten as

$$v_{qs} = -\frac{1}{\omega_B}\frac{d}{dt}\psi_{qs} - R_s i_{qs} + \omega\psi_{ds} \tag{3.47}$$

$$v_{ds} = -\frac{1}{\omega_B}\frac{d}{dt}\psi_{ds} - R_s i_{ds} - \omega\psi_{qs} \tag{3.48}$$

$$v_{qr} = -\frac{1}{\omega_B}\frac{d}{dt}\psi_{qr} - R_r i_{qr} + (\omega - \omega_r)\psi_{dr} \tag{3.49}$$

$$v_{dr} = -\frac{1}{\omega_B}\frac{d}{dt}\psi_{dr} - R_r i_{dr} - (\omega - \omega_r)\psi_{qr} \tag{3.50}$$

$$\psi_{qs} = L_{ss} i_{qs} + L_m i_{qr} \tag{3.51}$$

$$\psi_{ds} = L_{ss} i_{ds} + L_m i_{dr} \tag{3.52}$$

$$\psi_{qr} = L_{rr} i_{qr} + L_m i_{qs} \tag{3.53}$$

$$\psi_{dr} = L_{rr} i_{dr} + L_m i_{ds} \tag{3.54}$$

3.10 Converter Model

The back to back HVDC-link converter connected between the DFIG rotor and grid is Figure 3.3. The back-to-back converter is divided into two components: the Rotor-Side Converter (RSC) and the Grid-Side Converter (GSC) with a dc- link capacitor between them in order to keep the voltage variations in the dc-link voltage small. Both of these converters are Voltage-Sourced Converters (VSC) equipped with IGBTs and diodes to synthesize an *ac* voltage from a *dc* voltage source, which enable a bi-directional power flow [68-69]. The VSC is used to convert the *ac* voltage source into the *dc* voltage source and vice versa.

3.11 Conclusion

In this chapter a wind turbine system model with double fed induction generator was presented. The turbine performance was described by means of the energy conversion theory and general considerations regarding simulations for wind turbines in electrical power systems were presented. Simple turbine model assuming fixed sped and variable wind speed were discussed including their advantages and disadvantages. Simple turbine model assuming variable wind speed, rotor speed can be used in studies.

Non-linear algebraic models in which power output is obtained from the wind speed were used in power system small signal stability analysis. The drive train was modelled by the two-mass model approach in order to represent correctly the shaft dynamics. The electrical system model was expressed in per-unit notation and *d-q* reference frame. The converter configuration was described and the machine side controller will be explained with detail in next chapter.

CHAPTER 4

Modelling and Small-Signal Stability Assessment of DIFG Connected To Grid

The seventh order model of gird connected DFIG is first setup and the whole model is formulated by a set of differential algebraic equations (DAE). Then different oscillatory modes are obtained with their eigenvalue, oscillation frequency, damping ratio and participation factor. The results from eigenvalues assessment are presented to demonstrate the small signal stability of power system for improving active and reactive power, finally numerical results offer the better understanding of the DFIG intrinsic dynamics, which can also be useful for control design and model justification.

4.1 Background

Modern life cannot go without electricity. Electricity is mainly generated from fossil fuel like petroleum, natural gas, etc. Because of tremendous demand of electric power, fossil energy is being diminished very quickly. In recent years the environmental pollution has become a major concern in daily life and a possible energy crisis has led to the development of new technologies for generating clean and sustainable energy. Therefore, renewable energy is becoming a viable alternative to meet the crisis. Renewable energy is generally defined as energy that comes from resources which are naturally replenished on a human timescale such as sunlight, wind, rain, tides, waves and geothermal heat. In this thesis wind.

From the above renewable energy sources wind energy is one of the most competitive and efficient renewable energy sources and, as a result, its use is continuously increasing. At present, the

capacity of the installed wind power in the world is stood at 336'327 MW [137]. With the growing penetration of wind power into gird, the effective inertia of power networks reduces [138]. Thus, the impact of wind turbine's generator, on power system stability is of increasing concern, and the dynamics of wind turbines generator should be carefully considered in power system stability.

Traditionally, the oscillatory behavior of power systems has been controlled by the electromechanical interactions between the synchronous generators through the network [115]. Several papers and researcher's experience have been shown that by using induction generator the generation of wind power from the wind energy conversion system increasing significantly. Now the important thing is to analyze the impact of this kind of asynchronous generation on the system stability and vice versa.

The dynamic behavior of the doubly fed induction generator (DFIG) has been investigated by various authors. The majority of these studies are based on time-domain simulations to show the impact on power system dynamics [2,139], the performance of small-signal stability analysis of a grid connected DFIG under decoupled P-Q control and maximum power tracking [140], the response to grid disturbance [141], the ride-through behavior of DFIG during a voltage dip [142], the controlling strategies to make the DFIG behave as a synchronous generator [143], small signal stability assessment of DFIG including series dynamic breaking resistor (SDBR)[144]etc. Time-domain studies propose a direct appreciation of the dynamic behavior of DFIG in terms of visual clarity. However, they are not able to identify and quantify the cause and nature of interactions and problems [115]. Study of eigenvalue and participation factor enables the identification of the stability scenario of a dynamic system.

In this thesis the grid-connected DFIG is studied which has been explained in 3rd chapter with detail and the single-machine infinite-bus (SMIB) approach is followed.

The small signal stability of a DFIG based wind turbine has been assessed under different operating modes [115,145]. However the study was carried out using the 5th order model of the induction generator and the control representation was simplified and based on decoupled vector control principles.

To assess the small signal stability more accurately, this study uses a full 7th order DFIG model. The model comprises the drivetrain, the DFIG and its associated back to back HVDC link and its associated controls.

This study is particularly useful to check the stability of DFIG itself and also for control design and model justification

4.2 Modeling

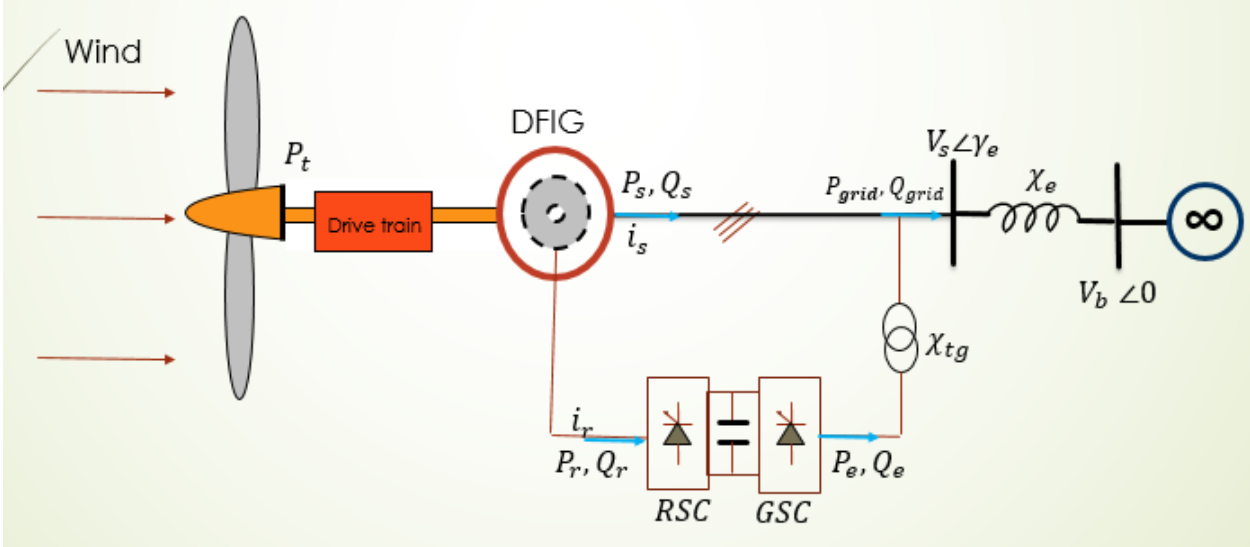

Fig. 4.1: Grid-connected WECS with DFIG [25]

The single machine infinite-bus (SMIB) model studied in this thesis is illustrated in figure 4.1. In this system the wind turbine is connected to the DFIG through a drive-train system. The DFIG system is an induction type generator in which the stator winding are directly connected to the grid

and rotor winding are fed through back to back IGBT based PWM converter . The DFIG model has been explained in detail in 3rd chapter. The model of DFIG is overviewed here for better understanding.

The turbine power P_t is transformed in to electrical power via DFIG and the produced power from DFIG to grid in the stator winding is always positive P_S. Using the back-to-back converter allows bidirectional power flows and hence the rotor power P_r can be positive and negative. This allows the machine to operate at both sub-and super synchronous speeds [140, 146].

4.3 Wind Turbine Based DFIG

The wind turbine is structured from blades and hub. It's a revolving machine that convert the kinetic wind energy into electrical energy through generator squirrel-cage induction generator (SCIG) or doubly fed induction generator (DFIG) and then fed into grid. In a wind turbine two conversion process take place. The kinetic energy is first converted into mechanical energy. Next, that mechanical energy is converted into electrical energy. For stability studies of wind turbine an algebraic model is used and the dynamics related to turbine, yaw system, and tower can be ignored [115, 12, 147].which is explained and simulated in matlab software in 3rd chapter of this thesis.

4.4 Model for Drive Train

The drive train system consist of turbine, a low and a high speed shaft, and a gear box. For small signal stability analysis of VSWTs equipped with DFIG, a two mass drive train model [115, 148] is considered and the dynamics can be expressed by the following differential equations .it may be mentioned that the drive train model is defined and derived in chapter 3 with more details.

$$2H_t \frac{d\omega_t}{dt} = \frac{p_t}{\omega_t} - T_{sh} \tag{4.1}$$

$$\frac{1}{\omega_{elB}} \frac{d\theta_{tw}}{dt} = \omega_t - \omega_r \tag{4.2}$$

$$2H_g \frac{d\omega_r}{dt} = T_{sh} - T_e \tag{4.3}$$

$$T_{sh} = K_{sh}\theta_{wt} + c\frac{d\theta_{wt}}{dt} \tag{4.4}$$

$$T_e = \left(\frac{e'_{qs}}{\omega_s}\right) i_{qs} + \left(\frac{e'_{ds}}{\omega_s}\right) i_{ds} \tag{4.5}$$

Where

H_t The inertia constant of the turbine;

H_g The inertia constants of the generator;

ω_t The wind turbine angle speed;

ω_r The generator rotor angle speed;

θ_{tw} The shaft twist angle;

K_{sh} The shaft stiffness coefficient;

c The damping coefficient;

T_{sh} The shaft torque;

T_e The generator torque;

p_t The turbine input power (here assumed as constant);

ω_{elB} The electrical base speed in (rad/s);

It should be mentioned that all the turbine variables are per unit [pu].

4.5 DFIG Model for Stability Studies

In the case of small signal stability studies variable speed DFIGs are usually represented by Thevenin's equivalent model as a voltage source based on transient impedance [36, 149].

Equations 3.47-3.54 can be rewritten so that the DFIG is represented as shown in figure 4.2

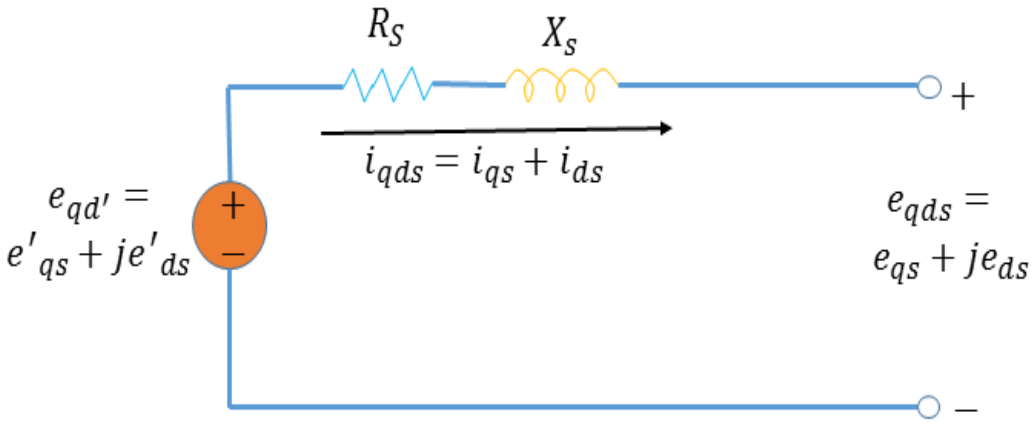

Fig. 4.2: DFIG model for stability studies

This is done by defining the variables

$$e'_{qs} = (L_m / L_{rr})\omega_s \psi_{dr} \tag{4.6}$$

$$e'_{ds} = -(L_m / L_{rr})\omega_s \psi_{qr} \tag{4.7}$$

$$X'_s = \omega_s \left(L_{ss}L_{rr} - L_m^2\right) / L_{rr} \tag{4.8}$$

$$T_r = \omega_s L_{rr} / R_r \tag{4.9}$$

$$K_{mrr} = L_m / L_{rr} \tag{4.10}$$

$$R_1 = R_s + R_2 \tag{4.11}$$

$$R_2 = K_{mrr}^2 R_r \tag{4.12}$$

Now, by manipulation of equations 4.6-4.9 into 3.51-3.54 we will get the following equations,

$$\mathrm{i_{qr}} = -\left(1/\omega_s \mathrm{L_m}\right)\mathrm{e'_{ds}} - \left(\mathrm{L_m}/\mathrm{L_{rr}}\right)\mathrm{i_{qs}} \tag{4.13}$$

$$\mathrm{i_{dr}} = \left(1/\omega_s \mathrm{L_m}\right)\mathrm{e'_{qs}} - \left(\mathrm{L_m}/\mathrm{L_{rr}}\right)\mathrm{i_{ds}} \tag{4.14}$$

$$\psi_{\mathrm{qs}} = -\left(1/\omega_s\right)\mathrm{e'_{ds}} + \left(\mathrm{X'_s}/\omega_s\right)\mathrm{i_{qs}} \tag{4.15}$$

$$\psi_{\mathrm{ds}} = \left(1/\omega_s\right)\mathrm{e'_{qs}} + \left(\mathrm{X'_s}/\omega_s\right)\mathrm{i_{ds}} \tag{4.16}$$

Now after some manipulation and substitution of equations 4.10-4.13 into 3.47-3-50, the DFIG-model in [pu] becomes.

$$\frac{di_{qs}}{dt} = \frac{\omega_{elB}}{\omega_s L'_s}\left(-R_1 i_{qs} + \omega_s L'_s i_{ds} + \frac{\omega_r}{\omega_s} e'_{qs} - \frac{1}{T_r \omega_s} e'_{ds} - v_{qs} + K_{mrr} v_{qr} \right) \tag{4.17}$$

$$\frac{di_{ds}}{dt} = \frac{\omega_{elB}}{\omega_s L'_s}\left(-R_1 i_{ds} - \omega_s L'_s i_{qs} + \frac{\omega_r}{\omega_s} e'_{ds} - \frac{1}{T_r \omega_s} e'_{qs} - v_{ds} + K_{mrr} v_{dr} \right) \tag{4.18}$$

$$\frac{de'_{qs}}{dt} = \omega_{elB}\left(R_2\, i_{ds} - \frac{1}{T_r \omega_s} e'_{qs} + \left(1 - \frac{\omega_r}{\omega_s}\right) e'_{ds} - K_{mrr} v_{dr} \right) \tag{4.19}$$

$$\frac{de'_{ds}}{dt} = \omega_{elB}\left(-R_2\, i_{qs} - \frac{1}{T_r \omega_s} e'_{ds} - \left(1 - \frac{\omega_r}{\omega_s}\right) e'_{qs} + K_{mrr} v_{qr} \right) \tag{4.20}$$

The parameters used in above equations are defined as follows:

ψ_{qr} The q axis rotor flux linkage;

ψ_{dr} The d axis rotor flux linkages;

L_{ss} The stator self-inductance;

L_{rr} The rotor self-inductance;

L_m The mutual inductance;

R_r The rotor resistance;

R_s The stator resistance

ω_s The synchronous angel speed;

X_s The stator reactance;

L'_s The stator transient reactance;

e'_{qs} The q axis voltage behind the transient reactance;

e'_{ds} The d axis voltage behind the transient reactance;

T_r The rotor circuit time constant;

i_{qs} The q axis stator current;

i_{ds} The d axis rotor current;

v_{qs} The q axis stator terminal voltages;

v_{ds} The d axis stator terminal voltages;

v_{qr} The q axis rotor terminal voltages;

v_{dr} The d axis rotor terminal voltages.

The DFIG equivalent model for the small signal stability studies is shown in figure 2.4. The variables e'_{qds}, e'_{qds}, z_s and i_{qds} are complex values with the real and imaginary components equal to $q-$ and $d-$ axis components respectively .

4.6 Converter Model

The back to back HVDC-link converter connected between the DFIG rotor and grid consist of two pulse width modulation as shown in Figure 4.1. The back-to-back converter is divided into two components: the rotor-side converter (RSC) and the grid-side converter (GSC) with a dc- link capacitor between them in order to keep the voltage variations in the dc-link voltage small. Both of these converters are Voltage-Sourced Converters (VSC) equipped with IGBTs and diodes to synthesize an *ac* voltage from a *dc* voltage source, which enable a bi-directional power flow [36, 149]. The VSC is used to convert the *ac* voltage source into the *dc* voltage source and vice versa.

The rotor side converter (RSC) is used to control the torque production of the DFIG through direct control of the rotor current. The RSC does this by applying a voltage to the rotor winding at slip frequency of machine.

The range of rotor speed variation is dependent on the rating of the rotor voltage source converter. These voltages can be set depending on what current is required [150].The machine-side converter (MSC) can use either a torque controller, speed controller or active power flow control to regulate

the output power of the DFIG. The MSC is controlled such that maximum wind power is extracted at sub-synchronous regimes and constant torque is tracked at synchronous regime.

The grid-side VSC is used to regulate the active and reactive power exchange between the generator and the grid. This is represented as a controlled current source since it maintains the dc-link voltage constant and injecting an *ac* current at grid frequency to the network [140]. The reactive power set point is generated by the terminal voltage or power factor controller, based on the actual value of the terminal voltage or the power factor.

For the grid side converter the control has to be coordinated, so that the dc-link voltage is constant and high. Thus the total reactive power exchanged with these grid depends not only on the control of the GSC but also to the stator winding. The active and reactive power balanced equation for GSC expressed as

$$P_{total} = P_s + P_{gsc} \tag{4.21}$$

$$Q_{total} = Q_s + Q_{gsc} \tag{4.22}$$

Where

$$P_S = v_{qs} i_{qs} + v_{ds} i_{ds} \tag{4.23}$$

$$Q_S = -v_{qs} i_{ds} + v_{ds} i_{qs} \tag{4.24}$$

$$P_{gsc} = v_{qr} i_{qr} + v_{dr} i_{dr} \tag{4.25}$$

$$Q_{gsc} = \alpha Q_{total} \tag{4.26}$$

The parameters used in above equations are defined as follows:

P_{total} The total active power delivered to the grid;

Q_{total} The total reactive power delivered to the grid;

P_s The stator active power delivered to the grid;

Q_s The stator reactive power delivered to the grid;

P_{gsc} The active power of grid side converter;

Q_{gsc} The active power of the grid side converter;

α The reactive power sharing between stator and GSC;

i_{qr} The q axis rotor current;

i_{dr} ` The d axis rotor current.

For the minimum converter current rating, no sharing is done, and the reactive power delivered to the grid comes only from the stator (i.e. the grid side of the converter operates at unity power factor). Hence $\alpha = 0$, $Q_{gsc} = 0$ and $Q_{total} = Q_S$ [115, 151].

The back-to-back converter is assumed as lossless components, and the switching dynamics are not modeled since their frequency is not in the range of interest for small signal stability studies. Modal analysis of the open-loop DFIG is carried out to gain a solid understanding of the inherent strengths and weaknesses of the system with no control, i.e. the rotor voltage (v_{qr} , v_{dr}) remains constant at its initial value. Closed-loop controllers are not included in this chapter and it will be discussed in details in next chapter.

4.7 Power Exchange between Grid and DFIG

The model of the grid connected DFIG developed so far. In order to accomplish the complete model , two algebraic equations has to be added to the seventh order model of DFIG, namely the equations of active power and reactive power of the grid side converter exchange between the grid and generator , respectively.

In this thesis, the grid is modeled by its thevenin's equivalent [148-149]; i.e. an infinite bus behind a line reactance X_e, as shown in figure 4.1. The total reactive and active powers in [pu] grabbed by the grid are:

$$P_{total} = \frac{\sqrt{v_{qs}^2 + v_{ds}^2}\, v_b \sin\gamma}{X_e} \tag{4.27}$$

$$Q_{total} = \frac{\left(\left(v_{qs}^2 + v_{ds}^2\right) - \sqrt{v_{qs}^2 + v_{ds}^2}\, v_b \cos\gamma\right)}{X_e} \tag{4.28}$$

Where

γ The angle between DFIG stator voltage and infinite bus voltage;

X_e The reactance of the external line;

V_b The magnitude of the infinite bus voltage.

If the stator resistance is neglected and it is assumed that d-axis coincides with the maximum of the stator flux, which implies that v_{ds} equals zero and v_{qs} equals the terminal voltage, the electrical torque is dependent on the quadrature components of the rotor current[152]and the hence the network algebraic equations 4.27 and 4.28 can be simplified as following equations:

$$p_{total} = \frac{V_s V_b \sin \gamma_e}{X_e} \tag{4.29}$$

$$Q_{total} = \frac{V_s^2 - V_s V_b \cos \gamma_e}{X_e} \tag{4.30}$$

4.8 Simulation and Results

The small-signal stability of a DFIG directly connected to an equivalent grid is studied by examining the eigenvalues, eigenvalue properties and participation factors for a number of different system conditions. The simulation used for this analysis contains drive train, DFIG model, and electrical network.

It is important to emphasize how the dynamic behavior of the DFIG-based WT system changes under different modes of operation.

Modal analysis (analysis of eigenvalue locations, eigenvalue properties and participation factors) of the open-loop DFIG is carried out to study the inherent strengths and weaknesses of the system with no control.

4.8.1 Initial Conditions

The initialization of the power system is the first step in both studies (transient and small signal analysis). This is done in two steps. First, the equation 4.29 and 4.30 is calculated on the grid side in order to obtain the voltage magnitude, voltage angle and injected active and reactive powers at SMIB. Then, with obtained solution, the DFIG is initialized by solving 2.3-2.4 with time derivative

terms equal to zero and controlled outputs v_{qr} and v_{dr} equal to their reference value. It should be noticed that, the initialization is done by 'fsolve' which is a built-in function in MATLAB software for solving simultaneous equations.

4.8.2 Linearization of the Dynamic Model and State Matrix

Considering the system described by equation 2.3-2.4:

$$\dot{x} = f\left(x, z, u\right) \tag{4.31}$$

$$y = g\left(x, z, u\right) \tag{4.32}$$

If $\left(x_0, z_0, u_0\right)$ is the equilibrium point, we consider a nearby solution.

$$\Delta x = x - x_0 \quad \Delta z = z - z_0 \quad \Delta u = u - u_0$$

Taking the first order Taylor expansion, we find the relation

$$\frac{d}{dt}\Delta x = \frac{\partial f}{\partial x}\Delta x + \frac{\partial f}{\partial z}\Delta z + \frac{\partial f}{\partial u}\Delta u \tag{4.33}$$

$$0 = \frac{\partial g}{\partial x}\Delta x + \frac{\partial g}{\partial z}\Delta z + \frac{\partial g}{\partial u}\Delta u \tag{4.34}$$

Where

$$F_x = \frac{\partial f}{\partial x}, \quad F_z = \frac{\partial f}{\partial z}, \quad F_u = \frac{\partial f}{\partial u}, \quad G_x = \frac{\partial g}{\partial x}, \quad G_z = \frac{\partial g}{\partial z}, \quad G_u = \frac{\partial g}{\partial u}$$

We call F_x, F_z, F_u, G_x, G_z and G_u the Jacobean matrices. If G_z is non-singular we can write that.

$$\Delta \dot{x} = \left(F_x - F_z G_z^{-1}\ G_x \right) \Delta x + \left(F_u - F_z G_z^{-1} G_u \right) \Delta u \tag{4.35}$$

Now From the relationships of linearized DAE model equation 2.10 and equation 4.35 the system state matrix, A_{sys} can be obtained:

$$\Delta \dot{\mathbf{x}} = \mathbf{A}_{\text{sys}}\, \Delta \mathbf{x} + \mathbf{B}\, \Delta \mathbf{u} \tag{4.36}$$

Where

$$\mathbf{A}_{sys} = \left[F_x - F_z \left(G_z \right)^{-1} G_x \right]_{x_0, z_0, u_0} \tag{4.37}$$

$$\mathbf{B} = \left[F_u - F_z \left(G_z \right)^{-1} G_u \right]_{x_0, z_0, u_0} \tag{4.38}$$

The state vectors is defined by $x = \left[i_{qs}\ i_{ds}\ e'_{qs}\ e'_{ds}\ \omega_r\ \theta_{tw}\ \omega_t \right]^T$, $z = \left[V_s\ \gamma \right]^T$ and $u = \left[v_{qr}\ v_{dr}\ P_t \right]$. f is contained in equations 4.1-4.3 and 4.17-4.20 and g is contained in equations 4.29-4.30.

The linearized model of equation 4.36 is used for the small-signal stability analysis and the matrix A_{sys} is the state matrix. Its eigenvalues (real/complex) give the natural modes of the system. For the given case of the DFIG-based WT system, the characteristic equations is a seventh-order equation: thus, it will yield seven eigenvalues for a specific steady-state value of the rotor speed. Therefore, in general, one of the eigenvalues must be real and the other six eigenvalues form three sets of complex conjugate pairs.

4.8.3 Base Case Modes

The single machine infinite bus (SMIB) system shown in figure 4.1 is studied for the base case mode. The terminal voltage V_s is 1 pu and remains constant for most of the simulation work. The

reactive power output is zero, the active power injected to grid is 1 pu, and the system is operating at rated speed, which is assumed to be the synchronous speed ω_s. The parameters of the DFIG wind turbine system are listed in table 4.1[13]

Table 4.1: DFIG-WT Data

DFIG			Drive train			Constants		
R_r	0.005	$[pu]$	H_t	3	$[pu]$	ω_s	1	$[pu]$
R_s	0.00706	$[pu]$	H_g	0.5	$[pu]$	ω_{elB}	$2\pi*50$	$rad/\sec$
X_m	6	$[pu]$	K_{sh}	0.3	$[pu]$	V_b	1	$[pu]$
L_m	2.9	$[pu]$	c	0.001	$[pu]$			
R_r	$0.8\,R_s$	$[pu]$						
L_s	0.171	$[pu]$						
L_r	0.156	$[pu]$						
L_{ss}	$L_s + L_m$	$[pu]$						
L_{rr}	$L_r + L_m$	$[pu]$						

Table 4.2 (a) and (b) show the eigenvalues, eigenvalue properties and participation factors of the dominant states of the WT-DFIG at the base case. It can be seen that the system is dynamically stable, since all the real parts of the eigenvalues have negative values. There are three oscillating modes associated with stator and rotor dynamics and one non-oscillating mode associated with rotor dynamics.

Table 4.2: Base case mode

(a) Eigenvalues λ, nature of the mode, Oscillation frequency f_{osc} [Hz] and damping ratio ζ

	$\lambda = \sigma \pm j\omega$	Nature of the mode	$f_{osc} = \omega/2\pi$	$\zeta = -\sigma/\sqrt{\sigma^2 + \omega^2}$
λ_1	-10.27 + 313.88i	Stator mode (λ_1, λ_2)	49.98[Hz]	0.0325 [pu]
λ_2	-10.27 - 313.88i			
λ_3	-2.82 + 41.06i	Electro mechanical mode (λ_3, λ_4)	6.57[Hz]	0.068[pu]
λ_4	-2.82 - 41.06i			
λ_5	-6.27 + 0.00i	Non-oscillating mode (λ_5)	0 [Hz]	1 [pu]
λ_6	-2.64 + 4.67i	Mechanical mode (λ_6, λ_7)	0.743 [Hz]	0.492 [pu]
λ_7	-2.64 - 4.67i			

(b) Participation factors for base case mode

	λ_1	λ_2	λ_3	λ_4	λ_5	λ_6	λ_7
i_{qs}	0.50	0.50	0.02	0.02	0.00	0.00	0.00
i_{ds}	0.50	0.50	0.02	0.02	0.06	0.06	0.01
e'_{qs}	0.01	0.01	0.02	0.02	0.76	0.19	0.19
e'_{ds}	0.01	0.01	0.49	0.49	0.03	0.04	0.04
ω_t	0.00	0.00	0.00	0.00	0.00	0.48	0.48
θ_{tw}	0.00	0.00	0.01	0.01	0.04	0.80	0.80
ω_r	0.00	0.00	0.32	0.32	0.00	0.00	0.00

The mode with the highest oscillation frequency is an electrical mode associated with the DFIG stator state variables (i_{qs}, i_{ds}) which oscillates around 49.98 Hz. The medium frequency, at about 6.571 Hz, is an electro-mechanical mode associated with rotor electrical and rotor mechanical

dynamics. It is contributed by the internal voltage e'_{ds} , and generator speed ω_r . The lowest frequency mode is a mechanical mode associated with shaft and turbine dynamics by torsion angle θ_{wt} and turbine speed ω_t , of frequency about 0.743 Hz. It is the dominant mode. The non-oscillating mode is a real eigenvalue associated with rotor electrical dynamics, by the internal voltage e'_{qs} . As it can be seen from Table 4.2, the stator mode (λ_1, λ_2) is a poorly damped mode ($\sim$ 3.25%). All other modes are well damped ($\zeta > 6$ %).

The three oscillating modes can be visualized, as shown in figure 4.3. The figure shows the time-domain response of the DFIG active power injected to grid when the wind turbine speed is disturbed by 0.5 pu. The disturbance time start at 0.1s and end at 0.2s.

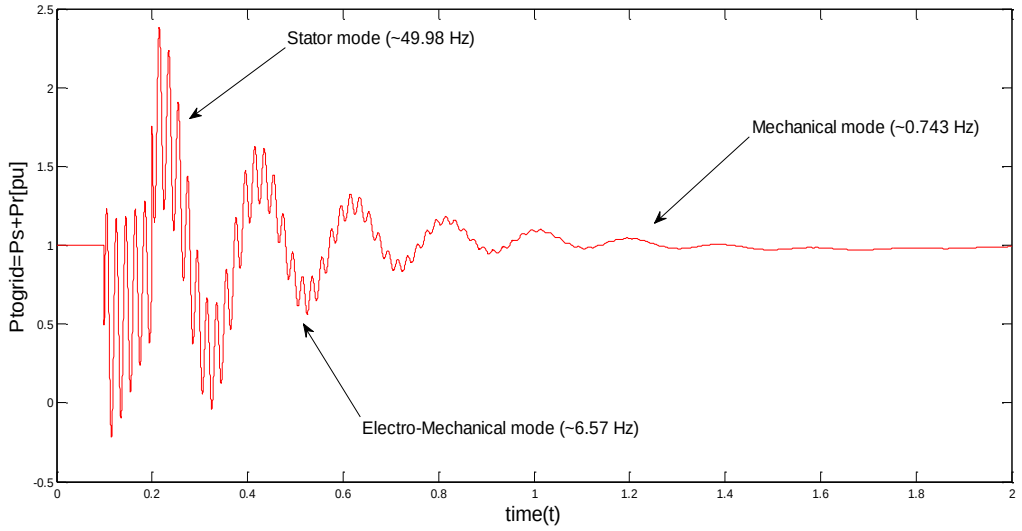

Fig. 4.3: visualization of the DFIG modes in time domain: active power response in base case mode

4.8.4 Effect of Machine Parameters on Model Analysis

The drive-train and DFIG parameters vary with the machine size, design and working conditions, so it is useful to consider the order of magnitude of the various parameters and the extent to which each parameter influences particular modes.

In this subsection, a modal analysis of DFIG is carried out to investigate the effect of changing DFIG parameters on eigenvalues and the degree of participation of state variables in the system modes.

For the drive train, the effect of stiffness and inertia values are considered. For the generator, the effects of the mutual inductance and resistance values and initial terminal voltages are considered.

4.8.5 Generator Parameters:

(A) Stator and Rotor Machine Resistances

The machine resistances R_S and R_r exert a significant effect on the open-loop eigenvalue placement and on the participation factor. The relationship between stator and rotor resistance is $R_r = 0.8R_S$. Smaller resistance values alter the system stability at non- synchronous speed. Displacement of real part magnitude of all eigenvalues σ_i, is directly proportional to resistances variation, i.e., it tends to increase negatively with resistance value increases.

Varying the resistance R_S / X_m (1/567 to 1/38) while keeping all other parameters constant causes noticeable displacement for all eigenvalues as shown in figure 4.4. The real part magnitudes of the high-frequency and medium-frequency oscillating modes have an almost linear variation with resistance variation for the whole operating range and they are better damped since they move farther away from the imaginary axis. The frequency of the high-frequency and medium-frequency oscillating modes are affected more with resistance variation. The most significant changes are for

the oscillation frequency of the stator mode (λ_1, λ_2) and electro-mechanical mode (λ_3, λ_4). The oscillation frequency of electro-mechanical mode (λ_3, λ_4) decreases up to R_S / X_m (1/45) at synchronous speed, and the frequency of mechanical mode (λ_6, λ_7) is affected to a lesser extent for the whole range of resistance variation. The non-oscillating mode becomes more and more negative up to a point (R_S / X_m =1/50).then it suddenly moves back toward the origin. As we observed from the results below the system is dynamically stable for tested range of resistance variation as it can be seen from the eigenvalues and eigenvalue loci. The low-frequency mode is the dominant mode. It is real part magnitude and damping ratio decreases by up to -50% for resistances values of 0.01% and increases almost twice as much for resistance values of 200%.

The damping ratio of the high and medium-frequency modes improve linearly with increasing resistance values and oscillations are damped out faster. As shown in figure 4.4 participation factors are modified significantly for all modes especially for medium- frequency and high frequency modes. It should be mentioned that at point $\left(R_S / X_m = 1/35\right)$ there is no electro-mechanical mode.

Table 4.3 Modes for resistive machine $\left(R_S / X_m = 1/35\right)$

(a) Eigenvalues λ, nature of the modes, Oscillation frequency f_{osc} [Hz] and damping ratio ζ

	$\lambda = \sigma \pm j\omega$	Nature of the mode	$f_{osc} = \omega/2\pi$	$\zeta = -\sigma/\sqrt{\sigma^2 + \omega^2}$
λ_1, λ_2	-122.22 ± 276.13i	Electrical mode	43.96[Hz]	0.405 [pu]
λ_3, λ_4	-79.50 ± 34.15i	Electrical mode	5.4378[Hz]	0.1181[pu]
λ_5, λ_6	$-7.40 \pm 4.63i$	Mechanical mode	0.737[Hz]	0.851[pu]
λ_7	-4.89 + 0.00i	Non-oscillating mode	0 [Hz]	1 [pu]

(b) Participation factors for heavy resistive machine $\left(R_S / X_m = 1/35\right)$

	λ_1	λ_2	λ_3	λ_4	λ_5	λ_6	λ_7
i_{qs}	0.63	0.63	0.23	0.23	0.03	0.03	0.02
i_{ds}	0.62	0.62	0.17	0.17	0.00	0.00	0.00
e'_{qs}	0.19	0.19	0.68	0.68	0.00	0.00	0.00
e'_{ds}	0.19	0.19	0.79	0.79	0.06	0.06	0.04
ω_t	0.00	0.00	0.00	0.00	0.47	0.47	0.19
θ_{tw}	0.00	0.00	0.00	0.00	0.45	0.45	0.05
ω_r	0.00	0.00	0.17	0.17	0.09	0.09	1.00

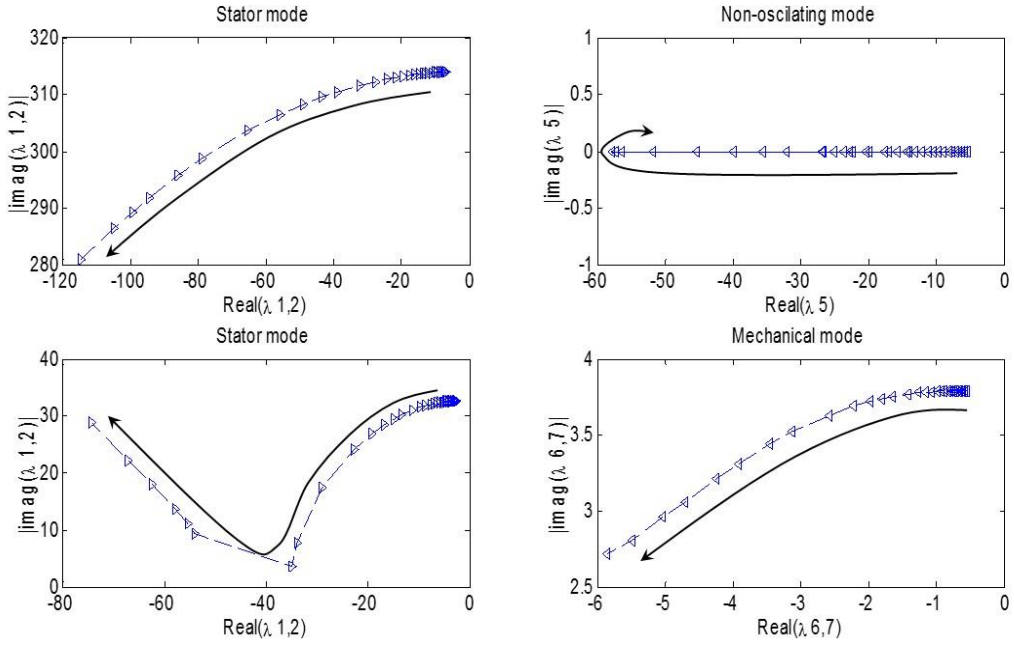

Fig. 4.4: Eigenvalue loci of the stator, non-oscillating, electromechanical and Mechanical modes for increasing stator resistance $\left(R_S / X_m = 1/567 \, to \, 1/35\right)$

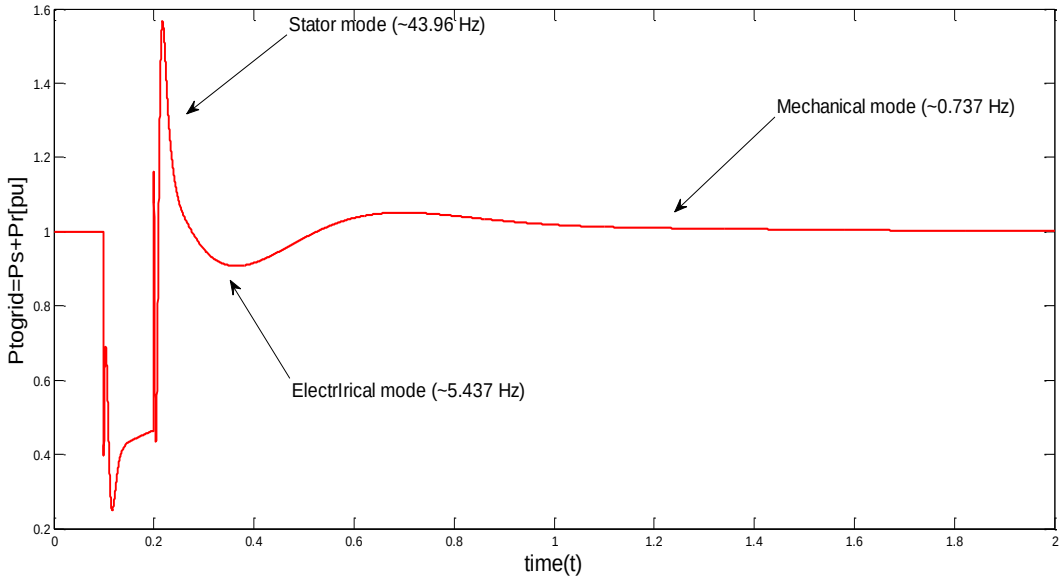

Fig. 4.5: Visualization of the DFIG modes in time domain: active power response to change in stator and rotor resistance at point $\left(R_S \middle/ X_m = 1 \middle/ 35\right)$

(B) Magnetization Inductance

Variation on magnetization inductance L_m seems to alter only the stability of the real mode at synchronous operation when it increase $(L_m = 1 \sim 7.5)$ as shown in the figure 4.6. The electrical modes (stator mode (λ_1, λ_2) and non-oscillating mode (λ_5)) are affected more with increasing L_m since the eigenvalues are going further away from origin. For the electro-mechanical mode (λ_3, λ_4) and mechanical mode (λ_6, λ_7) the magnitude of the imaginary part decreases slowly and that of the real part increases with the increase of L_m . As a result the stability margin of all modes increases as shown in the figure 4.6. Hence, the damping ratio increases up to 50%, the oscillation frequency of the lowest frequency mode increases up to 30%.

The magnetization inductance can be seen as a representation of the airgap length, with a large inductance accounting for a small airgap hence, the observation indicate that small-airgap

machines are better damped and their oscillation frequencies are lower compared to large-airgap machines[115].

Table 4.4 Modes for mutual inductance at point $(X_m = 7.5)$

(a) Eigenvalues λ, nature of the modes, Oscillation frequency f_{osc} [Hz] and damping ratio ζ

	$\lambda = \sigma \pm j\omega$	Nature of the mode	$f_{osc} = \omega/2\pi$	$\zeta = -\sigma/\sqrt{\sigma^2 + \omega^2}$
λ_1, λ_2	-17.95 + 313.34i	Electrical mode	49.89[Hz]	0.0571 [pu]
λ_3, λ_4	-6.42 ± 32.26i	Electrical mod	5.14[Hz]	0.195[pu]
λ_5, λ_6	-14.56 + 0.00i	Non-oscillating	0 [Hz]	1 [pu]
λ_7	-0.94 ± 3.79i	Mechanical mode	0.60 [Hz]	0.240 [pu]

(b)Participation factors for mutual inductance at point $(X_m = 7.5)$

	λ_1	λ_1	λ_1	λ_1	λ_1	λ_1	λ_1
i_{qs}	0.50	0.50	0.01	0.01	0.00	0.00	0.00
i_{ds}	0.50	0.50	0.01	0.01	0.00	0.00	0.00
e'_{qs}	0.02	0.02	0.02	0.02	0.99	0.00	0.00
e'_{ds}	0.02	0.02	0.48	0.48	0.01	0.04	0.04
ω_t	0.00	0.00	0.00	0.00	0.00	0.50	0.50
θ_{wt}	0.00	0.00	0.04	0.04	0.00	0.46	0.46
ω_r	0.00	0.00	0.51	0.51	0.00	0.00	0.00

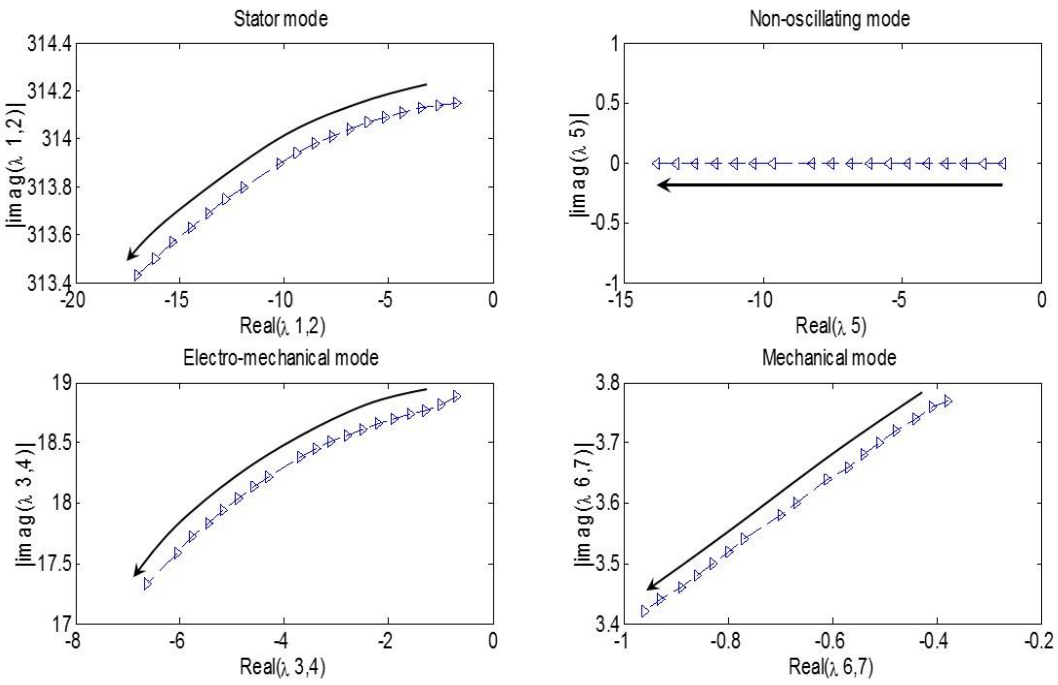

Fig. 4.6: Eigenvalue loci of the stator, non-oscillating, electro-mechanical and mechanical modes for increasing mutual inductance in the range of $(X_m = 1 \sim 7.5)$

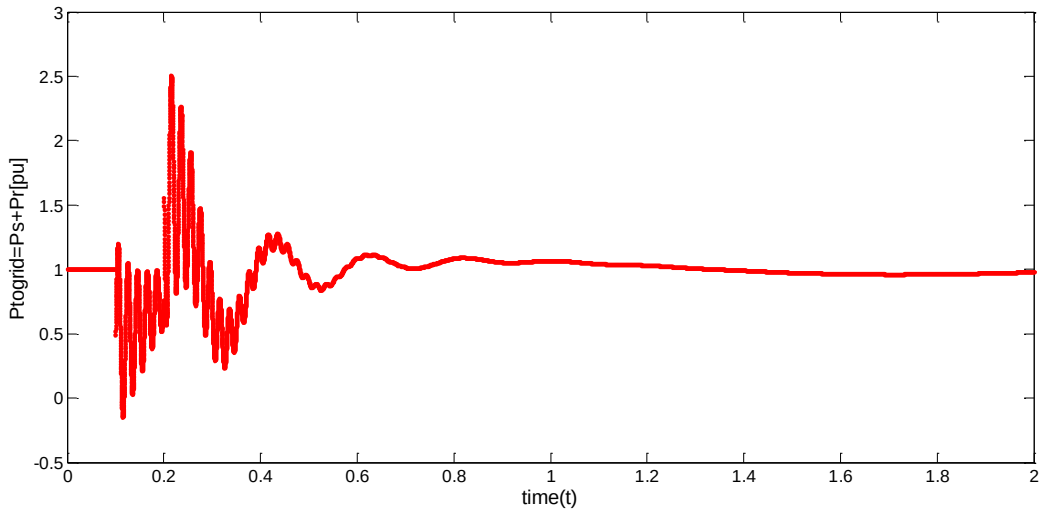

Fig. 4.7: Visualization of the DFIG modes in time domain: active power response to change in mutual inductance at point $(X_m = 7.5)$

4.8.6 Modal Analysis- Effect of the Operating Point

In this this section, the effects of power generation at different operating speeds, non-unity power factors, and non-unity terminal voltages are discussed.

Table 4.5:- Investigated initial rotor speed and corresponding active power level to grid

(a) Sub-synchronous speed operation at maximum active power tracking regime

P_{togrid}	0.3	0.4	0.5	0.6	0.7	0.8	0.9
ω_r	0.7	0.74	0.78	0.82	0.86	0.9	0.92

(b) Super-synchronous speed operation at constant active power tracking regime

P_{togrid}	0.9	0.9	0.9	0.9	0.9	0.9	0.9
ω_r	0.93	0.95	0.98	1	1.02	1.05	1.1

4.8.6.1 Effects of Operating Points

Since the DFIG may operate at large slips, it is important to study how its dynamic behavior changes with rotor speed. In this case the total active power injected at the point of common coupling is (0.3~0.9 p.u) at the sub-synchronous regime and constant active power of 0.9 p.u at the super-synchronous regime as shown in table 4.5 (a) and (b).

Table 4.6 shows the eigenvalues, eigenvalue properties and participation factors of the dominant state of the DFIG at sub-synchronous speed and table 4.7 shows similar information but for the super-synchronous speed. It can be observed that the system is dynamically stable at both operating modes.

There are three oscillating modes associated with stator and rotor dynamics and one nonoscillating mode associated with mechanical dynamics. The mode with the highest oscillation frequency is

an electrical mode associated with the DFIG stator state variables (i_{qs}, i_{ds}) which oscillates around 49.96~49.98 Hz for both operating speed sub-synchronous and as well as super-synchronous. The medium frequency electrical mode for sub-synchronous speed, about 13.97 Hz, is associated with the rotor through the dynamics of the internal voltages e'_{qs} and e'_{sd} . In other way the super-synchronous operates at medium frequency about 5.88 Hz as an electro-mechanical mode, it is contributed by rotor dynamics (e'_{qs}, e'_{ds}) and generator speed ω_r . The lowest frequency mode is contributed by shaft and rotor dynamics, by (θ_{wt}, ω_t) , ω_r and to a lesser extent by e'_{qs} ($\sim 25\%$), with an oscillation frequency of about 0.97~1.55 Hz. The non-oscillating mode is the dominant mode and consists in a mechanical mode contributed by the generator speed ω_r , and turbine speed ω_t . The stability margin of the low frequency and non-oscillating mode is smaller at sub-synchronous operation than super-synchronous operation.

Table 4.6: Effects of Sub-synchronous operation at point $(\omega_r = 0.74\, p.u, P_{togrid} = 0.4\, p.u)$

(a) Eigenvalues λ , nature of the modes, Oscillation frequency f_{osc} [Hz] and damping ratio ζ

	$\lambda = \sigma \pm j\omega$	Nature of the mode	$f_{osc} = \omega/2\pi$	$\zeta = -\sigma/\sqrt{\sigma^2 + \omega^2}$
λ_1, λ_2	-10.28 + 313.81i	Electrical mode	49.96[Hz]	0.0327 [pu]
λ_3, λ_4	-6.49 + 87.74i	Electrical mod	13.97[Hz]	0.073[pu]
λ_5, λ_6	-1.58 + 9.74i	Electro-mechanical	1.55[Hz]	0.160[pu]
λ_7	-0.98 + 0.00i	Mechanical mode (non-oscillating mode)	0 [Hz]	1 [pu]

(a) Participation factor for Sub-synchronous operation at point $(\omega_r = 0.74\, p.u, P_{togrid} = 0.4\, p.u)$

	λ_1	λ_2	λ_3	λ_4	λ_5	λ_6	λ_7
i_{qs}	0.50	0.50	0.01	0.01	0.00	0.00	0.00
i_{ds}	0.50	0.50	0.02	0.02	0.01	0.01	0.00
e'_{qs}	0.01	0.01	0.45	0.45	0.04	0.04	0.01
e'_{ds}	0.01	0.01	0.50	0.50	0.00	0.00	0.00
ω_t	0.00	0.00	0.00	0.00	0.08	0.08	0.84
θ_{wt}	0.00	0.00	0.00	0.00	0.51	0.51	0.01
ω_r	0.00	0.00	0.06	0.06	0.37	0.37	0.14

Table 4.7: Effects of Super-synchronous operation at point $(\omega_r = 1.05\, p.u, P_{togrid} = 0.9\, p.u)$

(a) Eigenvalues λ, nature of the modes, Oscillation frequency f_{osc} [Hz] and damping ratio ζ

	$\lambda = \sigma \pm j\omega$	Nature of the mode	$f_{osc} = \omega/2\pi$	$\zeta = -\sigma/\sqrt{\sigma^2 + \omega^2}$
λ_1, λ_2	-10.26 + 313.91i	Electrical mode	49.98[Hz]	0.0327 [pu]
λ_3, λ_4	-6.52 + 35.72i	Electro-mechanical	5.688[Hz]	0.1795[pu]
λ_5, λ_6	-1.33 + 5.76i	Electro-mechanical	0.917[Hz]	0.299[pu]
λ_7	-1.46 + 0.00i	Non-oscillating mode	0 [Hz]	1 [pu]

(b) Participation factor for Sub-synchronous operation at point $(\omega_r = 1.05\ p.u, P_{togrid} = 0.9\ p.u)$

	λ_1	λ_2	λ_3	λ_4	λ_5	λ_6	λ_7
i_{qs}	0.50	0.50	0.01	0.01	0.00	0.00	0.00
i_{ds}	0.50	0.50	0.02	0.02	0.01	0.01	0.01
e'_{qs}	0.01	0.01	0.08	0.08	0.25	0.25	0.38
e'_{ds}	0.01	0.01	0.49	0.49	0.05	0.05	0.02
ω_t	0.00	0.00	0.00	0.00	0.22	0.22	0.56
θ_{wt}	0.00	0.00	0.03	0.03	0.49	0.49	0.02
ω_r	0.00	0.00	0.41	0.41	0.06	0.06	0.11

The operating point has a significant effect on all the eigenvalues, except of the high frequency mode which is stator mode (i_{qs}, i_{ds}). For the no oscillating mode, the eigenvalue is the furthest away from the imaginary axis at synchronous speeds, while its absolute values decrease dramatically at sub-synchronous and super-synchronous speed at large slip.

Figure 4.8 shows the eigenvalue displacement of the electro-mechanical mode for operating points of table 4.5. From the stability viewpoint, small-slip speed (operating point around connection point between red line and blue line) is the region of least stability.it also means that assuming the rated operation as synchronous operation, dynamics tend to be more coupled and it is more conservative approach. For the mechanical mode, the operating points which is shown by red line, it contains plus sign (+) and blue lines contains circles (0) are the most stable for sub-and super

synchronous operations, respectively. This means that in both the maximum active power tracking regime and constant active power tracking regime, there is an optimal speed for the stability of the critical mode.

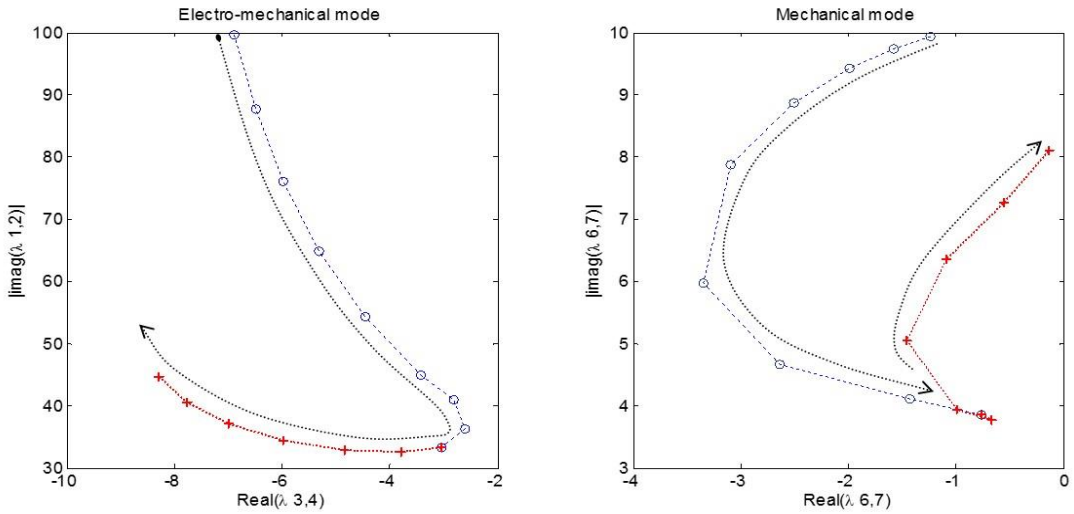

Fig. 4.8: Eigenvalue loci of the electromechanical and mechanical modes for increasing rotor speed ($\omega_r = 0.67 \sim 1.3\ p.u$)

The indicated operating points are: blue lines which contains symbols in shape of circles (0) for ($\omega_r = 0.7 \sim 0.9\ p.u$) ; red lines which contains symbols in the shape of (+) for ($\omega_r = 0.92 \sim 1.1\ p.u$) The red line with symbols (+) are used for super synchronous speed and the blue line with symbols (o) used for sub-synchronous speed.

4.8.7 Initial Reactive Power Loading

For the base case the grid side converter operates at unity power factor that is why the reactive power is zero and the reactive power delivered to the grid comes only from the stator winding. Now we are going to check for less than unity power factor and see the effects at small signal

stability properties, suppose the reactive power absorption and production at power factor 0.7 corresponding to the reactive power range ($Q_{togrid} = \pm 1$) which is shown in table (4.8) . It shows that there is slight significant change in eigenvalues in all modes except in stator mode, so we can say that the reactive power level does not affect the small-signal stability significantly. The participation factors are not shown, because there is no significant effect.

Table 4.8: Modes for different reactive power ranges with $P_{togrid} = 1\,p.u., V_s = 1\ p.u.$

(a) Eigenvalues $\lambda = \sigma \pm j\omega$

	$Q_{togrid} = -1\,p.u$	$Q_{togrid} = 0\,p.u$	$Q_{togrid} = +1\,p.u$
λ_1, λ_2	-10.24 ±313.90i	-10.27 ± 313.90i	-10.31 + 313.90i
λ_3, λ_4	-3.64 ± 27.36i	-3.78 ± 32.59i	-3.83 + 37.10i
λ_7	-8.30 + 0.00i	-8.27 + 0.00i	-8.25 + 0.00i
λ_5, λ_6	-0.83 ± 3.71i	-0.68 ± 3.78i	-0.60 ±3.82i

(b) Oscillation frequency f_{osc} [Hz] and damping ratio ζ

	$Q_{togrid} = -1\,p.u$		$Q_{togrid} = 0\,p.u$		$Q_{togrid} = +1\,p.u$	
	f_{osc}	ζ	f_{osc}	ζ	f_{osc}	ζ
λ_1, λ_2	49.98[Hz]	0.0326 [pu]	49.98[Hz]	0.0326 [pu]	49.98[Hz]	0.0328 [pu]
λ_3, λ_4	4.35[Hz]	0.132 [pu]	5.19[Hz]	0.115 [pu]	5.90[Hz]	0.102 [pu]
λ_7	0[Hz]	1[pu]	0[Hz]	1[pu]	0[Hz]	1[pu]
λ_5, λ_6	0.59[Hz]	0.218 [pu]	0.60[Hz]	0.21 [pu]	0.60[Hz]	0.15 [pu]

4.8.8 Initial Terminal Voltage

In the case of constant active power tracking (CAPT) to grid and maximum active power tracking (MAPT) to grid the effect of voltage is different, it is discussed below with details.

(a) Variation of Terminal Voltage at CAPT Regime.

Figure 4.9 shows the eigenvalue loci for increasing terminal voltage in range of $(V_S = 0.5 \sim 2.5\ p.u)$ while keeping active power to grid equals to one per unit $(P_{togrid} = 1\ p.u)$ and rotor speed should be equal to synchronous speed of the machine ($\omega_r = \omega_r$). The eigenvalues, eigenvalue properties and participation factors for a points ($V_S = 0.5,\ P_{togrid} = 1$ and $V_S = 2.5,\ P_{togrid} = 1$)

Are shown in table 4.9 and 10.10 for better understanding of the figure.

Table 4.9: Effects of variation of terminal voltage at point $(V_S = 0.5\ p.u, P_{togrid} = 1\ p.u)$

(a) Eigenvalues λ, nature of the modes, Oscillation frequency f_{osc} [Hz] and damping ratio

	$\lambda = \sigma \pm j\omega$	Nature of the mode	$f_{osc} = \omega/2\pi$	$\zeta = -\sigma/\sqrt{\sigma^2 + \omega^2}$
λ_1, λ_2	$-10.25 \pm 313.90i$	Electrical mode	$49.98[Hz]$	$0.0326\ [pu]$
λ_3, λ_4	$-2.91 \pm 18.47i$	Electro-mechanical	$2.94[Hz]$	$0.156[pu]$
λ_5	$-8.52 + 0.00i$	non-oscillating mode	$0\ [Hz]$	$1\ [pu]$
λ_6, λ_7	$-1.45 + 3.31i$	Mechanical mode	$0.53[Hz]$	$0.401\ [pu]$

(b)Participation factor for variation of terminal voltage at point $(V_S = 0.5\ p.u, P_{togrid} = 1\ p.u)$

	λ_1	λ_2	λ_3	λ_4	λ_5	λ_6	λ_7
i_{qs}	0.50	0.50	0.02	0.02	0.00	0.00	0.00
i_{ds}	0.50	0.50	0.03	0.03	0.03	0.00	0.00
e'_{qs}	0.01	0.01	0.03	0.03	0.98	0.00	0.00
e'_{ds}	0.01	0.01	0.50	0.50	0.00	0.00	0.00
ω_t	0.01	0.01	0.39	0.39	0.01	0.16	0.16
θ_{wt}	0.00	0.00	0.15	0.15	0.00	0.37	0.37
ω_r	0.00	0.00	0.51	0.51	0.00	0.03	0.03

Table 4.10: Effects of variation of terminal voltage at point $(V_S = 2.5\,p.u, P_{togrid} = 1\,p.u)$

(a) Eigenvalues λ, nature of the modes, Oscillation frequency f_{osc} [Hz] and damping ratio

	$\lambda = \sigma \pm j\omega$	Nature of the mode	$f_{osc} = \omega/2\pi$	$\zeta = -\sigma/\sqrt{\sigma^2 + \omega^2}$
λ_1, λ_2	$-10.58 + 313.90i$	Electrical mode	$49.98[Hz]$	$0.0337\ [pu]$
λ_3, λ_4	$-3.81 + 81.32i$	Electro-mechanical	$12.95[Hz]$	$0.047[pu]$
λ_5	$-8.19 + 0.00i$	non-oscillating mode	$0\ [Hz]$	$0.160[pu]$
λ_6, λ_7	$-0.38 + 3.93i$	Mechanical mode	$0.63[Hz]$	$0.096\ [pu]$

(b)Participation factor for variation of terminal voltage at point $(V_S = 2.5\,p.u, P_{togrid} = 1\,p.u)$

	λ_1	λ_2	λ_3	λ_4	λ_5	λ_6	λ_7
i_{qs}	0.53	0.53	0.03	0.03	0.00	0.00	0.00
i_{ds}	0.50	0.50	0.01	0.01	0.00	0.00	0.00
e'_{qs}	0.01	0.01	0.00	0.00	1.00	0.00	0.00
e'_{ds}	0.03	0.03	0.53	0.53	0.00	0.00	0.00
ω_t	0.00	0.00	0.00	0.00	0.00	0.50	0.50
θ_{wt}	0.00	0.00	0.00	0.00	0.00	0.49	0.49
ω_r	0.00	0.00	0.50	0.50	0.00	0.00	0.00

With increasing of terminal voltage, the highest frequency oscillation mode associated with stator state variables (i_{qs}, i_{ds}) oscillates around $49.98[Hz]$. Real part of the eigenvalues moves away from the origin and damping ratio improves to the some extent, the magnitude of the imaginary part remains same as the base case.

The non-oscillating mode associated with stator dynamics (e'_{qs}) moves toward the origin as the real part of the eigenvalues decreases.

The medium frequency electro-mechanical mode, about $2.94 \sim 12.95[Hz]$, is associated with the rotor through the dynamics of the internal voltage e'_{sd} and contribution of the rotor speed ω_r. With increasing terminal voltage its oscillating frequency increases and damping ratio drop from 15.6% to 4.7% which is a huge margin. As the magnitude of the imaginary part increases so the system goes to less stable mode.

The lowest frequency mode is mechanical mode associated with shaft and turbine dynamics by torsion angle θ_{tw} and the turbine speed ω_t of frequency about $0.53 \sim 0.63[Hz]$. With increasing terminal voltage its real part of eigenvalue decreases, as it moves toward the origin and the magnitude of the imaginary part of the eigenvalue increases that's why the system goes less stable mode. With increasing of terminal voltage the damping ratio of mechanical mode (λ_6, λ_7) drops form 40% to 9.6% , which is a huge margin.

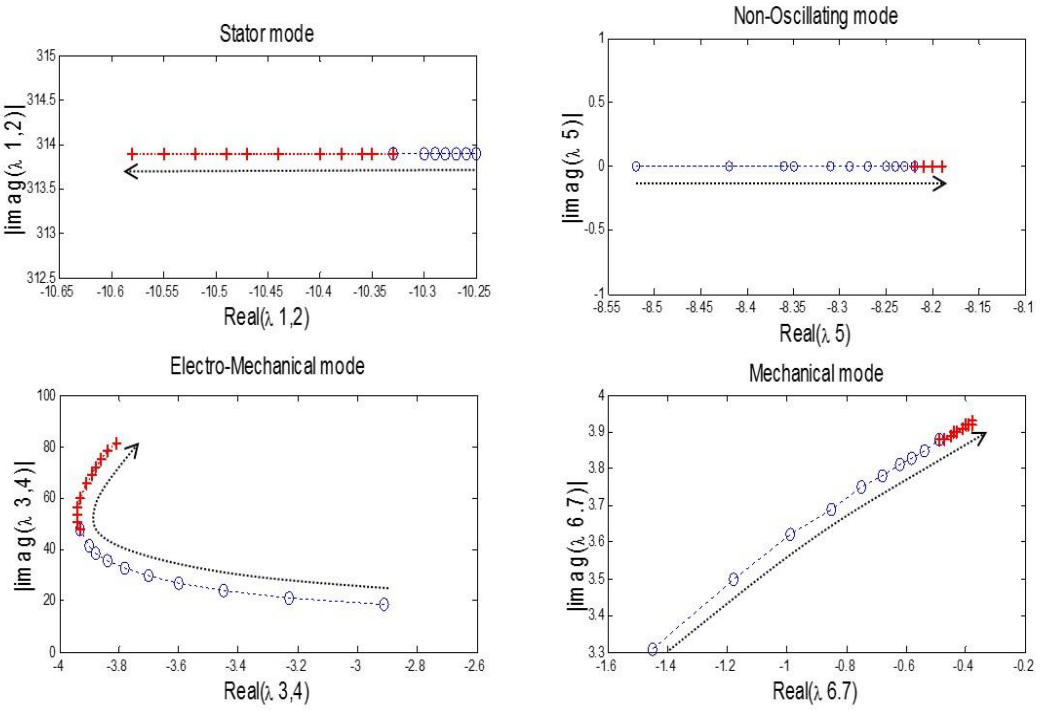

Fig. 4.9: Eigenvalue loci for increasing terminal voltage($V_S = 0.5 \sim 2.5$ p.u) with $P_{togrid} =$ 1p.u, $Q_{togrid} = 0$ p.u the symbols "0" and "+" are used for voltages below and above 1.5. Respectively

The loci are drawn with $V_S = 0.5 \sim 2.5\, p.u$ while keeping $P_{togrid} = 1\, p.u$, $Q_{togrid} = 0\, p.u$ and $\omega_r = \omega_s$. The blue lines contains symbols "o" and red lines contains symbols "+" are used for voltages below 1.5 p.u and above 1.5 p.u, respectively.

The main outcomes are that, in the case of constant active power tracking regime, the system is less stable for the over voltage condition, as we observe from the figure 4.9 with the increasing of terminal voltage the stator and the non-oscillating modes are not significantly affected but we see a huge change in electro-mechanical and mechanical mode. Electro mechanical mode to some extent moves away from the origin but immediately as terminal voltage crossed 1.5 p.u it turn back toward the origin. As the dominant mode (mechanical mode) moves closer to the imaginary axis.

(b) Variation of Terminal Voltage at MAPT Regime

Figure 4.10 shows the eigenvalue loci for increasing terminal voltage in range of $(V_S = 0.5 \sim 2.5\, p.u)$ in the MAPT regime $(P_{togrid} < 1 p.u)$ and rotor speed should be smaller than synchronous speed of the machine ($\omega_r < \omega_s$). The eigenvalues, eigenvalue properties and participation factors for a points $(V_S = 0.5,\ P_{togrid} = 1$ and $V_S = 2.5,\ P_{togrid} = 1)$ are shown in table 4.11 and 4.12.

Table 4.11: Effects of variation of terminal voltage at point $(V_S = 0.5\, p.u, P_{togrid} = 0.5\, p.u)$

(a) Eigenvalues λ, nature of the modes, Oscillation frequency f_{osc} [Hz] and damping ratio

	$\lambda = \sigma \pm j\omega$	Nature of the mode	$f_{osc} = \omega/2\pi$	$\zeta = -\sigma/\sqrt{\sigma^2 + \omega^2}$
λ_1, λ_2	−10.24 ± 313.85i	Electrical mode	49.98[*Hz*]	0.0326 [*pu*]
λ_3, λ_4	−5.68 ±49.90i	Electrical mode	7.94[*Hz*]	0.113[*pu*]
λ_7	−1.22 + 0.00i	Mechanical mode (Non-oscillating mode)	0 [*Hz*]	1[*pu*]
λ_6, λ_5	−2.31 ±9.71i	Mechanical mode	1.54[*Hz*]	0.231 [*pu*]

(b) Participation factor for variation of terminal voltage at point $(V_S = 0.5\,p.u, P_{togrid} = 0.5\,p.u)$

	λ_1	λ_2	λ_3	λ_4	λ_5	λ_6	λ_7
i_{qs}	0.50	0.50	0.02	0.02	0.00	0.00	0.00
i_{ds}	0.50	0.50	0.01	0.01	0.01	0.00	0.00
e'_{qs}	0.01	0.01	0.45	0.45	0.03	0.03	0.01
e'_{ds}	0.01	0.01	0.51	0.51	0.01	0.01	0.00
ω_t	0.00	0.00	0.00	0.00	0.08	0.08	0.85
θ_{wt}	0.00	0.00	0.00	0.00	0.52	0.52	0.02
ω_r	0.00	0.00	0.07	0.07	0.40	0.40	0.15

Table 4.12: Effects of variation of terminal voltage at point $(V_S = 2.5\,p.u, P_{togrid} = 0.5\,p.u)$

(a) Eigenvalues λ, nature of the modes, Oscillation frequency f_{osc} [Hz] and damping ratio

	$\lambda = \sigma \pm j\omega$	Nature of the mode	$f_{osc} = \omega/2\pi$	$\zeta = -\sigma/\sqrt{\sigma^2 + \omega^2}$
λ_1, λ_2	–10.61 ± 313.86i	Electrical mode	49.98[*Hz*]	0.0338 [*pu*]
λ_3, λ_4	–3.78 ±91.31i	Electro-mechanical	14.53[*Hz*]	0.0414[*pu*]
λ_5	–5.17 + 0.00i	non-oscillating mode	0 [*Hz*]	1.00[*pu*]
λ_6, λ_7	–1.87 ±4.87i	Mechanical mode	0.775[*Hz*]	0.361 [*pu*]

(b)Participation factor for variation of terminal voltage at point $(V_S = 2.5\,p.u, P_{togrid} = 0.5\,p.u)$

	λ_1	λ_2	λ_3	λ_4	λ_5	λ_6	λ_7
i_{qs}	0.53	0.53	0.03	0.03	0.00	0.00	0.00
i_{ds}	0.50	0.50	0.06	0.06	0.12	0.02	0.02
e'_{qs}	0.01	0.01	0.19	0.19	0.69	0.00	0.00
e'_{ds}	0.03	0.03	0.53	0.53	0.00	0.00	0.00
ω_t	0.00	0.00	0.00	0.00	0.28	0.42	0.42
θ_{wt}	0.00	0.00	0.00	0.00	0.40	0.69	0.69
ω_r	0.00	0.00	0.36	0.36	0.30	0.07	0.07

Increasing terminal voltage affects the participation factor of the stator mode (λ_1, λ_2) to a less extent , its participation factors improves by 3% (50%~53%) as the real part of the eigenvalues of stator mode moves further away from the origin, so it becomes more negative. It helps the stator modes to be more stable.

At MAPT regime with $P_{togrid} = 0.5, \omega_r < \omega_s$ and ($V_S < 1.5 p.u$) the non-oscillating mode associated with mechanical dynamics by turbine speed ω_t which is observed from participation factor in table 4.11(b). Just after the crossing of terminal voltage from ($V_S > 1.5 p.u$) the nonoscillating mechanical mode shifted to the non-oscillating electrical mode. Which associated by the internal terminal voltage of stator dynamics (e'_{qs}). With increasing of terminal voltage the non-oscillating mode in MAPT regime goes to more stable mode as the eigenvalues tends to increase negatively.

With increasing of voltage from (0.5 ~ 1.5 p.u) in the MAPT regime ($P_{togrid} < 1 \text{and} \omega_r < \omega_s$) the medium frequency mode, operates as electrical mode about $7.94[Hz]$. Thus, electrical mode associated with the rotor through the dynamics of the internal voltages (e'_{qs}, e'_{ds}), which is observed by participation factors (λ_3, λ_4) in table 4.11(b). Just after the crossover of terminal voltage at point ($V_S > 1.5 \text{p.u}$) the nature of the system changed from electrical mode to electromechanical mode. Which is observed with help of participation factors. Now the electoro-mechanical mode is contributed by stator dynamics and rotor dynamics (e'_{ds}, ω_r). With increasing of terminal voltage at MAPT regime the electro-mechanical modes move toward the imaginary axis and the magnitude of imaginary axis is increasing , the damping ratio drops from 11% to 4%. It is indicating a less stable condition.

With the increasing of terminal voltage in the MAPT regime ($P_{togrid} < 1 \text{p.u and} \omega_r < \omega_s$) the lowest frequency mode which is called mechanical mode contributed by the generator speed ω_r and the turbine speed ω_t up to some extent ($V_S \leq 1.5 \text{p.u}$), it is observed by participation factor (λ_5, λ_6) in table 4.12 (b). After the point ($V_S > 1.5 \text{p.u}$) the participation factor (λ_5, λ_6) tend to shift to (λ_6, λ_7), which is corresponding with shaft and turbine dynamics, by torsion angle θ_{wt} and turbine speed ω_t, of frequency $0.775[Hz]$. It is the dominant mode. With the increase of terminal voltage the mechanical mode tends toward the imaginary axis, so we can say that in an overvoltage condition the mechanical modes is indicating a less stable condition. For the depressed voltage condition $V_S \leq 0.5 \text{p.u}$ the system is over damped.

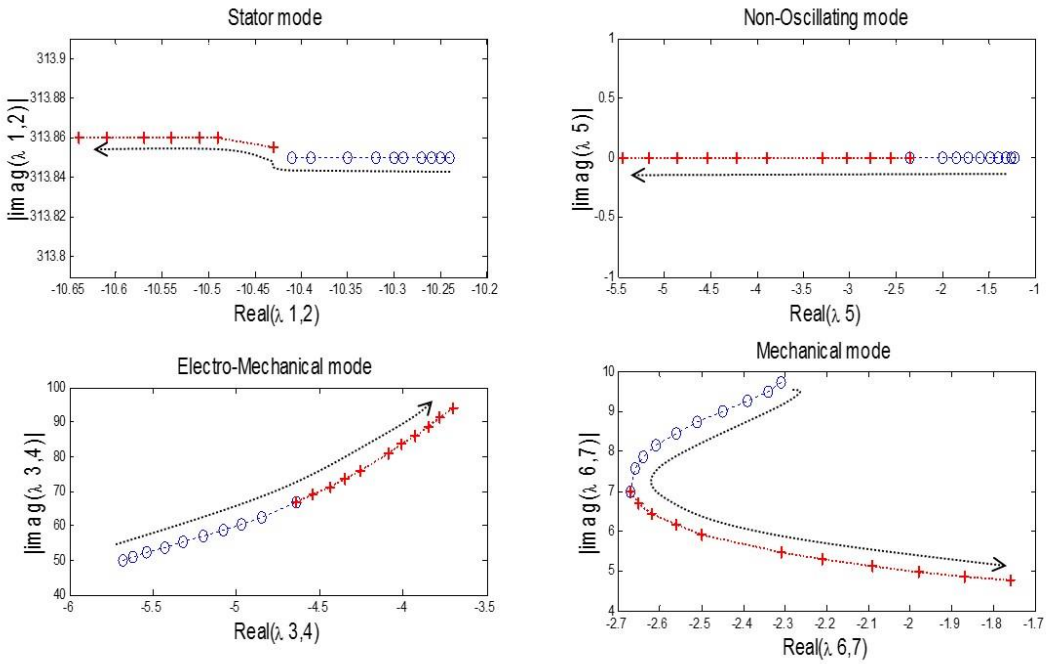

Fig. 4.10: Eigenvalue loci for increasing terminal voltage$\left(V_S = 0.5 \sim 2.5\ \mathrm{p.u}\right)$ with $P_{togrid} = 0.5\ \mathrm{p.u}$, $Q_{togrid} = 0\ \mathrm{p.u}$ the symbols "0" and "+" are used for voltages below and above 1.5. Respectively

4.8.9 Drive Train Parameters

As expected, varying the values of inertia constants and stiffness while keeping all other parameters at their base-case values does not affect the eigenvalues displacement of the electrical mode (stator mode and non-oscillating mode) significantly. Hence the following discussion describes only the effect on the mechanical and electromechanical modes.

For a tow-mass drive train, the mechanical state variables contribute to two modes, one is of a lower frequency, which is the non-torsional mode (cause in-phase oscillations of inertias). The other is of a higher frequency, which is the torsional mode (causes antiphase oscillations of inertias) [115]. The mechanical parameters determine which of these two modes is dominant and whether they are mechanical or electro-mechanical.

Table 4.13: Non-torsional and torsional mode for drive train parameters at point

$$(k = 0.3\,pu/el.rad\,, H_t = 0.5\,s)$$

(a) Eigenvalues λ, nature of the modes, Oscillation frequency f_{osc} [Hz] and damping ratio

	$\lambda = \sigma \pm j\omega$	Nature of the mode	$f_{osc} = \omega/2\pi$	$\zeta = -\sigma/\sqrt{\sigma^2 + \omega^2}$
λ_1, λ_2	$-10.58 + 313.90i$	Electrical mode	$49.98[Hz]$	$0.0337\ [pu]$
λ_3, λ_4	$-4.28 + 80.41i$	Electro-mechanical	$12.80[Hz]$	$0.0531[pu]$
λ_5	$-8.27 + 0.00i$	non-oscillating mode	$0\ [Hz]$	$1.00[pu]$
λ_6, λ_7	$-0.88 + 9.25i$	Mechanical mode	$1.472[Hz]$	$0.094\ [pu]$

(b) Participation factor for drive-train parameters at point $(k = 0.3\,pu/el.rad\,, H_t = 0.5\,s)$

	λ_1	λ_2	λ_3	λ_4	λ_5	λ_6	λ_7
i_{qs}	0.53	0.53	0.05	0.05	0.00	0.00	0.00
i_{ds}	0.50	0.50	0.04	0.04	0.00	0.00	0.00
e'_{qs}	0.00	0.00	0.04	0.04	1.00	0.00	0.00
e'_{ds}	0.03	0.03	0.49	0.49	0.01	0.00	0.00
ω_t	0.00	0.00	0.00	0.00	0.00	0.49	0.49
θ_{wt}	0.00	0.00	0.04	0.04	0.00	0.45	0.45
ω_r	0.00	0.00	0.50	0.50	0.00	0.00	0.00

In this thesis the relationship between generator and turbine inertia constant is $H_g = 0.2667 H_t$ and the stiffness function $(k < 1\,p.u/el.rad)$. In such a case the non-torsional mode is the dominant mode [131, 153], which is mechanical mode contributed by torsional angle θ_{wt} and wind turbine speed ω_t. That is shown in table 4.13. Where the lowest frequency mode (λ_6, λ_7) about $1.472[Hz]$ is closest to the imaginary axis and has significant participation factor from shaft and turbine states

(ω_t , θ_{wt}).with increasing of inertia constants from $0.5H_t$ to $4H_t$ the mechanical mode, stator mode and electro-mechanical mode is shown in the figure 4.11. The non-oscillating mode is not significantly affected and it is not shown in the figure.

The stability margin of the electro-mechanical mode tends to decrease as its real part of eigenvalues approaches to origin.

For the electrical high frequency mode which is stator mode, changes do take place in the real part but to a lesser extent.

In the figure 4.11 shows the dominant mode is the lowest mechanical mode (λ_6, λ_7) the imaginary part tends to decrease with inertia constants increases , the real part of the mechanical mode tends to decrease up to some extent ($H_t \leq 2.5$) behind that the real part of the mechanical mode again started to increase ,it give a massage for better stability. Which is nicely explained in figure 4.11.

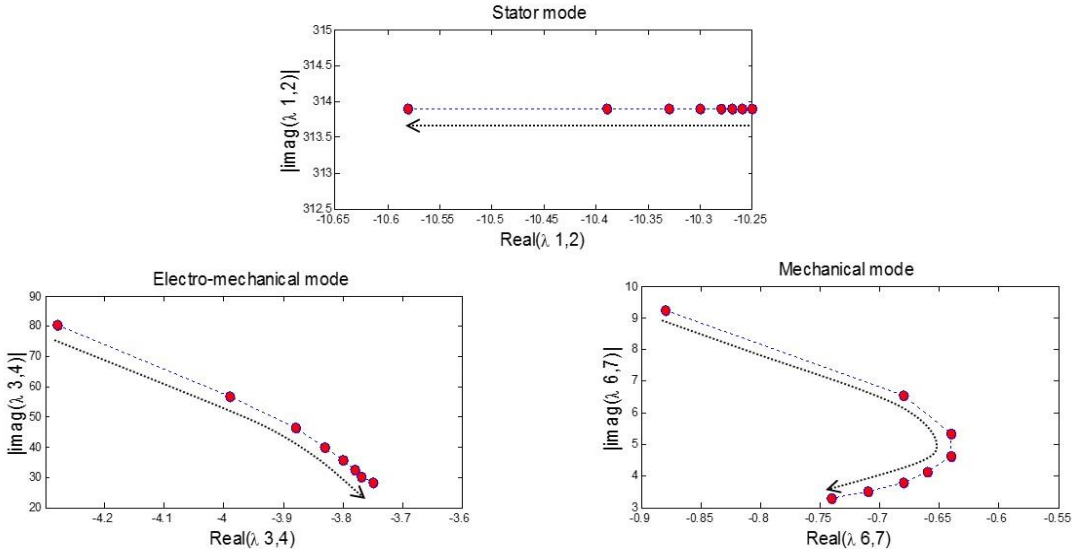

Fig. 4.11: Effect of inertia constants variation at synchronous regime for increasing inertia constant ($H_t 0.5 \sim 4\, p.u/el.rad$)while keeping stiffness function

$(k < 1\ p.u/el.rad)$

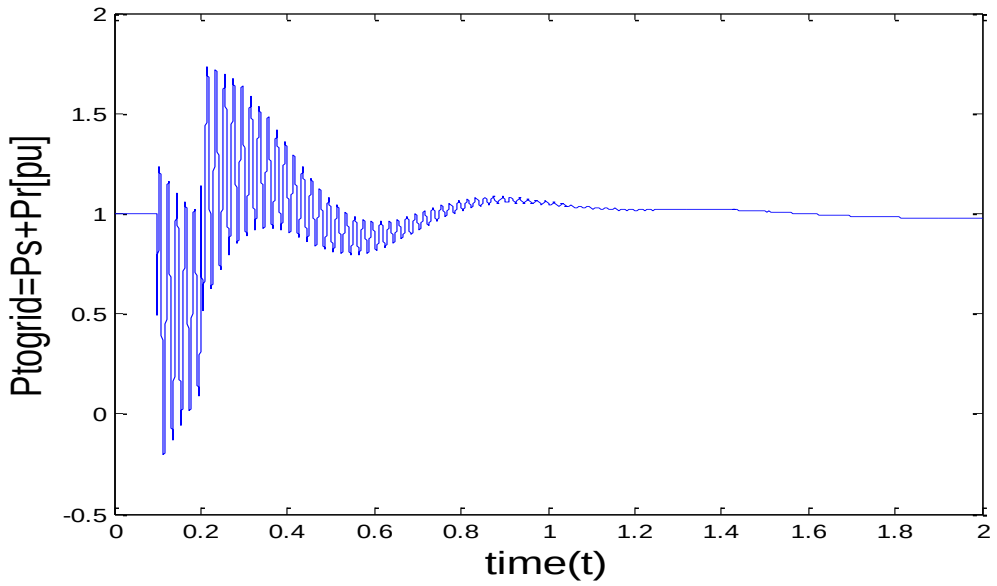

Fig:-4.12 Visualization of the DFIG modes in time domain: active power response to change in inertia constant at point ($k = 0.3\ pu/el.rad, H_t = 0.5s$)

Now concerning the shaft stiffness variations, and keeping the machine inertia constant value equals to the base case mode. Changes are significant only in the medium-frequency and in the low-frequency modes. For stiffer drive trains, the stability margin of the medium-frequency which is the electro-mechanical modes decreases whereas the low-frequency mode which is mechanical tend to increase. Oscillation frequency increases with stiffness function (k) value increases and the damping ratios deteriorate for the whole range speed. The participation factors are also affected negatively. For synchronous generator the stiffness is relatively higher and inertias are of the same order ($k \geq 50\ p.u/el.rad, H_t \approx H_g \approx 1s$) [3, 115, 152] in such a case the torsional mode is the dominant mode, which is the mechanical mode. In this thesis the stiffness values increases from

($0.3 \sim 8\ p.u/el.rad$) and the relationship between generator and turbine inertia constant is $H_g = 0.2667 H_t$. Tables 4.14 and 4.15 shows the eigenvalues, eigenvalue properties and participation factor for better understanding of the figure 4.13.

Table 4.14: Non-torsional and torsional mode for drive train parameters at point $(k = 0.3\,pu/el.rad, H_t = 3s)$

(a) Eigenvalues λ, nature of the modes, Oscillation frequency f_{osc} [Hz] and damping ratio

	$\lambda = \sigma \pm j\omega$	Nature of the mode	$f_{osc} = \omega/2\pi$	$\zeta = -\sigma/\sqrt{\sigma^2 + \omega^2}$
λ_3, λ_4	$-3.78 \pm 32.59i$	Electro-mechanical	$5.18[Hz]$	$0.115[pu]$
λ_6, λ_7	$-0.68 + 3.78i$	Mechanical mode	$0.601[Hz]$	$0.177\ [pu]$

	λ_1	λ_2	λ_3	λ_4	λ_5	λ_6	λ_7
e'_{ds}	0.01	0.01	0.47	0.47	0.00	0.04	0.04
ω_t	0.00	0.00	0.00	0.00	0.00	0.49	0.49
θ_{wt}	0.00	0.00	0.04	0.04	0.00	0.45	0.45
ω_r	0.00	0.00	0.50	0.50	0.00	0.00	0.00

Table 4.15: Non-torsional and Torsional mode for drive train parameters at point $(k = 8\,pu/el.rad, H_t = 3s)$

(b) Eigenvalues λ, nature of the modes, Oscillation frequency f_{osc} [Hz] and damping ratio

	$\lambda = \sigma \pm j\omega$	Nature of the mode	$f_{osc} = \omega/2\pi$	$\zeta = -\sigma/\sqrt{\sigma^2 + \omega^2}$
λ_3, λ_4	-0.94 +67.24i	Electro-mechanical	$10.70[Hz]$	$0.014[pu]$
λ_6, λ_7	-3.52 +10.24i	Mechanical mode	$1.63[Hz]$	$0.325\ [pu]$

	λ_1	λ_2	λ_3	λ_4	λ_5	λ_6	λ_7
e'_{ds}	0.01	0.01	0.10	0.10	0.00	0.42	0.42
ω_t	0.00	0.00	0.04	0.04	0.00	0.46	0.46
θ_{wt}	0.00	0.00	0.40	0.40	0.00	0.10	0.10
ω_r	0.00	0.00	0.45	0.45	0.00	0.05	0.05

At synchronous speed the system dynamics change with increasing shaft stiffness above $k > 2$, as shown in figure 4.13. The dominant mode changes for stiffer drive-train at this regime, as observed from the results presented in table 4.14 and 4.15.

With k less than $k < 6$, the mechanical mode (λ_6, λ_7) is the dominant mode, otherwise, with increase of stiffness function $(k \geq 6)$ the dominance passes onto electro-mechanical mode (λ_3, λ_4). Now the (λ_3, λ_4) is the non-torsional mode, as it is the slowest mode for $(k \geq 6)$ and (λ_6, λ_7) operates as torsional mode. At $k < 2$ the medium frequency mode λ_3, λ_4 about $(5.18 \sim 6[Hz])$ which is electro-mechanical contributed by the rotor through the dynamic of the internal voltage (e'_{ds} 47%) and rotor speed (ω_r 50%) respectively .with increasing of stiffness function the nature of the electro-mechanical mode changes at point ($k \geq 7$), the electro-mechanical mode contributed by rotor dynamics (ω_r 45%) and the shaft which is turbine torsional angle (θ_{tw} 40%)and to a lesser extent by (e'_{sd} 10%) with oscillation frequency of about $10.70[Hz]$,this is shown in table (4.14).

The oscillation frequency of the mechanical mode λ_6, λ_7 varies between $0.601[Hz]$ and $3.35[Hz]$ For $0.3 < k < 3$ and remains constant up to about $1.63[Hz]$ above k=7. The λ_6, λ_7 tends to become an electro-mechanical mode from $k > 3$. The λ_6, λ_7 mode is mainly contributed by turbine speed ω_t and internal voltage e'_{sd} . It can be seen in figure 4.13 that for stiffer drive-trains, the λ_3, λ_4 mode is a poorly damped mode about 1.4% having the longest time constant. The λ_3, λ_4 diminishes below 10% for $k > 3$ and passes to mechanical mode which has been explained above.

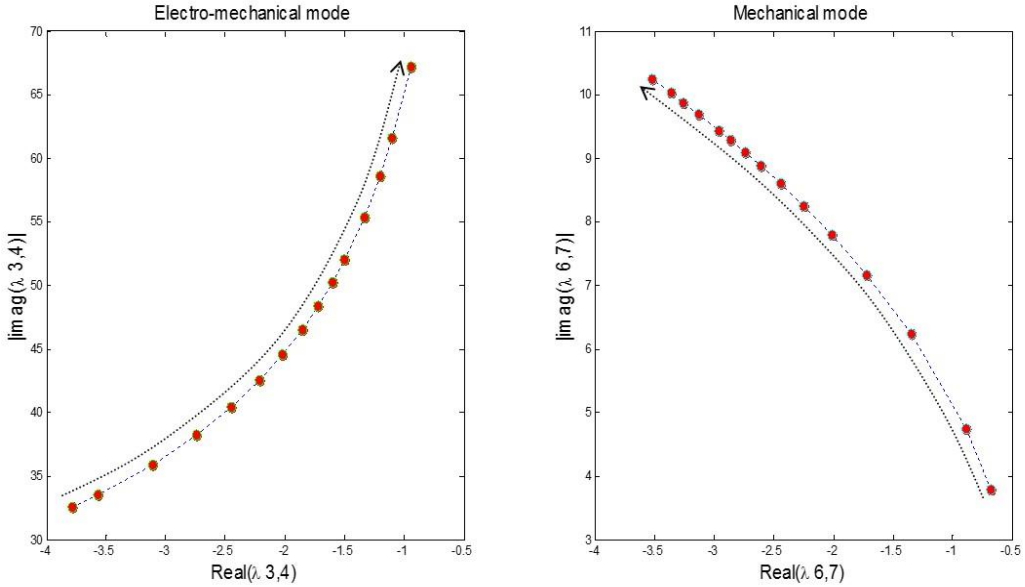

Fig. 4.13: Eigenvalue loci of electro-mechanical and mechanical modes for increasing stiffness function $(k = 0.3 \sim 8\ p.u/el.rad)$ while keeping inertia constant same as base case mode ($H_t = 3 and\ H_g = 0.2667 H_t$).

Where the higher frequency mode $(10.70[Hz])$ is closest to the imaginary axis and has significant participation factor only from the mechanical states (ω_r, θ_{wt}) .in general, this mode is out of the frequency range of interest and is not considered in stability studies of low-frequency oscillations.

4.9 Conclusion

This chapter presented the modal analysis of an SMIB system with DFIG. A seventh order model has been used with four state variables for the DFIG (stator and rotor dynamics) and three for the drive train (two-mass model). The results give the machine local modes, i.e., oscillations of the DFIG against the external system. The small-signal behavior is characterized by four modes, three

of which are oscillating. The slowest mode (which is the dominant mode) is the drive-train non-torsional mode. Oscillating at ~0.74 Hz, it is a mechanical mode associated with shaft and turbine dynamics. The second slowest mode is the drive-train torsional mode. Oscillating at ~6.57 Hz, at base case mode, it is an electromechanical mode associated with rotor dynamics (generator speed and rotor q-axis flux). The third oscillating mode is an electrical mode. Oscillating at ~49.8 Hz, it is associated with the stator dynamics. The no-oscillating mode has a small time constant of ~0.05 s and is associated with the rotor d-axis flux dynamics. The effects of several parameters (drive-train inertias, stiffness, generator mutual inductance, and stator resistance), operating points (rotor speed, reactive power loading, and terminal voltage level) on the system modes have been studied. The result of this study offer a good starting point for the small-signal stability analysis of multi machine power systems with both conventional synchronous generator (SC) and wind-drive DFIG. Finally numerical results offer the better understanding of the DFIG intrinsic dynamics, which can also be useful for control design and model justification. The control part will be studied in next chapter.

CHAPTER 5

Small Signal Stability Enhancement Using Genetic Algorithm

This chapter presents the dynamics and the state space modelling of the Doubly-fed induction generator (DFIG) with a closed-loop PI controller for small signal stability assessment. The discussion consider generic PI controller is used in rotor side converter for regulation of active and reactive power, rotor speed and pitch angle. Tuning these PI controllers is a tedious work and it is difficult to tune the PI gains optimally due to the nonlinearity and high complexity of the system. This thesis presents an approach to use Genetic algorithm to design the optimal PI controllers for tuning the gains in inner and outer control loop of rotor-side converter of DFIG for optimization of the system parameters. These optimized parameters results in improved damping ratio of DFIG and minimizes the oscillations in rotor voltage, rotor current and electro-magnetic torque. A new-fitness function is defined to measure the performance of the controllers. Simulation results show that the proposed design approach is efficient to find the optimal parameter of the PI controllers and therefore improve the small-signal stability performance of DFIG connected to grid over a wide range of operating condition. Eigenvalue analysis and time-domain simulations are performed on a single machine infinite bus (SMIB) system to illustrate the control performance of the system with and without Genetic algorithm for tuning of controller gains for optimization of the system parameters.

5.1 Background of the Study

Over the last few years the usage of wind power has been increased significantly, and its integration with the power system is now an important topic of study. In the present the capacity

of the installed wind power in the world stood at 333,337MW [137]. USA, China, Germany, Spain and India are the most wind energy producing countries in the world. With the growing penetration of wind energy into power grids, it is reducing the effective inertia of power networks [138]. Thus, the impact of wind turbine's generator on power system stability is of increasing concern, and the dynamics of wind turbines generator should be carefully considered in power system stability.

The wind energy conversion system (WECS) could be operationally classified into fixed speed and variable speed wind turbine generating system (WTGS). In the early stage of wind power generations, most wind farms were equipped with fixed speed induction generators (FSIG). The operation of FSIG is fairly simple but it is unable to extract maximum power at varying wind speed as its slip can be varied in a very small range. The development in technology has encouraged to switch from the fixed speed WTGS to variable speed WTGS mainly due to its advantages such as improved efficiency for wider range of wind speeds, independent control of active and reactive power, better fault ride through capability, etc. Currently the most common variable-speed wind turbine configurations are DFIG wind turbine and fully rated converter (FRC) wind turbine based on a synchronous or induction generator. Among the variable speed generators, the doubly-fed induction generator (DFIG) equipped wind turbine is currently one of the most preferred technologies in wind conversion systems due to its operation over a wide range of rotor speed[55, 154-157] high energy efficiency, reduced mechanical stress on the wind turbine and relatively low power rating of the connected power electronics converter [153]. Speed variability is possible due to the ac-dc-ac converter in the rotor circuit required to produce rotor voltage at slip frequency. Using a back-to-back converter allows bidirectional power flows and hence operation at both sub and super synchronous speed formulating the control algorithm of the converters in a synchronous rotating frame allows decoupled control of the generator speed (or active power) and terminal

voltage(or reactive power) . As the increasing penetration level of DFIG wind power generation into the grid, the stability issue of the DFIG wind turbine system is of particular increasing concern. It is very important to assess the role of DFIG on overall system stability both in transient and small signal sense. In order to carry out this task the authors investigated several ways to keep the system stable, the majority of studies based on neglecting the effect of stator and rotor transients [157-158], the performance of decoupled control strategy for active and reactive power proposed in [159], the performance of small-signal stability analysis of a grid connected DFIG under decoupled P-Q control and maximum power tracking [140],small signal stability assessment of DFIG including series dynamic breaking resistor (SDBR)[144], the response to grid disturbance [141], the ride-through behavior of DFIG during a voltage dip [142], the controlling strategies to make the DFIG behave as a synchronous generator [143], crowbar circuits in the rotor winding [163-166] etc. It has been studied that the stator transient of the DFIG in closed-loop controls is largely determined by its controllers [160]. Unlike synchronous generator, neglecting stator and rotor transient from DFIG model will produce a simplified but inaccurate model. So it is very essential to design a controller in rotor side converter to make certain that the stator transients are stable over a wide range of rotor speed and output power. And formulating the control algorithm of converters in synchronous rotating frame allows decoupling of active and reactive power. Once the controller gains are tuned, the simplified model can be included for stability analysis. On the other hand, the power electronics (IGBT-switches) in ac-dc-ac converter are the most sensitive part of the DFIG, when subjected to small signal and transient disturbances in the power network. As a result of such disturbances, the rotor side converter (RSC) may be blocked (it stops switching and trips) due to the protection from over-current in rotor circuit and the wind turbine might be tripped from the system. So the behavior of the switches and the associated DFIG relies on the

performance of its control system. With well-designed controllers. It is possible to increase the chances of the DIFG to remain in services during grid disturbances. To do this the various modern control techniques such as adaptive control, variable structure control and intelligent control [161-162] are proposed for controlling the nonlinear components in power system. However, these control techniques have few real applications probably due to their complicated structure or the lack of confidence in their stability. In [166], Hu *et al.* propose the use of a virtual resistance in combination with demagnetization control to limit the rotor side overcurrent. This method manages to enlarge the control range in relation to the control method proposed in [167], but the drawbacks that were met in [167] still cannot be avoided. The study described in [168] suggests that a properly designed fuzzy controller (FC) presents a better performance in presence of variations of parameters and external disturbances than a traditional proportional integral (PI) controller. Comparative results between the two controllers showed that the FC manages to limit the generator currents during the fault, avoiding the use of the crowbars. However, it would be interesting to see what would be the response of this control system and what changes should possibly be done, for the case where the DFIG would be connected to an infinite bus in small signal stability. In this thesis the protection and switching logics are generally assumed to be neglected for low frequency small-small signal stability studies as the switching frequency is far above the dynamics under study. Therefore, the conventional PI controllers, because of their simple structures and a low cost, are still the most commonly used control techniques in power systems, as can be seen in the control of the WTs equipped with DFIGs [55,142, 169]. PI controllers allow, in general a quick convergence between the reference and actual values of the active and reactive power delivered, when a change in the reference value occurs [170]. The tuning of the PI gains is very important task and even more vital to have optimized performance for a varying operating

conditions. The sound knowledge of the dynamic modelling of DFIG integrated to power system is required to adjust the PI gains in order to have optimized performance of DFIG in normal operation conditions as well as under sever disturbance on the system [168]. The authors investigated several techniques to tune PI gains, for example the classic control theory techniques, such as Ziegler-Nichols method and Cohen-coon method [171-172] and also trial and error method. The Ziegler-Nichols method can be used for both closed-loop and open loop systems, while Cohen-coon method is typically used for open loop system. In general the classic control techniques offer reasonable results in simple system, but unfortunately in the case of more complicated control system, the tuning of the controller gains are tedious work. As the system controller is complicating, the tuning process increases its complexity [171]. On the other hand the trial and error tuning method is probably the most known and the most widely used method for tuning of PID and PI controllers which is based on guess-and-check. Also known as online or continuous cycling or ultimate gain tuning method. In this method, the proportional action is the main control, while the integral and derivative actions refine it. The advantage of trial and error method is that it is case-dependent, it doesn't require the process model. The disadvantage of this technique that it is time consuming, it force the process into a condition of marginal stability that may lead to unstable operation or hazardous situation due to set point changes or extra disturbances and therefore is less attractive. As a result in the case of two-loop PI controllers in the rotor side converter, it will be difficult to achieve proper tuning by using Ziegler-Nichols method, this happens due to the complexity of DFIG control system, also trial and error method is less attractive, when DFIG connected to grid is in islanding operation, as a result of stronger coupling of active and reactive power. Last several years, heuristic search based algorithm such as evolutionary algorithms, taboo- search algorithm, simulated annealing (SA) have been used for optimization of

power system stabilizers design [173-174] due to its high efficiency in searching global optimal solutions on the search space. However, when the parameters being optimized are highly correlated, the performance of this heuristic search algorithms degrades [175-176]. Among these methods Particle Swarm Optimization (PSO) is a relatively recent heuristic search method whose mechanics are inspired by the swarming or collaborative behavior of biological populations. PSO is similar to the Genetic Algorithm (GA) in the sense that these two evolutionary heuristics are population-based search methods. In other words, PSO and the GA move from a set of points (population) to another set of points in a single iteration with likely improvement using a combination of deterministic and probabilistic rules [177]. The GA and its many intelligent computation techniques have been used as optimization tools in various research areas, including the design of controllers [178-179] mainly because of its intuitiveness, ease of implementation, and the ability to effectively solve highly nonlinear, mixed integer optimization problems that are typical of complex engineering systems. In reference [145, 180], Qiao .W and Wu.F, Zhang X .Particle swarm optimization technique (PSO) has been used to adjust the DFIG controllers gains with the objective of reducing over-current in the rotor circuit and improving the small-signal stability of the system. The results obtained with the application of the PSO techniques in reference [145,180] are compared with the results of trial and error technique. Which is not good to compare since the trial and error technique does not guarantee an optimal performance for the PI controller. Yufei Tang [146] used PSO for tuning PI gains to identify a uniformed dominate control parameters (UDCP) and optimize the UDCP to improve the dynamic performance of the wind generation system. Yateendra Mishra [181] proposed the Bacteria Foraging optimization method for tuning and adjustment of the PI controllers gains to enhance the damping of the oscillatory mode in the DIFG. However, the characteristic of exhibiting a robust damping and also improving

the stability margin may not be guaranteed simultaneously when a change in the operation condition occurs. Vrionis. D .Theodoros [182] proposed Genetic Algorithm (GA) for tuning the triangular membership functions (TMFs) of fuzzy controller to coordinate the control strategy of the DFIG converters during a grid fault, managing to ride-through the fault without the use of any auxiliary hardware. By this concept, the overcurrent's at the rotor windings and the dc side overvoltage's are effectively eliminated.

In the research of B.C. Pal and F. Mei [25] the modeling and small signal analysis of a grid connected DFIG were discussed without the optimization of the controller gains. This chapter focuses on the optimizing controller parameters of a DFIG wind turbine to enhance its small signal stability under grid connection. The Genetic Algorithm (GA) is used to determine the optimal gains for the PI controller to the rotor side converter of DFIG. A new fitness function is defined with the objective to shift all the eigenvalue as far to the left of the left hand side of the s-plane. It will improve the overall power system stability margin. Eigenvalue analysis and time-domain simulations are performed on a single machine infinite bus (SMIB) system to illustrate the control performance of the system with the optimized controller parameters. The result are shown with and without optimized controller in the table below.

5.2 Optimization Theory

Optimization is the act of obtaining the best result under given circumstances. The word 'optimum' is taken to mean 'maximum' or 'minimum' depending on the circumstances. In design, construction, and maintenance of any engineering system, engineers have to take many technological and managerial decisions at several stages. The ultimate goal of all such decisions is either to minimize the effort required or to maximize the desired benefit. Since the effort required

or the benefit desired in any practical situation can be expressed as a function of certain decision variables, so optimization can be defined as the process of finding the conditions that give the minimum or maximum value of a function, where the function represents the effort required or the desired benefit.

5.2.1 Objectives of Optimization

- Understand the need and origin of the optimization methods.
- Get a broad picture of the various applications of optimization methods used in engineering.

In this thesis the main objective of engineering optimization is to propose an easy technique for tuning of the PI controller gains for overall stability of the DFIG dynamics.

5.2.2 Engineering Applications of Optimization

- Design of structural units in construction, machinery, and in space vehicles.
- Maximizing benefit/minimizing product costs in various manufacturing and construction processes.
- Optimal path finding in road networks/freight handling processes.
- Optimal production planning, controlling and scheduling.
- Optimal Allocation of resources or services among several activities to maximize the benefit.

5.2.3 The Main Technique of Optimization

(a) Classical Optimization Technique:

The classical methods of optimization are useful in finding the optimum solution of continuous and differentiable functions. These methods are analytical and make use of the techniques of differential calculus in locating the optimum points. Since some of the practical problems involve objective functions that are not continuous and/or differentiable, the classical optimization techniques have limited scope in practical applications. However, a study of the calculus methods of optimization forms a basis for developing most of the numerical techniques of optimization presented more suitable to today's practical problems. Three main types of problems can be handled by the classical optimization techniques: single variable functions, multivariable functions with no constraints, multivariable functions with both equality and inequality constraints. The several types of classical optimization technique is listed below.

Linear programming: studies the case in which the objective function *f* is linear and the set A is specified using only linear equalities and inequalities. (A is the design variable space).

Integer programming: studies linear programs in which some or all variables are constrained to take on integer values.

Quadratic programming: allows the objective function to have quadratic terms, while the set A must be specified with linear equalities and inequalities.

Nonlinear programming: studies the general case in which the objective function or the constraints or both contain nonlinear parts.

Stochastic programming: studies the case in which some of the constraints depend on random variables.

Dynamic programming: studies the case in which the optimization strategy is based on splitting the problem into smaller sub-problems.

Combinatorial optimization: is concerned with problems where the set of feasible solutions is discrete or can be reduced to a discrete one.

Infinite-dimensional optimization: studies the case when the set of feasible solutions is a subset of an infinite-dimensional space, such as a space of functions.

Constraint satisfaction: studies the case in which the objective function *f* is constant (this is used in artificial intelligence, particularly in automated reasoning).

(b) Advanced Technique of Optimization:

Many difficulties such as multi-modality, dimensionality and differentiability are associated with the optimization of large-scale problems. Traditional techniques such as steepest decent, linear programing and dynamic programing generally fail to solve such large-scale problems especially with nonlinear objective functions. Most of the traditional techniques require gradient information and hence it is not possible to solve non-differentiable functions with the help of such traditional techniques. Moreover, such techniques often fail to solve optimization problems that have many local optima. To overcome these problems, there is a need to develop more powerful optimization techniques which is called advanced technique of optimization. Research is still going on to find more effective optimization techniques. Some of the well-known population-based advanced optimization techniques developed during last three decades are: Genetic Algorithms (GA) [183] which works on the principle of the Darwinian theory of the survival-of-the fittest and the theory of evolution of the living beings; Artificial Immune Algorithms (AIA) [184] which works on the principle of immune system of the human being; Particle Swarm Optimization (PSO) [185] which works on the principle of foraging behavior of the swarm of birds; Differential Evolution (DE)

[186] which is similar to GA with specialized crossover and selection method; Bacteria Foraging Optimization (BFO) [187] which works on the principle of behavior of bacteria; Shuffled Frog Leaping (SFL) [188] which works on the principle of communication among the frogs, Artificial Bee Colony (ABC) [189] which works on the principle of foraging behavior of a honey bee; Biogeography-Based Optimization (BBO) [190] which works on the principle of immigration and emigration of the species from one place to the other; Gravitational Search Algorithm (GSA) [191] which works on the principle of gravitational force acting between the bodies and Grenade Explosion Method (GEM) [192] which works on the principle of explosion of grenade. These algorithms have been applied to many engineering optimization problems and proved effective to solve some specific kind of problems.

5.3 Objective Function

The conventional design procedures aim at finding an acceptable or adequate design that merely satisfies the functional and other requirements of the problem. In general, there will be more than one acceptable design, and the purpose of optimization is to choose the best one of the many acceptable designs available. Thus a criterion has to be chosen for comparing the different alternative acceptable designs and for selecting the best one. The criterion with respect to which the design is optimized, when expressed as a function of the design variables, is known as the criterion or merit or objective function. The choice of objective function is governed by the nature of problem. The objective function for minimization is generally taken as weight in aircraft and aerospace structural design problems. In civil engineering structural designs, the objective is usually taken as the minimization of cost. The maximization of mechanical efficiency is the

obvious choice of an objective in mechanical engineering systems. In electrical engineering, the objective is usually taken as the minimization of disturbance and maximization of stability.

5.4 Constraints in Optimization

Any optimization problem can be classified as constrained or unconstrained, depending on whether or not constraints exist in the problem. A problem that does not entail any equality or inequality constraints is said to be an unconstrained optimization problem

5.5 Numerical Method of Optimization

The numerical method of optimization are used for solving both unconstrained and constrained optimization problems. The iterative method and heuristic method are the two main branch of numerical method.

(a) Iterative Method

Iterative method is a mathematical procedure that generates a sequence of improving approximate solutions for a class of problems. A specific implementation of an iterative method, including the termination criteria, is an algorithm of the iterative method. An iterative method is called convergent if the corresponding sequence converges for given initial approximations.

The iterative methods used to solve problems of nonlinear programming differ according to whether they evaluate Hessians, gradients, or only function values. While evaluating Hessians (H) and gradients (G) improves the rate of convergence, for functions for which these quantities exist and vary sufficiently smoothly, such evaluations increase the computational complexity (or computational cost) of each iteration. In some cases, the computational complexity may be

excessively high. Iterative method contains several types such as steepest decent method, modified Newton's method, conjugate gradient's method, reduced gradient's method etc.

(b) Heuristic Method

In computer science, artificial intelligence, and mathematical optimization, a heuristic is a technique designed for solving a problem more quickly when classic methods are too slow, or for finding an approximate solution when classic methods fail to find any exact solution. This is achieved by trading optimality, completeness, accuracy, or precision for speed. In a way, it can be considered a shortcut. The objective of a heuristic is to produce a solution in a reasonable time frame that is good enough for solving the problem at hand. This solution may not be the best of all the actual solutions to this problem, or it may simply approximate the exact solution. But it is still valuable because finding it does not require a prohibitively long time. The type of heuristic problems Genetic algorithms, Hill climbing, Simulated annealing, Tabu search, Particle swarm optimization, Evolutionary algorithms, Differential evolution.

With the increasing complexity of the modern control system researchers and control system engineers investigated the idea of applying new techniques in order to solve design problems for different control engineering problems. Among the aforementioned methods the Genetic Algorithm (GA) is the optimum choice for tuning the PI controller gains and is used in this thesis. As GA is a promising heuristic approach for locating near-optimal tuning solutions, they are easy to implement. Based on a criterion a new fitness function is defined with the objective to shift all the eigenvalue as far to the left of the left hand side of the s-plane. It will improve the overall power system stability margin. The simulation results obtained using Matlab/Simulink showed that the proposed controller had on one hand a good dynamic and static performance and on other hand had a better robustness compared to the conventional PI controller.

5.6 Genetic Algorithm

A genetic algorithm is a search technique used in finding true or approximate solutions to optimization and search problems. Genetic algorithms are categorized as global search heuristics. Genetic algorithms form particular class of evolutionary algorithms that use techniques inspired by evolutionary biology such as inheritance, mutation, selection and crossover (also called recombination). Genetic Algorithms are implemented as a computer simulation in which a population of abstract representations (called chromosomes or the genotype or the genome) of candidate solutions (called individuals, creatures, or prototypes) to an optimization problem evolves toward better solutions. Traditionally, solutions are represented in binary strings of 0s and 1s, but other encodings are also possible. The evolution usually starts from a population of randomly generated individuals. Genetic algorithms form on of the best ways to solve a problem for which a little is known. They are very general algorithms that work well in any search space. A genetic algorithm is able to create a high quality solution [193].

5.6.1 Background of Ga

The famous naturalist Charles Darwin defined natural selection or survival of the fittest in his book (Darwin, 1929) as the preservation of favorable individual differences and variations, and the destruction of those that are injurious. In nature, individuals have to adapt to their environment in order to survive in a process called evolution, in which those features that make an individual more suitable to compete are preserved when it reproduces, and those features that make it weaker are eliminated. Such features are controlled by units called genes, which form sets known as chromosomes. Over subsequent generations not only the fittest individuals survive, but also their genes which are transmitted to their descendants during the sexual recombination process, which is called crossover.

In the late 60s, John H. Holland became interested in the application of natural selection to machine learning. He developed a technique known as reproductive plans that allowed computer programs to mimic the process of evolution. This technique became popular after the publication of his book (1975). He renamed this technique using the term genetic algorithm (GA). The main goals of the research of Holland and his students were

- to abstract and rigorously explain the adaptive processes of natural systems.
- to design artificial systems software that retained the important mechanisms of natural systems.

Basically, the central thrust of the research on genetic algorithm GA has been due to its robustness and the balance between efficiency and efficacy necessary for survival in many different environments.

GA has been recognized as an effective and efficient technique to solve optimization problems. Compared with other optimization techniques, such as simulating annealing and random search method techniques, GA is superior in avoiding local minima, which is a significant issue in the case of nonlinear systems [196]. GA starts with an initial population containing a number of chromosomes (gens) where each one represents a solution of the problem, the evolution of the species is simulated through a fitness function and some genetic operators such as reproduction, crossover and mutation. The application of these three basic operations allows the creation of new individuals, which may be better than their parents. This algorithm is repeated for many generations. As this process is iterated, sequence of successive generation evolves and the average fitness of the chromosomes tends to increases until some stopping criterion is reached and finally stops when reaching individuals that represent the optimum solution to the problem. That is why,

GA “evolves” a best solution to any problem [194-195]. The GA flow chat is shown in figure 5.3 [122-124].

5.6.2 Fitness Function

A fitness function is a particular type of objective function that is used to summarize, as a single figure of merit, how close a given design solution is to achieve the set aims. In the GA each individual within the population is assigned a fitness value, which express how good the solution is at solving the problem. The fitness value probabilistically determines how successful the individual will be at propagating it genes (its code) to subsequent generations. Better solutions are assigned higher values of fitness than worse performing solutions.

5.6.3 Selection

The selection procedure implements the natural selection or the survival-of-the fittest principle and selects good individuals out of the current population for generating the next population according to the assigned fitness. For example choosing two parents from the population for crossing. After deciding on an encoding, the next step is to decide how to perform selection. Darwin stated in his theory of evolution that best ones survive to create new offspring. Selection is a method that randomly picks chromosomes out of the population according to their evaluation function. The higher the fitness function, the more chance an individual will be selected. Four common methods for selection are:

1. Roulette Wheel selection
2. Stochastic Universal sampling
3. Normalized geometric selection
4. Tournament selection

After selection, crossover and mutation recombine and alter parts of the individuals to generate new solutions.

5.6.4 Crossover

Crossover is a genetic recombination operator that combine two parents (chromosomes) to form children (offspring) for the next generation. The children are different from their parents but which inherit apportion of their parents' genetic materials. The main idea behind crossover is that the new chromosome may be better than both of parents (mates) if it takes best characteristics from each of the parents. Typically this operator is applied at a rate of 60% to 80% of the population, and the crossover point and each pair is randomly selected [200]. Various forms of crossover operator have been developed. The simplest form, single point crossover, is illustrated in figure 5.1. When using one-point crossover, only one crossover point is chosen at random. For example let there be two parents choses a random position in the genetic coding, and exchange genetic information to the right of this points, thus creating two new offspring.

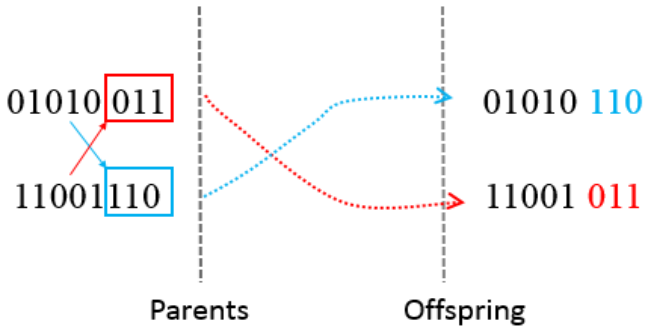

Fig. 5.1: single point crossover

5.6.5 Mutation

After crossover, the strings are subjected to mutation. Mutations are applying random changes to individual parents (chromosomes) to form children (offspring). It helps to keep diversity in the

population by discovering new or recovering the lost genetic materials by searching the neighborhood solution space. Despite the fact that mutation can serve a vital role in a genetic algorithm, it prevents the algorithm to be trapped in a local minimum. For a binary encoding, this involves swapping gene 1 for gene 0 with small probability (typically at the rate of 0.1% to 10%) [200] of each bit in the chromosome as shown in the figure 5.2.

Fig. 5.2: binary mutation operator

5.7 The Pi Controller Gains Using The Genetic Algorithm Approach

Genetic algorithm (GA) can be applied in the tuning of the PI controller gains to ensure optimal parameter optimization.it will help the optimal control performance in the DFIG. Considering small signal stability analysis, the main purpose of the PI controller in the rotor side converter based on GA is to increase the system damping ratio as well as to guarantee enough stability margin. To do this the fitness function of GA is used to obtain eigenvalues of state matrix $\mathbf{A}_{sys}$ to achieve satisfactory closed loop poles via controller to the desired reign in the complex plane.

The following paragraphs will describe the methodology to adjust the controllers' gains of the rotor-side converter based on the GA procedure.

The chromosome structure that will be used by the GA in the search procedure to obtain the best set of gains for the controllers of the rotor-side converter is presented in figure 5.3 [197-199]. This structure is composed of as set of eight gains where the first four are related to the inner loop of PI controller associated by reactive power and electrical torque and the last four are related to the outer loop of PI controller associated by rotor current as tabulated 5.1. The searching method

developed in this work using a GA technique for the PI controllers' gains tuning and adjustment is described by a flowchart with the following steps:

Step1:-initialization: - . Start the process by randomly generating (N–1) individuals of the initial population. Where each individual is a candidate solution of the problem. The numerical values that each gain may assume are constrained by low boundary and high boundary values, in p.u., as described in the following

$$low boundry \leq gains' values \leq high boundry$$

The set of gains obtained by the poles placement procedure composes one of the individuals of the initial population.

The set of gains of the two loop generic PI controller to be obtained forms one of the individuals of the initial population.

Table 5.1: chromosome structure

K_{Qs}	T_{Qs}	K_{id}	T_{id}	K_{Te}	T_{Te}	K_{iq}	T_{iq}

Step 2: Evaluation: Calculate the fitness value of each individual in the generation. The fitness value of individuals is given by:

$$g = -\min\left\{\frac{-real(\lambda_i)}{abs(\lambda_i)}\right\} \qquad (5.1)$$

$$for\, i = 1,2,3,...,N,....$$

Where g is the fitness value, λ_i are the eigenvalues and i is the number of eigenvalues of the closed loop system. In optimization the aim is to minimize g in order to shift all the eigenvalues as far to the left of the left hand side of the complex plane as possible.

Step 3: New generation: After the initial evaluation is concluded, the genetic operators are applied to obtain new individuals in the search space of the optimal solution. The search space of the optimal solution is consist of cross over and mutation.

Step 4: Stopping criteria: If one of the stopping criteria is satisfied, then stop, else go to Step2. Here, the stopping criteria may be the maximal number of iterations, or the fitness value of best smaller than a specified negative value.

Step 5: Updating velocities and positions:-if the convergence or termination criterion is not satisfied, the iterative process returns to step 2.

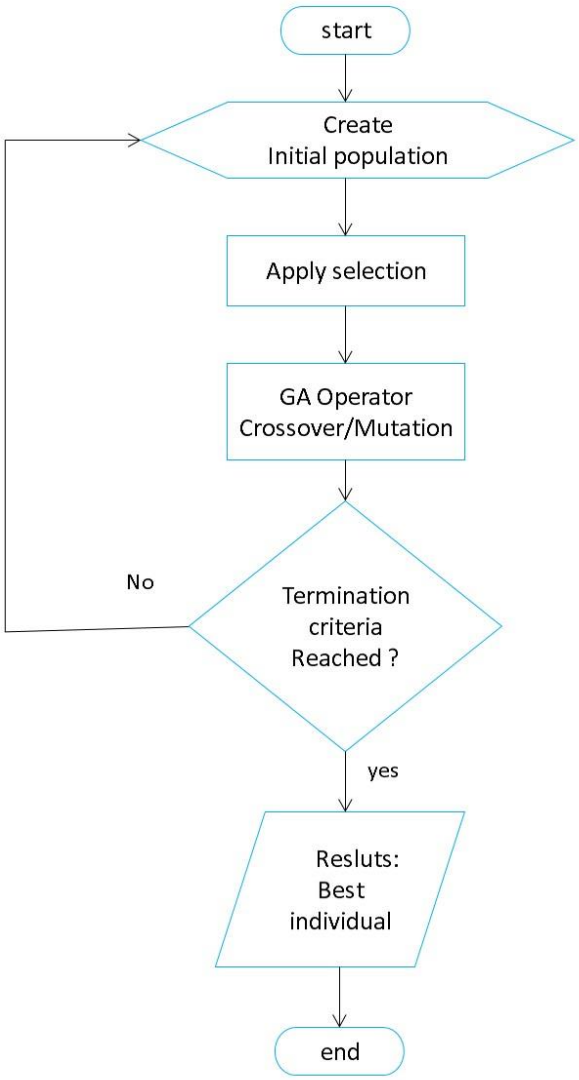

Fig. 5.3: Flowchart for the PI controllers' gains design

5.8 Modeling of DFIG Connected To Grid

Since SMIB system is adequate to investigate the dynamics, small signal stability and control design of a DFIG. Modeling of DFIG wind turbine connected to SMIB system has been presented earlier in chapter 3 and 4 as it is shown in figure (4.1). The DFIG wind turbine system, including

wind turbine, two mass drive train, induction generator and back-to-back PWM converter connected to grid is derived in chapter 3.9 and simulated with matlab in chapter 4.9. In this chapter GA is considered for the optimal design of generic PI controller in the rotor side converter of the DFIG. Where the RSC control consist in two decoupled loops. Each loop is a cascade of simple PI-control. The slower outer loop achieves the power or torque control and produces the set point for the faster inner current control loop this chapter just focus on the rotor side controller based GA. The pitch controller and the grid side controller can be found in [44, 146].

5.9 Rotor Side Converter Controllers' Model

In the article 4.7 the back to back PWM converter has been studied based on open loop design of DFIG, no controller has been added in the rotor side converter i.e. the rotor voltage (v_{qr} , v_{dr}) were remained constant at its initial value . In this chapter we will discuss the close loop controller in the rotor side converter. The rotor side voltages (v_{qr} , v_{dr}) are not any more constant rather they work as controller input variables.

As we mentioned in article 3.8, the vector control strategy (standard d-q axis frame) is used for the active power and reactive power control of wind turbine with DFIG system. For the RSC controller, the active power and electric torque are controlled independently via v_{qr} and v_{dr} .aligning the direction of the q axis of the d-q reference frame with the stator voltage, V_{ds} become zero and V_{qs} is equal to the terminal voltage value.

The controller of the rotor-side converter is a two-stage controller which is comprised of a real and reactive power controller [203-204] or reactive power and electric Torque controller as shown in figure 5.4. The rotor-side converter uses a torque controller to regulate the wind turbine output

power and the reactive power (or terminal voltage) measured at the machine stator terminals. The power is controlled in order to follow a pre-defined turbine power-speed characteristic to track the maximum power point. The actual electrical output power from the generator terminals, added to the total power losses (mechanical and electrical) is compared with the reference power obtained from the wind turbine characteristic. Usually, a proportional-integral (PI) controller is used at the outer control loop to reduce the power error (electric torque error) to zero. The output of this regulator is reference rotor current i_{qr-ref} that must be injected in the rotor winding by rotor-side converter. The q-axis component controls the electromagnetic torque T_e the actual i_{qr} component of rotor current is compared with i_{qr-ref} and the error is reduced to zero by a current PI regulator at the inner control loop. The output of this current controller is the voltage v_{qr} generated by the rotor-side converter. In d-axis frame with another similar PI controller obtained for i_{dr} , Q_s and v_{dr} components.

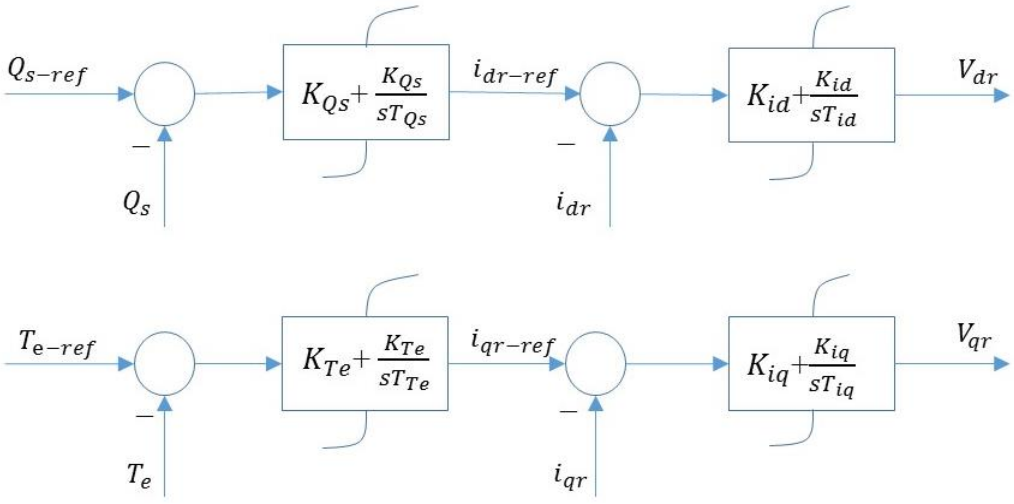

Fig. 5.4: Genetic control loops of the DFIG rotor side converter

As shown in the figure 5.4 the reference reactive power is a constant determined by the wind farm control center or a variable determined by an additional outer voltage control loop. In sub-rated wind speed, the reference torque is $T_{e-ref} = K_{OPT}\omega_r^2$, where K_{OPT} a constant is (defined in 3rd chapter) the set of differential and algebraic equations (DAEs) of the closed loop PI controllers are written as below:

The control equations for the q-axis inner control loop:

$$\dot{\Phi}_{T_e} = T_{e-ref} - T_e \tag{5.2}$$

The equation 5.2 is the torque error which can be written as,

$$\dot{\Phi}_{T_e} = T_{e-err} \tag{5.3}$$

$$\dot{\Phi}_{i_{qr}} = i_{qr-ref} - i_{qr} \tag{5.4}$$

Where i_{qr-ref} is equal to

$$i_{qr-ref} = T_{e-err}\left(K_{T_e} + \frac{K_{T_e}}{sT_{T_e}}\right) \tag{5.5}$$

$\because\ T_{e-err} = s\Phi_{T_e}$

$$i_{qr-ref} = K_{T_e}T_{e-err} + \frac{K_{T_e}}{T_{T_e}}\Phi_{T_e} \tag{5.6}$$

Putting equation 5.6 into 5.4 we get

$$\frac{d\Phi_{iqr}}{dt} = K_{T_e}T_{e-ref} + \frac{K_T}{T_T}\Phi_{T_e} - i_{qr} \tag{5.7}$$

$$\therefore\ \dot{\Phi} = \frac{d\Phi}{dt}$$

The control equations for the q-axis outer control loop:

$$V_{qr} = \dot{\Phi}_{iqr}\left(K_{iq} + \frac{K_{iq}}{sT_{iq}}\right) \tag{5.8}$$

$$\because\ \dot{\Phi}_{iqr} = s\Phi_{iqr}$$

After some simplification the equation 5.8 can be written as

$$V_{qr} = \dot{\Phi}_{iqr}K_{iq} + \frac{K_{iq}}{T_{iq}}\Phi_{iqr} \tag{5.9}$$

Now we will imply equation 5.7 into equation 5.9 then we will get the following equation of V_{qr} respectively,

$$V_{qr} = K_{iq}K_{Te}K_{e-err} + K_{iq}\frac{K_{Te}}{T_{Te}}\Phi_{T_e} - K_{iq}i_{qr} + \frac{K_{iq}}{T_{iq}}\Phi_{iqr} \tag{5.10}$$

The control equations for the d-axis inner control loop:

$$\dot{\Phi}_{Qs} = Q_{s-ref} - Q_s \tag{5.11}$$

The equation 5.11 is the torque error we can write it, as the following equation,

$$\dot{\Phi}_{Qs} = Q_{s-err} \tag{5.12}$$

The rotor actual current i_{dr} and reference current i_{dr-ref} can be compared as the following equation

$$\dot{\Phi}_{id} = i_{dr-ref} - i_{dr} \tag{5.13}$$

Where i_{dr-ref} is equal to

$$i_{dr-ref} = Q_{s-err}\left(K_{Qs} + \frac{K_{Qs}}{sT_{Qs}}\right) \tag{5.14}$$

$\because \Phi_{Qs} = \frac{Q_{s-err}}{s}$

After some simplification the Eq (4.14) can be written as

$$i_{dr-ref} = Q_{s-err}K_{Qs} + \frac{K_{Qs}}{T_{Qs}}\Phi_{Qs} \tag{5.15}$$

From the manipulation of equation 5.15 into 5.13 we get

$$\dot{\Phi}_{id} = Q_{s-err}K_{Qs} + \frac{K_{Qs}}{T_{Qs}}\Phi_{Qs} - i_{dr} \tag{5.16}$$

The control equations for the d-axis outer control loop:

$$v_{dr} = \dot{\Phi}_{id}\left(K_{id} + \frac{K_{id}}{sT_{id}}\right) \tag{5.17}$$

$\because \dot{\Phi}_{idr} = s\Phi_{idr}$

After some simplification the equation 5.17 can be written as

$$v_{dr} = \dot{\Phi}_{idr}K_{id} + \frac{K_{id}}{T_{id}}\Phi_{id} \tag{5.18}$$

Now we will imply equation 5.16 into 5.18, then we will get the following equation of V_{dr} respectively,

$$v_{dr} = K_{id} K_{Qs} Q_{s-err} + K_{id} \frac{K_{Qs}}{T_{Qs}} \Phi_{Qs} - K_{id} i_{dr} + \frac{K_{id}}{T_{id}} \Phi_{id} \qquad (5.19)$$

Equations 5.2–5.10 represent the q-axis control loop, $T_{e-err=}T_{e-ref} - T_e$ is the torque error, Φ_{Te} the state variable of the outer controller and Φ_{iq} is the state variable of the inner controller. Similarly, 5.11–5.19 represent the d-axis control loop, Φ_{Qs} and Φ_{id} are the state variables of the outer and inner controllers respectively, $Q_{s-err} = Q_{s-ref} - Q_s$ is the reactive power output error. The parameters K_{iq}, K_{id}, K_{Te} and K_{Qs} are the controller proportional gains (P-gains). From figure 5.4, K_{iq} and K_{id} have units of impedance, K_{Te} has units of speed over voltage and K_{Qs} has units of voltage inversed. Below, their values are given in per-unit on machine base. The parameters T_{iq}, T_{id}, T_{Te} and T_{Qs} are the controller reset times or integral times and have units of second.

5.10 GA-Multi Objective Optimal Control

The problem of adjusting the controller's gains of the rotor-side DFIG converter, considering a specific operating point, may be formulated as a multi-objective optimization problem. The objectives to be optimized are the absolute errors between the rotor reference currents, which are established by the PI controllers, and the rotor measured currents along the q and d axis respectively and the magnitude of the rotor voltage. By considering the DFIG vector control formulation as presented in above topic, it can be shown that the q and d components of the rotor current are very effective in controlling both the DFIG electric torque and the terminal voltage respectively. This way, improving the rotor current dynamic response (which may be obtained by minimizing the error between the rotor reference and measured currents) may reflect also in a

better dynamic performance for the DFIG stator active power and terminal voltage. Besides that, the minimization of an additional term in the objective function that will be responsible for obtaining optimized responses for the magnitude of the rotor voltage may improve the dynamic behavior of other variables which are controlled by the grid side converter, as for example the rotor active power which is a function of the rotor voltage, as well as the dc-link voltage, and the current and reactive power of the grid-side converter. This way the global objective is to improve the DFIG dynamic behavior after the occurrence of faults in the electrical network enhancing the ride-through capability, voltage control, and also increasing the small-signal margins of the power system. A measure that indicates if a good adjustment for the parameters of the rotor side converter has been achieved is given by the fitness function which is composed by the eigenvalues of state space matrix which will be minimized by the genetic algorithm optimization procedure.

5.11 Simulation Results

Initialization and linearization of 7th full-order dynamic model has been studied in 4th chapter. While considering the rotor voltage (v_{qr} , v_{dr}) remains constant at its initial value. To assess the effect of the machine-side controller the rotor voltage (v_{qr} , v_{dr}) works as controller state variables and a new control algorithm are applied to the 7th full-order model of DFIG. This simulation is carried out for the whole range of rotor speed.

Now the WT-DIFG system under new control algorithm is in fact an eleventh order model. The state vector is defined by

$$x = \left[i_{qs} \;\; i_{ds} \;\; e'_{qs} \;\; e'_{ds} \;\; \omega_r \;\; \theta_{tw} \;\; \omega_t \;\; x_c \right]^T \tag{5.20}$$

With

$$x_c = \left[\Phi_{id} \; \Phi_{iq} \; \Phi_{Te} \; \Phi_{Qs} \right]^T$$

Where x_c is the state variables of the PI controller in the machine-side converter. The state vector of the DFIG system under small signal stability studies are defined in chapter 4. The linearized model of equation 4.36 is used for the small-signal stability analysis and the matrix A_{sys} is the state matrix .its eigenvalues (real/complex) give the natural modes of the system. For the given case of the DFIG-based WT system, the characteristic equations is an eleventh-order equation: thus, it will yield eleven eigenvalues for a specific steady-state value of the rotor speed. Therefore, in general, most of the eigenvalues must be real and the other form 2 or 3 sets of complex conjugate pairs. The steady state initial operating points for these varying operating conditions are tabulated in table 4.1.

5.11.1 Controllers Tuning Procedure

In the research of Mei F and B.C. Pal [25] the controller gains are manually tuned by applying some theorems such as Gershgorin theorem and some other assumptions. In my opinion manually adjusting of the PI gains are tedious work and wastage of time. In other hand it is difficult to tune PI gains optimally. For example once we may obtain stable results but not satisfactory, as the eigenvalues may be close to the imaginary axis. Or we may obtains some eigenvalues in the right half plane, which shows the system is unstable. Also it happens with very small change in a single gain, the system is going toward unstable system. However, it is noticed from the eigenvalue analysis and the figures ,which using the optimal gains of the GA projected PI controller the DFIG system presents a better time response , eigenvalues , damping ratio and participation factors . Both cases are compared in the following tables and figures. Thus, the improvement is evident in all results. Table 5.2 shows the manually tuned controller parameters and optimized controller

parameters obtained after minimizing the objective function given in equation 5.1 with the help of GA.

Table 5.2 Controller parameters without GA and with GA

PI gains	Without GA	With GA
K_{Qs}	1	-1.4379
T_{Qs}	0.5	0.0976
K_{id}	-0.01	0.3519
T_{id}	5	0.6823
K_{Te}	-0.1	-0.9087
T_{Te}	0.5	0.9549
K_{iq}	-2.8	-0.1259
T_{iq}	0.001	0.0866

The results of eigenvalue analysis including frequency of oscillation, damping ration and percentage participation of all the states for two scenarios are tabulated in tables 5.3-5.4.

Table 5.3: Eigenvalues and properties of the eigenvalues with closed-loop PI controlled DFIG at synchronous speed without optimization

	$\lambda = \sigma \pm j\omega$	f_{osc},Hz	ζ	Dominant states (contribution in %)	
λ_1	-470.45 +j 0.00	0.00	1.00	Stator electrical	$i_{qs} = 87$
λ_2, λ_3	-22.37 ± j311	49.52	0.07	Stator and rotor electrical	$i_{ds} = 49, e_{ds} = 50$
λ_4	-8.02 + j0.00	0.00	1.00	Rotor electrical	$e'_{qs} = 95$
λ_5	-4.11 + j0.00	0.00	1.00	q-axis current control	$\Phi_{iqr} = 85$
λ_6, λ_7	-1.2 ± j9.11	1.45	0.36	Rotor mechanical	$\theta_{wt} = 50, \omega_r = 45$
λ_8, λ_9	-0.03 ± j0.40	0.063	0.074	d-axis current control and reactive power control	$\Phi_{iqs} = 50, \Phi_{idr} = 50$
λ_{10}	-0.13 +j0.00	0.00	1.00	Torque control	$\Phi_{Te} = 97$
λ_{11}	-0.01 + 0.00i	0.00	1.00	Turbine speed control	$\omega_t = 90$

Table 5.4: Participation factor of closed loop PI controlled DFIG without optimization

	λ_1	λ_2	λ_3	λ_4	λ_5	λ_6	λ_7	λ_8	λ_9	λ_{10}	λ_{11}
i_{qs}	0.87	0.02	0.02	0.00	0.00	0.00	0.00	0.00	0.00	0.00	0.00
i_{ds}	0.00	0.49	0.49	0.06	0.00	0.00	0.00	0.00	0.00	0.00	0.00
e'_{qs}	0.00	0.12	0.12	0.95	0.00	0.00	0.00	0.02	0.02	0.00	0.00
e'_{ds}	0.01	0.50	0.50	0.01	0.00	0.00	0.00	0.00	0.00	0.00	0.00
ω_t	0.00	0.00	0.00	0.00	0.00	0.04	0.04	0.00	0.00	0.00	0.90
θ_{tw}	0.00	0.00	0.00	0.00	0.00	0.50	0.50	0.00	0.00	0.00	0.00
ω_r	0.00	0.00	0.00	0.00	0.02	0.45	0.45	0.00	0.00	0.00	0.09
Φ_{Te}	0.00	0.00	0.00	0.00	0.00	0.00	0.00	0.00	0.00	0.97	0.00
Φ_{iqr}	0.00	0.00	0.00	0.00	0.85	0.01	0.01	0.00	0.00	0.00	0.00
Φ_{iqs}	0.00	0.00	0.00	0.00	0.00	0.00	0.00	0.50	0.50	0.00	0.00
Φ_{idr}	0.00	0.00	0.00	0.00	0.00	0.00	0.00	0.50	0.50	0.00	0.00

Table 5.5: Eigenvalues and properties of the eigenvalues with closed-loop PI controlled DFIG at synchronous speed with optimization.

	$\lambda = \sigma \pm j\omega$	f_{osc}, Hz	ζ	Dominant states (contribution in %)	
λ_1	-7680.46 + j0.00	0.00	1.00	Stator electrical	$i_{qs} = 99$
λ_2	-4725.9 + j0.00	0.00	1.00	Stator electrical	$i_{ds} = 98$
λ_3, λ_4	-26.77 ± j307.62	48.88	0.09	Rotor electrical	$e'_{qs} = 49, e'_{ds} = 48$
λ_5	-24.33 + j0.00	0.00	1.00	Reactive power control	$\Phi_{iqs} = 100$
λ_6	-425.05 + j0.00	0.00	1.00	q-axis current control	$\Phi_{iqr} = 92$
λ_7, λ_8	-6.59 ± j9.52	1.51	0.57	Rotor mechanical	$\theta_{wt} = 56, \omega_r = 44$
λ_9	-211 + j0.00	0.00	1.00	d-axis current control	$\Phi_{idr} = 100$
λ_{10}	-37.11 + j0.00	0.00	1.00	Torque control	$\Phi_{Te} = 100$
λ_{11}	-0.12 + 0.00	0.00	1.00	Turbine speed	$\omega_t = 93$

Table 5.6: Participation factor of closed loop PI controlled DFIG with optimization.

	λ_1	λ_2	λ_3	λ_4	λ_5	λ_6	λ_7	λ_8	λ_9	λ_{10}	λ_{11}
i_{qs}	0.99	0.01	0.16	0.16	0.00	0.00	0.00	0.00	0.00	0.00	0.00
i_{ds}	0.00	0.98	0.27	0.27	0.00	0.00	0.00	0.00	0.00	0.00	0.00
e'_{qs}	0.00	0.27	0.49	0.49	0.06	0.00	0.00	0.00	0.00	0.00	0.00
e'_{ds}	0.14	0.01	0.48	0.48	0.00	0.02	0.00	0.00	0.00	0.00	0.00
ω_t	0.00	0.00	0.00	0.00	0.00	0.00	0.06	0.06	0.00	0.06	0.93
θ_{tw}	0.00	0.00	0.00	0.00	0.00	0.12	0.56	0.56	0.00	0.00	0.00
ω_r	0.00	0.00	0.00	0.00	0.00	0.27	0.44	0.44	0.00	0.00	0.09
Φ_{Te}	0.00	0.00	0.00	0.00	0.00	0.01	0.00	0.00	0.00	1.00	0.01
Φ_{iqr}	0.01	0.00	0.00	0.00	0.00	0.92	0.13	0.13	0.00	0.05	0.01
Φ_{iqs}	0.00	0.07	0.00	0.00	1.00	0.00	0.00	0.00	0.48	0.00	0.00
Φ_{idr}	0.00	0.01	0.00	0.00	0.50	0.00	0.00	0.00	1.04	0.00	0.00

In the table 5.3-5.4 the eigenvalues, its properties and the participation factors of dominant states of the WT-DFIG under closed-loop PI controllers without optimizations are analyzed. There are three oscillation modes, the highest frequency mode, unlike the mode in open-loop, is associated with a coupling between the d-axis stator current component (i_{ds}) and rotor electrical dynamics

(e_{sd}). It is noticed that the damping ratio is slightly higher than open loop control. In general its damping ratio is lower around 7%. The medium frequency mode is mechanical mode contributed by θ_{wt} and ω_r, oscillating with a frequency of around 1.45 Hz, with an acceptable damping of ($>10\%$). The lowest frequency mode is the d-axis current control and reactive power control mode, contributed by Φ_{iqs} and Φ_{idr} oscillating with frequency of around 0.063 Hz. With damping ratio of ($<10\%$) which is not satisfactory result. Other modes are well damped. It should be noticed that for the closed-loop controlled DFIG, the controllers effectively separate the

mechanical dynamics from the electrical once and there is no electromechanical mode as opposed to the open-loop control case discussed in chapter four.

Now table 5.5-5.6 shows the results with optimized parameters of PI controllers with help of GA, as compared to table 5.3-5.4, respectively. There is two oscillating mode and nine non-oscillating mode. The physical nature of the modes can be identified by observing the participation factors in table 5.4: mode1 ($\lambda_{1,2}$) are non-oscillating mode associated with stator electrical dynamics i_{qs} and i_{ds} .mode1 has a large real part magnitude with zero frequency oscillations which results in highest damping ratio around 100%. Mode2 ($\lambda_{3,4}$) is the highest frequency oscillating mode, associated with rotor electrical dynamics e'_{qs} and e'_{ds} . Mode 2 has a large imaginary part magnitude and the much highest frequency of oscillations which results in lower damping ratio around 9% which is better compared to the without optimization mode in table 5.3. Mode 3(λ_5) is non-oscillating mode associated with reactive power control dynamics (Φ_{iqs}). It has a large real part magnitude and zero frequency oscillation which results in highest damping ratio. Mode 4(λ_6) is also non-oscillating mode associated with q-axis current control dynamics (Φ_{iqr}) it has a very large real part magnitude and zero frequency oscillation which results in highest damping ratio. Mode 5($\lambda_{7,8}$) is the lowest frequency mode which is a mechanical mode contributed by θ_{wt} and ω_r oscillating with a frequency of around 1.51Hz with acceptable damping ratio ($>10\%$).mode 6 and 7 (λ_9, λ_{10}) are non-oscillating mode, associated with d-axis current control dynamics (Φ_{idr})and torque control dynamics (Φ_{Te}) they has large real part magnitude in the left hand of S-plane, with zero frequency , which results in highest damping ratio.

Mode 8(λ_{11}) is also non-oscillating mode associated with turbine dynamics (ω_t). It has small real part magnitude but better than table 2.3 without optimization. In general It can be seen that with the optimized controller parameters, the number of oscillation modes decreases. All the damping ratios increase. All of the eigenvalues have shifted to the left in the *s*-plan. Which means that all the eigenvalues are into the left region which has larger stability margin.

In order to verify the effectiveness of the optimal controller design, the dynamic responses of the electrical torque (T_e), stator electrical dynamics (i_{qs}, i_{ds}), rotor electrical dynamics (e_{qs}, e_{ds}), turbine speed (ω_t), turbine torsion angle (θ_{wt}) and rotor speed (ω_r) at synchronous speeds of DFIG , with and without optimized controller are shown in figure 5.5 (a)-(h), respectively. To study the dynamic responses, the disturbance considered is the same as in chapter 4.

It can be seen that, with optimized controller parameters, the dynamic performance of studied variable speed wind turbine DFIG at synchronous speed are well improved where the oscillations after small-disturbance are well damped.

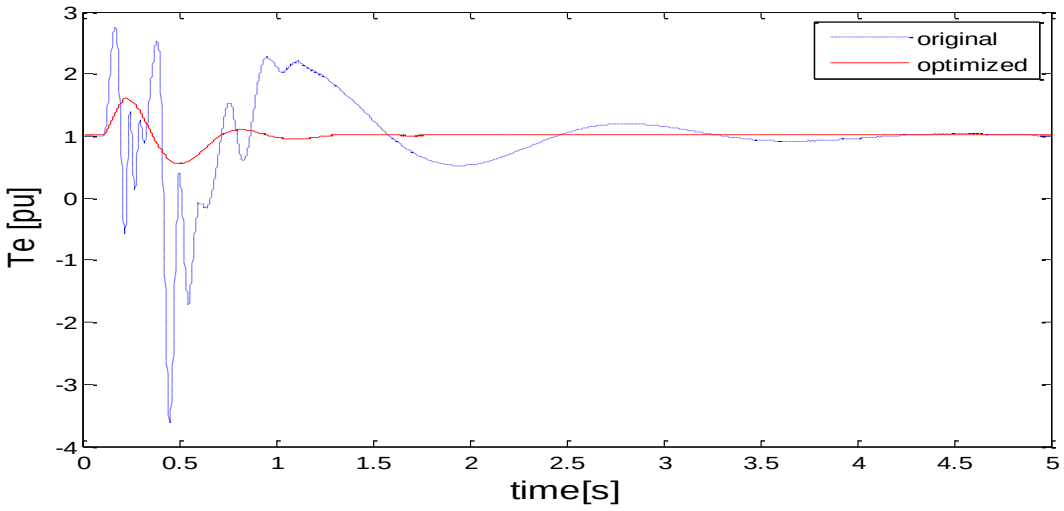

(a) Electrical torque(T_e)

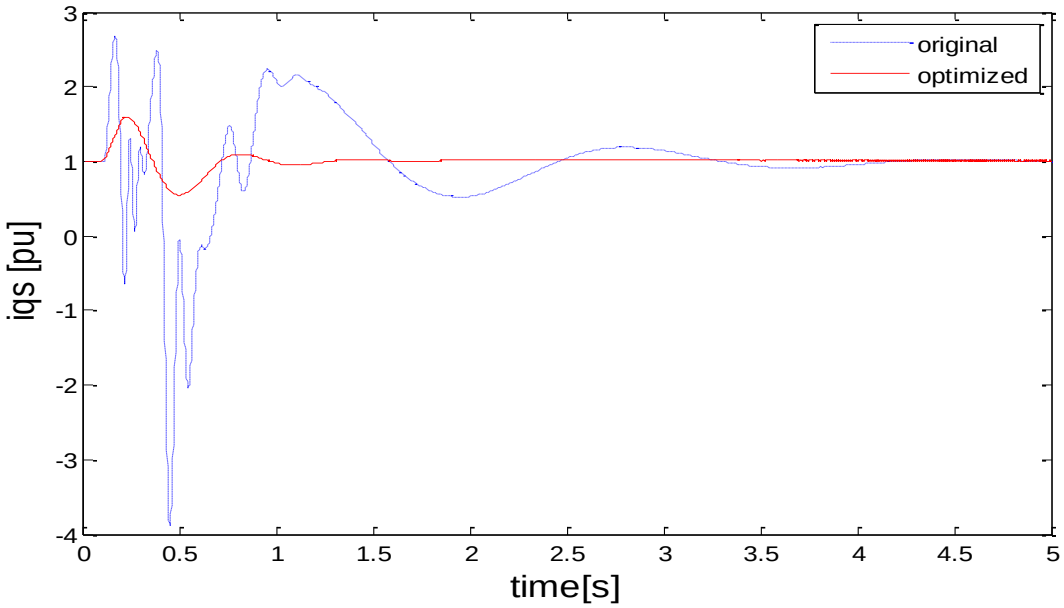

(b) q-axis stator electrical current (i_{qs})

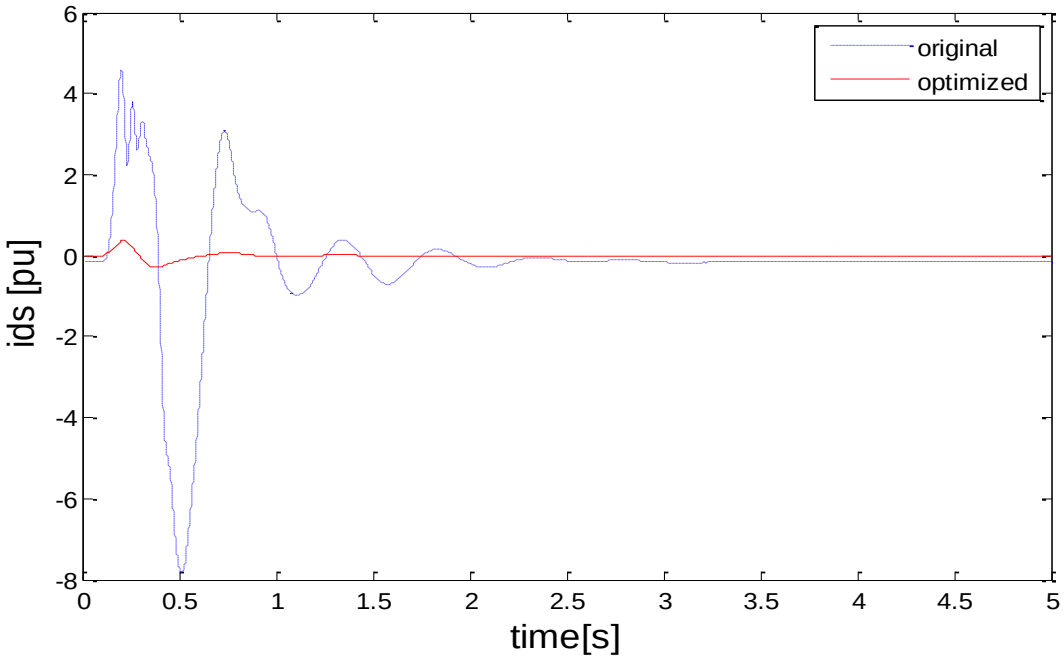

(c) d-axis stator electrical current (i_{ds})

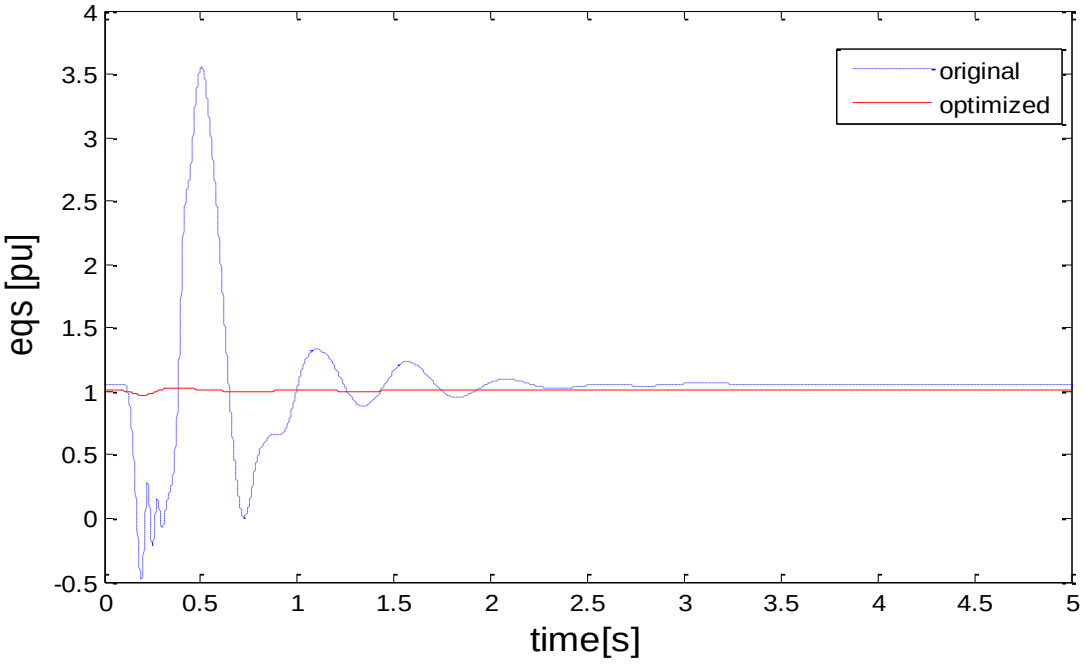

(d) q-axis rotor electrical voltage (e'_{qs})

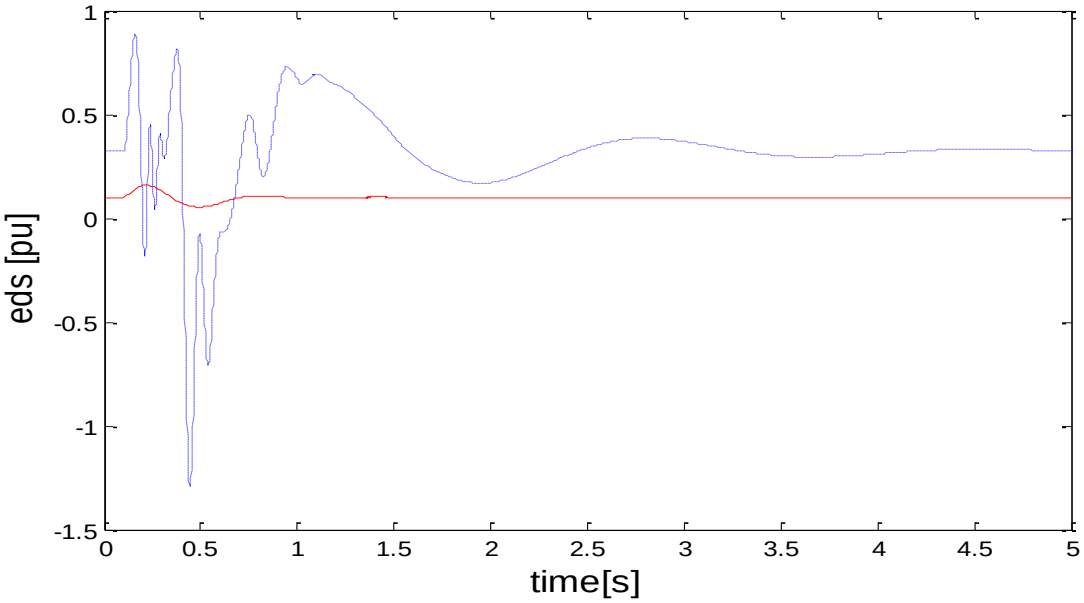

(e) d-axis rotor electrical voltage (e'_{ds})

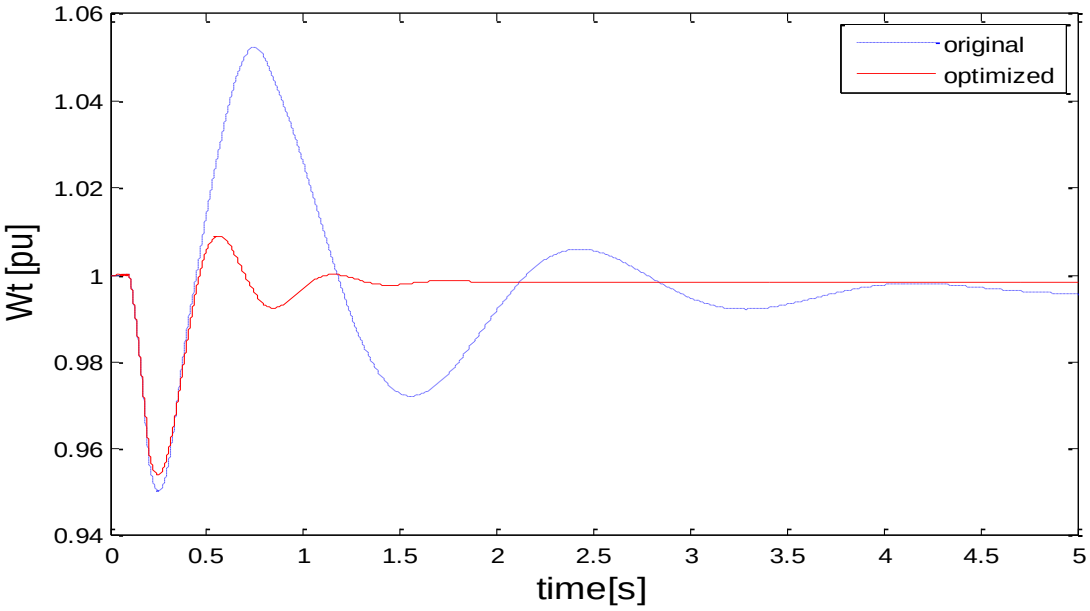

(f) wind turbine speed(ω_t)

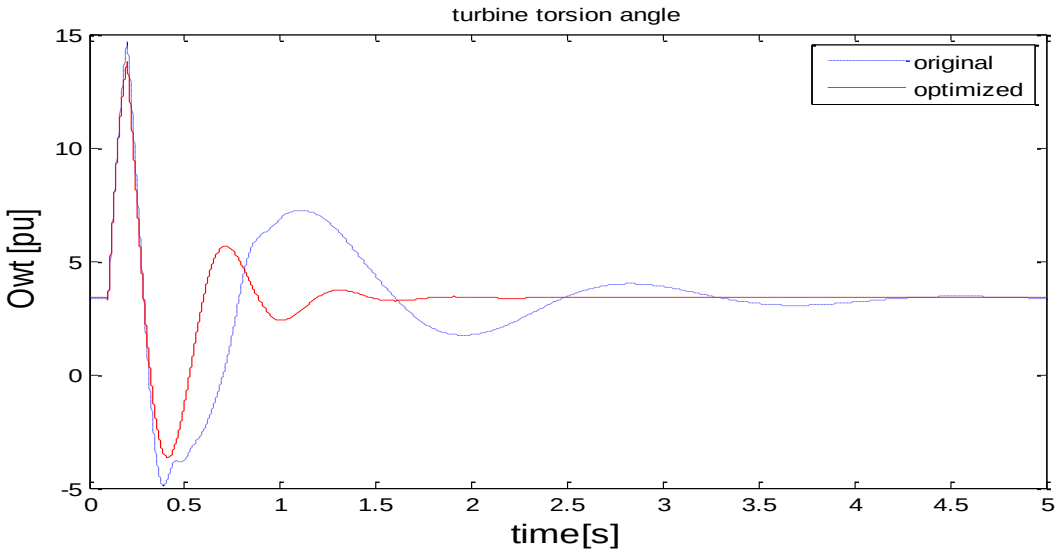

(g) turbine torsion angle (θ_{wt})

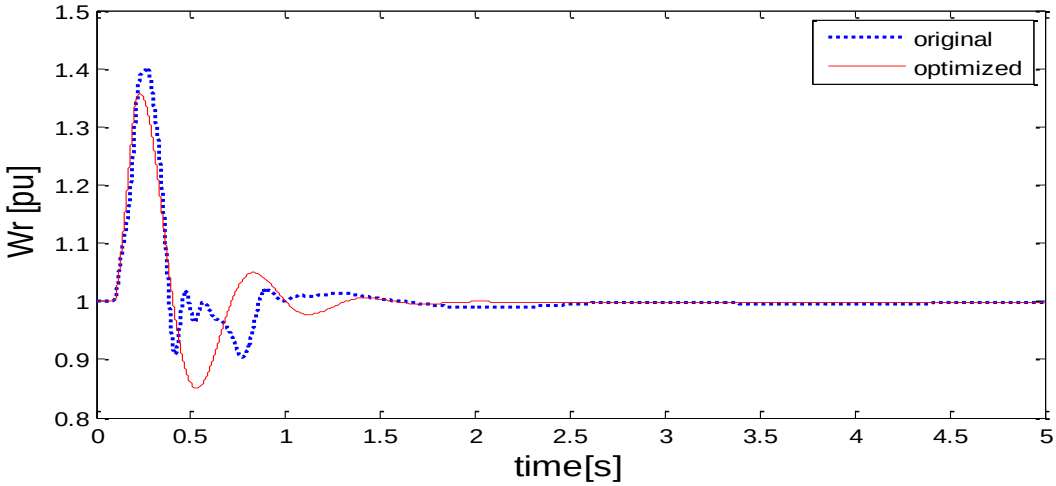

(h) rotor speed (ω_r)

Fig 5.5: The dynamic responses of the DFIG with and without optimization

CHAPTER 6

Conclusion

This research work basically focuses on the effect of introducing doubly-fed induction generator wind turbine to the grid system, of course, which is a renewable energy based system. Now it is clear that alternative source of energy like wind turbine based electric energy generation may be explored to continue generation of electrical power to meet the demand.

Although, among the renewable energy sources, the solar energy is considered one of the most popular because of the availability of free light energy from sun, but the solar energy is not going to the root level because of the cost of solar panel and complexity of using electronic circuit for maximum power point tracking. On the other hand countries like Afghanistan, New Zeeland, Germany where wind power is available in coastal or hilly areas, electricity can be generated using wind turbine. The challenge of using wind turbine is that it can be easily used in stand-alone way but difficulties arise if it is connected to grid. Therefore, in this thesis, a doubly fed induction generator (DFIG) has been studied with its dynamic model first. After that, modeling is done with the connection to grid. The complete grid connected DFIG has been designed for open loop and closed loop PI controller. Finally the system has been optimized using genetic algorithm.

6.1 Summary Of The Thesis:

Chapters 1 contain a general introduction to the thesis and to wind power technology. It was concluded that in some countries, as a result of legislation, governmental financial support and tax benefits to promote renewable energy sources, wind power has grown rapidly. It was also concluded that wind power fundamentally differs from conventional generation technologies, because the primary energy source is not controllable and because generating systems are used

that differ from the conventional directly grid coupled synchronous generator. Then the basics of wind turbine have been discussed. After that, literature review has been carried out on modeling of wind turbine equipped with DFIG. Literature Review has also been done on converter model, control strategies of wind turbine-generator system. Special attention has been given to the control strategies of DFIG from literatures. Finally the objectives of thesis have been explicitly mentioned with thesis organization.

It has been found very useful in order to contextualize the importance of the research i.e. chapter 2 starts with the general aspects of power system stability, definitions of stability , classification of power system stability, general category of stability more specifically transient stability and small signal stability. It should be mentioned that the impact of wind power on power system small signal stability is studied elaborately as it comes into discussion at later chapters in this thesis. For the contribution of DFIG and PI controller in case of power system operation. Furthermore, the mathematical treatment of the linearization of the non-linear equations describing a power system and of the relation between the eigenvalues and the time domain was given. Chapter 2 also include participation factor and it is definition which will use in chapter 4, and 5 for identification of state mode.

In chapter 3 a wind turbine system model equipped double fed induction generator was presented. The turbine performance was described by means of the energy conversion theory and general considerations regarding simulations for wind turbines in electrical power systems were presented. Simple turbine model assuming fixed speed and variable wind speed were discussed including their advantages and disadvantages. Simple turbine model assuming variable wind speed, rotor speed can be used in studies. Non-linear algebraic models in which power output is obtained from the wind speed were used in power system small signal stability analysis. The drive train was

modelled by the two-mass model approach in order to represent correctly the shaft dynamics. The electrical system model was expressed in per-unit notation and *d-q* reference frame and the mathematical model of electrical system is presented elaborately. The converter configuration was described and the machine side controller will be explained with detail in 5th chapter. Chapter 4 presents the modal analysis of an SMIB system with DFIG. A seventh order model has been used with four state variables for the DFIG (stator and rotor) dynamics and three for the drive train (two-mass model). The simulation results is carried out using Matlab software. Finally in the results of simulation it is has been shown that, the small-signal behavior is characterized by four modes, three of which were oscillation mode, and one mode was non-oscillating mode.

The Chapter 5 presents optimization theory, objective of optimization, engineering application of optimization, techniques of optimization, several techniques of optimization and genetic algorithm. Furthermore, the complete mathematical model of generic closed PI controller in the rotor side converter for the study of small signal stability of DFIG connected to grid presented in chapter 5. The model analysis results for this simplified representation of the power grid correctly include the effects of operating conditions, machine parameters and models and control system strategy. The results obtained certify that operating conditions, machine and system parameters affect markedly the location and nature of the oscillatory modes but also that the control approach adopted plays a major role. More specifically, it was found that stability of the DFIG-based wind turbine using conventional PI controller without optimization depends to a large extent on the tuning of the proportional-integral controllers and on having good knowledge of the machine parameters. It should be noticed the tuning of PI controller gains manually are tedious work. A change in operating scenarios or system topology may require a re-tuning of the PI controllers gains. Conversely, it was found that the tuning of PI controller gains with GA is a very convenient

vehicle to improve on the DFIG stability; it showed to be very robust under machine parameter and network variations. It yields electro-mechanical coupling cancellation without introducing additional modes and provides extra-damping which, in turn, reduces local oscillations. In brief, generic PI controller with Genetic algorithm presents a far better performance than the classical PI controller, in this application.

The conclusion, summery of the chapters, major contributions and future scopes are presented in chapter 6.

6.2 Major Contributions:

1. Mathematical formulation of full order nonlinear dynamic model of DFIG connected to grid is done.

2. A critical assessment of a parameters variation of a DFIG-based wind turbine led to the identification of the critical variables that affect most the frequency and damping ratio of the dominant oscillation modes is accomplished.

3. A better understanding of the dynamic performance of the DFIG based wind turbine has been achieved by implementation of the genetic algorithm optimization of closed loop PI controller. The obtained result is compared with the PI controller performance without optimization. The optimized results with genetic algorithm showed that the system presents far better performance than classical PI controller without GA.

4. A critical assessment of small signal stability analysis is carried out for different scenarios such as variation of parameters of drive train and DFIG, implementation of closed loop PI controller with and without optimization

It can be expected that this work may be helpful in feeding the grid with wind generated power for a stable operation.

6.3 FUTURE SCOPES:

I. The transient behavior of the DFIG-based wind turbine under proposed controller may be studied under large disturbance.

II. Eigenvalue analysis and time-domain simulations performance of Multi-machine power system under proposed controller may be studied.

III. Transient and small signal stability behavior of the DFIG-based wind turbine system under disturbance of grid failures may be studied.

IV. Reduced order model of the drive train system and the DFIG model under proposed controller may be studied.

References

[1] IEEE TF report, "Proposed terms and definitions for power system stability," *IEEE Trans. on Power Appart. and Syst.,*, Vol. PAS-101, pp.1894-1897, July 1982.

[2] J. G. Slootweg, "Wind power modelling and impact on power systems dynamics" Ph.D. dissertation, Delft Univ. Technol., Delft, The Netherlands,2003.

[3] Thomas Ackermann. (2012), Wind power on power system, Germany, A john Wiley& sons, Ltd, publications.

[4] Novak, P., Ekelund, T., Jovik, I., and Schmidtbauer, B., 1995, "Modeling and control of variable speed wind-turbine drive-system dynamics", *IEEE Control Systems*, Vol. 15, No. 4, pp. 28-38.

[5] Tao Sun, "Power Quality of Grid-Connected Wind Turbines with DFIG and Their Interaction with the Grid", Ph.D. dissertation, Aalborg University, Denmark, May 2004.

[6] S. M. Muyeen, Md. Hasan Ali, R. Takahashi, T. Murata, J. Tamura, Y. Tomaki, A. Sakahara and E. Sasano, "Comparative Study on Transient Stability Analysis of Wind Turbine Generator System Using Different Drive Train Models", *IET Renewable Power Generation*, Vol. 1, No, 2, pp. 131-141, June 2007.

[7] Stavros A. Papathanassiou and Michael P. Papadopoulos, "Mechanical Stresses in Fixed-Speed Wind Turbines Due to Network Disturbances", *IEEE Transactions on Energy Conversion*, Vol. 16, No. 4, pp. 361-367, December 2001.

[8] H. Li and Z. Chen, "Transient Stability Analysis of Wind Turbines with Induction Generators Considering Blades and Shaft Flexibility", *33rd Annual Conference of the IEEE Industrial Electronics Society*, Chongqing, China, pp. 1604 - 1609, November 2007.

[9] Gnanasambandapillai Ramtharanand and Nicholas Jenkins, "Influence of Rotor Structural Dynamics Representations on the Electrical Transient Performance of FSIG and DFIG Wind Turbines", *Wind Energy*, Vol.10, No. 4, pp. 293-301, August 2007.

[10] Boubekeur Boukhezzar and Houria Siguerdidjane, "Nonlinear Control of a Variable-Speed Wind Turbine Using a Two-Mass Model", *IEEE Transactions on Energy Conversion*, Vol. 26, No. 1, pp.149-162, March 2011.

[11] Wei Qiao, Wei Zhou, José M. Aller, and Ronald G. Harley, "Wind Speed Estimation Based Sensor less Output Maximization Control for a Wind Turbine Driving a DFIG", *IEEE Transactions on Power Electronics*, Vol. 23, No. 3, pp. 1156-1169, May 2008.

[12] Lucian Mihet-Popa, Frede Blaabjergand and Ion Boldea, "Wind Turbine Generator Modeling and Simulation Where Rotational Speed is the Controlled Variable", *IEEE Transactions on Industry Applications*, Vol. 30, No.1, pp. 3-10, January/February 2004.

[13] Francoise Mei and Bikash Pal, "Modal Analysis of Grid-Connected Doubly Fed Induction Generators", *IEEE Transactions on Energy Conversion*, Vol. 22, No.3, pp. 728-736, September 2007.

[14] Tomas Petru and Torbjörn Thiringer, "Modeling of Wind Turbines for Power System Studies", *IEEE Transactions on Power Systems*, Vol. 17, No. 4, pp. 1132-1139, November 2002.

[15] G. Quinonez-Varela and A. Cruden, "Modeling and Validation of a Squirrel Cage Induction Generator Wind Turbine during Connection to the Local Grid", *IET Generation, Transmission & Distribution*, Vol.2, No.2, pp. 301 -309, March 2008.

[16] Chen Wang and George Weiss, "Integral Input-to-State Stability of the Drive-Train of a Wind Turbine", *Proceedings of the 46th IEEE Conference on Decision and Control*, New Orleans, LA, USA, pp.6100-6105, December 2007.

[17] J. G. Slootweg, S. W. H. de Haan, H. Polinder and W. L. Kling, "General Model for Representing Variable Speed Wind Turbines in Power System Dynamics. Simulations", *IEEE Transactions on Power Systems*, Vol.18, No.1, pp.144-151, February 2003.

[18] Yazhou Lei, Alan Mullane, Gordon Lightbody, and Robert Yacamini, "Modeling of the Wind Turbine With a Doubly Fed Induction Generator for Grid Integration Studies", *IEEE Transactions on Energy Conversion*, Vol. 21, No. 1, pp. 257-264, March 2006.

[19] Janaka B. Ekanayake, Lee Holdsworth, Xueguang Wu and Nicholas Jenkins, "Dynamic Modeling of Doubly Fed Induction Generator Wind Turbines", *IEEE Transactions on Power Systems*, Vol.18, No.2, pp. 803-809, May 2003.

[20] L. J. Ontiveros, P. E. Mercado and G. O. Suvire, "A New Model of the Double-Feed Induction Generator Wind Turbine", *2010 IEEE Transmission and Distribution Conference and Exposition*, Latin America, pp. 263-269, November 2010.

[21] Daniel J. Trudnowski, Andrew Gentile, Jawad M. Khan, and Eric M. Petritz, "Fixed-Speed Wind-Generator and Wind-Park Modeling for Transient Stability Studies", *IEEE Transactions on Power Systems*, Vol. 19, No. 4, pp. 1911 -1917, November 2004.

[22] Wikipedia

[23] Kostyantyn Protsenko and Dewei Xu, "Modeling and Control of Brushless Doubly-Fed Induction Generators in Wind Energy Applications", *IEEE Transactions on Power Electronics*, Vol. 23, No. 3, pp.1191 - 1197, May 2008.

[24] Yongchang Zhang, Zhengxi Li, Jiefeng Hu, Wei Xu and Jianguo Zhu, "A Cascaded Brushless Doubly Fed Induction Generator for Wind Energy Applications Based on Direct Power Control", *2011 International Conference on Electrical Machines and Systems* , pp.1-6, August 2011.

[25] B.C. Pal and F. Mei : ' Modelling adequacy of the doubly fed induction generator for small-signal stability studies in power systems', IET Renew. Power Genre, 2008, Vol. 2, No. 3, pp. 181-190.

[26] Istvan Erlich, Jörg Kretschmann, Jens Fortmann, Stephan Mueller-Engelhardt and Holger Wrede, "Modeling of Wind Turbine Based on Doubly-Fed Induction Generators for Power System Stability Studies", *IEEE Transactions on Power Systems*, Vol.22, No.3, pp. 909-919, August 2007.

[27] Alvaro Luna, Francisco Kleber de Araujo Lima, David Santos, Pedro Rodríguez, Edson H. Watanabe, and Santiago Arnaltes, " Simplified Modeling of a DFIG for Transient Studies in Wind Power Applications" , *IEEE Transactions on Industrial Electronics*, Vol. 58, No. 1, pp. 9-20, January 2011.

[28] A. Samuel Neto, S. L. A. Ferreira, J. P. Arruda, F. A. S. Neves, P. A. C. Rosas and M. C. Cavalcanti, "Reduced Order Model for Grid Connected Wind Turbines with Doubly Fed Induction Generators", *IEEE International Symposium on Industrial Electronics*, pp. 2655-2660, June 2007.

[29] Pablo Ledesma and Julio Usaola, “Effect of Neglecting Stator Transients in Doubly Fed Induction Generators Models”, *IEEE Transactions on Energy Conversion*, Vol. 19, No. 2, pp. 459-461, June 2004.

[30] Katherine Elkington and Mehrdad Ghandhari, “Comparison of Reduced Order Doubly Fed Induction Generator Models for Nonlinear Analysis”, *IEEE Electrical Power & Energy Conference*, pp.1-6, October 2009.

[31] P. Sørensen, A. D. Hansen, T. Lund and H. Bindner, “Reduced Models of Doubly Fed Induction Generator System for Wind Turbine Simulations”, *Wind Energy*, Vol. 9, No. 4, pp. 299-311, August 2006.

[32] Alireza Abbaszadeh, Saeed Lesan and Vahid Mortezapour, “Transient Response of Doubly Fed Induction Generator Under Voltage Sag Using an Accurate Model”, *2009 IEEE PES/IAS Conference on Sustainable Alternative Energy (SAE)*, pp. 1-6, September 2009.

[33] Torbjörn Thiringer and Jorma Luomi, “Comparison of Reduced-Order Dynamic Models of Induction Machines”, *IEEE Transactions on Power Systems*, Vol.16, No. 1, pp. 119-126, February 2001.

[34] Gill G. Richards and Owen T. Tan, “Simplified Models for Induction Machine Transients under Balanced and Unbalanced Conditions”, *IEEE Transactions on Industry Applications*, Vol. IA-17, No. 1, pp. 15-21, January 1981.

[35] C. Hamon, “Doubly-fed Induction Generator Modeling and Control in Dig Silent Power Factory," Master Thesis, *KTH School of Electrical Engineering*, 2010.

[36] B. Pokharel, "Modeling, Control and Analysis of A Doubly Fed Induction Generator Based Wind Turbine System with Voltage Regulation," Master Thesis, *Tennessee Technological University*, December 2011.

[37] Vladimir Blasko and Vikram Kaura, “A New Mathematical Model and Control of a Three-Phase AC-DC Voltage Source Converter”, *IEEE Transactions on Power Electronics*, Vol. 12, No. 1, pp. 116-123, January1997.

[38] Bong-Hwan Kwon, Jang-Hyoun Youm and Jee-Woo Lim, "A Line-Voltage-Sensorless Synchronous Rectifier", *IEEE Transactions on Power Electronics*, Vol. 14, No. 5, pp. 966-972, September 1999.

[39] Yan Guo, Xiao Wang, Howard C. Lee and Boon-Teck Ooi, "Pole-Placement Control of Voltage-Regulated PWM Rectifiers Through Real-Time Multiprocessing", *IEEE Transactions on Industrial Engineering*, Vol. 41, No. 2, pp. 224-230, April 1994.

[40] Jae-Ho Choi, Hyong-Cheol Kim and Joo-Sik Kwak, "Indirect Current Control Scheme in PWM Voltage-Sourced Converter", *Proceedings of the Power Conversion Conference*, pp. 277-282, Nagaoka, August 1997.

[41] José R. Rodríguez, Juan W. Dixon, José R. Espinoza, Jorge Pontt and Pablo Lezana, "PW Regenerative Rectifiers: State of the Art", *IEEE Transactions on Industrial Electronics*, Vol. 52, No. 1, pp. 5-22, February 2005.

[42] N. Horiuchi and T. Kawahito, "Torque and Power Limitations of Variable Speed Wind Turbines Using Pitch Control and Generator Power Control", *2001 Power Engineering Society Summer Meeting*, Vol. 1, pp. 638-643, July 2001.

[43] Mohamed Mansour, M. N. Mansouri, and M. F. Mimouni, "Study of Performance of a Variable-Speed Wind Turbine with Pitch Control Based on a Permanent Magnet Synchronous Generator", *2011 8th International Multi-Conference on Systems, Signals & Devices*, pp. 1-6, March 2011.

[44] Eduard Muljadi and C. P. Butterfield, "Pitch-Controlled Variable-Speed Wind Turbine Generation", *IEEE Transactions on Industry Applications*, Vol. 37, No. 1, pp. 240-246, February 2001.

[45] Mohsen Faridi, Roghaiyeh Ansari, Seyed Ali Mousavi and Mahsa Dodman, "Pitch Control of Wind Turbine Blades in Noisy and Unstable Wind Conditions", *2010 9th International Conference on Environment and Electrical Engineering (EEEIC)*, pp. 22-25, May 2010.

[46] Jianzhong Zhang, Ming Cheng, Zhe Chen and Xiaofan Fu, "Pitch Angle Control for Variable Speed Wind Turbines", *2008 Third International Conference on Electric Utility Deregulation and Restructuring and Power Technologies*, pp. 2691-2696, April 2008.

[47] Tomonobu Senjyu, Ryosei Sakamoto, Naomitsu Urasaki, Toshihisa Funabashi, Hideki Fujita and Hideomi Sekine, "Output Power Leveling of Wind Turbine Generator for All Operating Regions by Pitch Angle Control", *IEEE Transactions on Energy Conversion,* Vol. 21, No. 2, pp. 467-475, June 2006.

[48] E.B. Muhando, T. Senjyu, A. Yona, H. Kinjo and T. Funabashi, "Disturbance Rejection by Dual Pitch Control and Self-Tuning Regulator for Wind Turbine Generator Parametric Uncertainty Compensation", *IET Control Theory & Applications*, Vol. 1, No. 5, pp. 1431-1440, September 2007.

[49] N. A. Schinas, N. A. Vovos and G. B. Giannakopoulos, "An Autonomous System Supplied Only by a Pitch-Controlled Variable-Speed Wind Turbine", *IEEE Transactions on Energy Conversion*, Vol. 22, No. 2, pp. 325- 331, June 2007.

[50] I. Hamzaoui, F. Bouchafaa, A. Hadjammar and A. Talha, A. "Improvement of the Performances MPPT System of Wind Generation", *2011 Saudi International on Electronics, Communications and Photonics Conference*, pp. 1-6, April 2011.

[51] Shuhui Li, Timothy A. Haskew and Eduard Muljadi, "Integrative Characteristic Evaluation of DFIG Maximum Power Extraction using Lookup Table Approach", *2010 IEEE Power and Energy Society General Meeting*, pp. 1-8, July 2010.

[52] H. Li, Z. Chen and John K. Pedersen, "Optimal Power Control Strategy of Maximizing Wind Energy Tracking and Conversion for VSCF Doubly Fed Induction Generator System", *IEEE 5th International Power Electronics and Motion Control Conference,* Vol.3, pp. 1-6, August 2006.

[53] H. Li, Z. Chen and John K. Pedersen, "Optimal Power Control Strategy of Maximizing Wind Energy Tracking and Conversion for VSCF Doubly Fed Induction Generator System", *IEEE 5th International Power Electronics and Motion Control Conference,* Vol.3, pp. 1-6, August 2006.

[54] Mohamed Hilal, Mohamed Maaroufi and Mohamed Ouassaid, "Doubly Fed Induction Generator Wind Turbine Control for a maximum Power Extraction", *2011 International Conference on Multimedia Computing and Systems*, pp. 1-7, April 2011.

[55] R. Pena, J. C. Clare and G. M. Asher, "Doubly fed induction generator using back-to-back PWM converters and its application to variable-speed wind-energy generation," *IEE Proceedings Electric Power Applications*, Vol. 143, No. 3, pp. 231-241, May 1996.

[56] Y. Zhao, X. D. Zou, Y. N. Xu, Y. Kang and J. Chen, "Maximal Power Point Tracking under Speed-Mode Control for Wind Energy Generation System with Doubly Fed Introduction Generator", *IEEE 5th International Power Electronics and Motion Control Conference*, Vol.1, pp. 1-5, August 2006.

[57] Xie Zhen, Zhang Xing, Yang Shuying, Li Qin and Zhai Wenfeng, "Study on Control Strategy of Maximum Power Capture For DFIG in Wind Turbine System", *2010 2nd IEEE International Symposium on Power Electronics Distributed Generation Systems*, pp. 110-115, June 2010.

[58] Yunqi Xiao and Pengxiao Jia, "VSCF Wind Turbine Control Strategy for Maximum Power Generation", *Proceedings of the 8th World Congress on Intelligent Control and Automation*, Jinan, China, pp. 4781-4786, July 2010.

[59] Wei Qiao, Wei Zhou, José M. Aller, and Ronald G. Harley, "Wind Speed Estimation Based Sensorless Output Maximization Control for a Wind Turbine Driving a DFIG", *IEEE Transactions on Power Electronics*, Vol. 23, No. 3, pp. 1156-1169, May 2008.

[60] Rajib Datta and V. T. Ranganathan, "A Method of Tracking the Peak Power Points for a Variable Speed Wind Energy Conversion System", *IEEE Transactions on Energy Conversion*, Vol. 18, No. 1, pp. 163-168, March 2003.

[61] Baike Shen, Bakari Mwinyiwiwa, Yongzheng Zhang and Boon-Teck Ooi, "Sensor-less Maximum Power Point Tracking of Wind by DFIG Using Rotor Position Phase Lock Loop (PLL)", *IEEE Transactions on Power Electronics*, Vol. 24, No. 4, pp. 942-951, April 2009.

[62] I. K. Buehring and L. L. Freris, "Control Policies for Wind Energy Conversion Systems," *IEE Proceedings on Generation, Transmission and Distribution*, Vol. 128, No. 5, pp. 253-261, September 1981.

[63] Quincy Wang and Liuchen Chang, "An Intelligent Maximum Power Extraction Algorithm for Inverter-Based Variable Speed Wind Turbine Systems", *IEEE Transactions on Power Electronics*, Vol. 19, No. 5, pp. 1242-1249, September 2004.

[64] Marcelo Godoy Simoes, Bimal K. Bose and Ronald J. Spiegel, "Fuzzy Logic Based Intelligent Control of a Variable Speed Cage Machine Wind Generation System", *IEEE Transactions on Power Electronics*, Vol. 12, No. 1, pp. 87-95, January 1997.

[65] R. Pena, J.C. Clare, G.M. Asher, "Doubly fed induction generator using back-to-back PWM converters and its application to variable speed wind-energy generation", IEEE Proceedings on Electric Power Applications, Vol. 143, No. 3, pp. 231-241, May 1996.

[66] Arantxa Tapia, Gerardo Tapia, J. Xabier Ostolaza and José Ramón Sáenz, "Modeling and Control of a Wind Turbine Driven Doubly Fed Induction Generator", *IEEE Transactions on Energy Conversion*, Vol. 18, No. 2, pp. 194-204, June 2003.

[67] S. Chondrogiannis and M. Barnes, "Stability of Doubly-Fed Induction Generator Under Stator Voltage Orientated Vector Control", *IET Renewable Power Generation*, Vol. 2, No. 3, pp. 170-180, September 2008.

[68] Carles Batlle, Arnau D`oria-Cerezo and Romeo Ortega, "A Stator Voltage Oriented PI Controller For The Doubly-Fed Induction Machine", *Proceedings of the 2007 American Control Conference*, New York City, USA, pp. 5438-5443, July 2007.

[69] Shuhui Li, Rajab Challoo and Marty J. Nemmers, "Comparative Study of DFIG Power Control Using Stator-Voltage and Stator-Flux Oriented Frames", *IEEE Power & Energy Society General Meeting*, pp. 1-8, July 2009.

[70] M. Tazil, V. Kumar, R. C. Bansal, S. Kong, Z. Y. Dong, W. Freitas and H. D. Mathur, "Three-phase doubly fed induction generators: an overview", *IET Electric Power Applications*, Vol. 4, No. 2, pp. 75-89, February 2010.

[71] I. Takahashi and T. Noguchi, "A New Quick-Response and High Efficiency Control Strategy of an Induction Machine," *IEEE Transaction on Industry Application*, Vol. 22, No. 5, pp. 820-827, October 1986.

[72] I. Takahashi and Y. Ohmori, "High-Performance Direct Torque Control of an Induction Motor," *IEEE Transaction on Industry Application*, Vol. 25, No. 2, pp. 257-264, March/April 1989.

[73] Toshihiko Noguchi, Hiroaki Tomiki, Seiji Kondo and Isao Takahashi, "Direct Power Control of PWM Converter Without Power-Source Voltage Sensors", *IEEE Transaction on Industry Application*, Vol. 34, No. 3, pp. 473-479, May/June 1998.

[74] D.W. Zhi, L. Xu, "Direct power control of DFIG with constant switching frequency and improved transient performance", IEEE Transactions on Energy Conversion, Volume: 22, Issue: 1, Pages: 110-118, March 2007.

[75] Jihen Arbi, Manel Jebali-Ben Ghorbal, Ilhem Slama-Belkhodja and Lotfi Charaabi, "Direct Virtual Torque Control for Doubly Fed Induction Generator Grid Connection", *IEEE Transactions on Industrial Electronics*, Vol. 56, No. 10, pp. 4163-4173, October 2009.

[76] Domenico Casadei, Francesco Profumo, Giovanni Serra and AngeloTani, "FOC and DTC: Two Viable Schemes for Induction Motors Torque Control", *IEEE Transactions on Power Electronics*, Vol. 17, No. 5, pp. 779-787, September 2002.

[77] Thomas G. Habetler, Francesco Profumo, Michele Pastorelli and Leon M. Tolbert, "Direct Torque Control of Induction Machines Using Space Vector Modulation", *IEEE Transactions on Industry Applications*, Vol. 28, No. 5, pp. 1045-1053, September / October 1992.

[78] S. Arnalte, J. C. Burgos and J. L. Rodríguez-Amenedo, "Direct Torque Control of a Doubly-Fed Induction Generator for Variable Speed Wind Turbines*", Electric Power Components and Systems*, Vol. 30, No. 2, pp. 199-216, November 2002.

[79] K. C. Wong, S. L. Ho and K. W. E. Cheng, "Direct Torque Control of a Doubly-fed Induction Generator with Space Vector Modulation", *Electric Power Components and Systems*, Vol. 36, No. 12, pp. 1337-1350, November 2008.

[80] Z. Liu, O. A. Mohammed and S. Liu, "A Novel Direct Torque Control Induction Generator Used for Variable Speed Wind Power Generation", *IEEE Power Engineering Society General Meeting*, pp. 1-6, June 2007.

[81] Etienne Tremblay, Sergio Atayde, and Ambrish Chandra, "Comparative Study of Control Strategies for the Doubly Fed Induction Generator in Wind Energy Conversion Systems: A DSP-Based Implementation Approach*", IEEE Transactions on Sustainable Energy*, Vol. 2, No. 3, pp. 288-299, July 2011.

[82] Mariusz Malinowski, Marian P. Kazmierkowski and Andrzej M. Trzynadlowski, "A Comparative Study of Control Techniques for PWM Rectifiers in AC Adjustable Speed Drives", *IEEE Transactions on Power Electronics,* Vol. 18, No. 6, pp. 1390-1396, November 2003.

[83] Rajib Datta and V. T. Ranganathan, "Direct Power Control of Grid-Connected Wound Rotor Induction Machine Without Rotor Position Sensors", *IEEE Transactions on Power Electronics,* Vol. 16, No. 3, pp. 390-399, May 2001.

[84] David Santos-Martin, Jose Luis Rodriguez-Amenedo and Santiago Arnalte, "Direct Power Control Applied to Doubly Fed Induction Generator Under Unbalanced Grid Voltage Conditions", *IEEE Transactions on Power Electronics,* Vol. 23, No. 5, pp. 2328-2336, September 2008.

[85] Gonzalo Abad, Miguel A´ngel Rodr´ıguez, Grzegorz Iwanskiand and Javier Poza, "Direct Power Control of Doubly-Fed-Induction-Generator-Based Wind Turbines Under Unbalanced Grid Voltage", *IEEE Transactions on Power Electronics*, Vol. 25, No. 2, pp. 442-452, February 2010.

[86] Lie Xu and Phillip Cartwright, "Direct Active and Reactive Power Control of DFIG for Wind Energy Generation", *IEEE Transactions on Energy Conversion*, Vol. 21, No. 3, pp. 750-758, September 2006.

[87] Jiefeng Hu, Jianguo Zhu and D. G. Dorrell, "A Comparative Study of Direct Power Control of AC/DC Converters for Renewable Energy Generation", *37th Annual Conference on IEEE Industrial Electronics Society*, pp. 3578-3583, November 2011.

[88] Sheng Yang and Venkataramana Ajjarapu, "A Speed-Adaptive Reduced-Order Observer for Sensorless Vector Control of Doubly Fed Induction Generator-Based Variable-Speed Wind Turbines", *IEEE Transactions on Energy Conversion*, Vol. 25, No. 3, pp. 891-900, September 2010.

[89] B. Hopfensperger, D. J. Atkinson and R. A. Lakin, "Stator-flux-oriented control of a doubly-fed induction machine with and without position encoder", *IEE Proceedings Electric Power Applications,* Vol.147, No. 4, pp. 241-250, July 2000.

[90] G. D. Marques, V. Fern˜ao Pires, S´ergio Sousa and Duarte M. Sousa, "A DFIG Sensorless Rotor-Position Detector Based on a Hysteresis Controller", *IEEE Transactions On Energy Conversion*, Vol. 26, No. 1, pp. 9-17, March 2011.

[91] G. D. Marques, V. Fern˜ao Pires, S´ergio Sousa and Duarte M. Sousa, "A DFIG Sensorless Rotor-Position Detector Based on a Hysteresis Controller", *IEEE Transactions On Energy Conversion*, Vol. 26, No. 1, pp. 9-17, March 2011.

[92] M.O. Mahmoudi, N. Madani, M.F. Benkhoris ″Cascade sliding mode control of a field oriented induction machine drive″, Eur. Phys, AP 7, 1999, pp.217-225.

[93] V.I Utkin, ″Sliding mode control design principles and applications to electric drives″, *IEEE Trans, on Industrial Electronics*, Vol.40, No.1, February 1993, pp.23-36.

[94] V. Utkin, J. Guldner, and J. Shi, *Sliding Mode Control in ElectroMechanical Systems, Second Edition*. CRC Press, 2 ed., May 2009.

[95] A. Sabanovic, L. Fridman, S. K. Spurgeon, and I. o. E. Engineers, *Variable structure systems: from principles to implementation*. IET, 2004.

[96] IEEE TF report, "Proposed terms and definitions for power system stability," *IEEE Trans. on Power Appart. and Syst.,*, Vol. PAS-101, pp.1894-1897, July 1982.

[97] P. Kundur, J. Paserba, V. Ajjarapu, G. Andersson, A. Bose,C. Canizares, N. Hatziargyriou, D. Hill, A.Stankovic, C. Taylor,T. Van Cutsem, and V. Vittal, "Definition and classification of power system stability IEEE/CIGRE joint task force on stability terms and definitions," *IEEE Transactions on Power Systems*,vol. 19, pp. 1387– 1401, Aug. 2004.

[98] Kundur, P. (1994) Power System Stability and Control, McGraw Hill, New York.

[99] Carlson, O., Hylander, J. and Thorborg, K. (1996) Survey of variable speed operation of wind turbines. 1996 European Union Wind Energy Conference, Sweden, pp. 406–409.

[100] "Proposed terms & definitions for power system stability," *IEEE Transactions on Power Apparatus and Systems*, vol. PAS-101, pp. 1894–1898, July 1982.

[101] K. R. Padiyar, *Power System Dynamics: Stability and Control*. John Wiley & Sons Ltd (Import), Pap/Dsk ed., Apr. 1999.

[102] "Power oscillation protection," Nov. 2002.

[103] K. Prasertwong, N. Mithulananthan, and D. Thakur, "Understanding low-frequency oscillation in power systems," *International Journal of Electrical Engineering Education*, vol. 47, no. 3,pp. 248–262, 2010.

[104] G. K. Morison, B. Gao, and P. Kundur, "Voltage stability analysis using static and dynamic approaches," *IEEE Trans. Power Systems*, vol. 8, pp.1159–1171, Aug. 1993.

[105] T. Van Cutsem, "Voltage instability: Phenomenon, countermeasures and analysis methods," *Proc. IEEE*, vol. 88, pp. 208–227, 2000.

[106] C. W. Taylor, *Power System Voltage Stability*. New York: McGrawHill, 1994.

[107] G. K. Morison, B. Gao, and P. Kundur, "Voltage stability analysis usingstatic and dynamic approaches," *IEEE Trans. Power Systems*, vol. 8, pp.1159–1171, Aug. 1993.

[108] J. Morren, S. W. de Haan, W. L. Kling, and J. A. Ferreira, "Wind turbines emulating inertia and supporting primary frequency control," *IEEE Transactions on Power Systems*, vol. 21, pp. 433– 434, Feb. 2006.

[109] G. Ramtharan, J. B. Ekanayake, and N. Jenkins, "Frequency support from doubly fed induction generator wind turbines," *IET Renewable Power Generation*, vol. 1, pp. 3–9, Mar. 2007.

[110] V. Akhmatov, H. Knudsen, M. Bruntt, A.H. Nielsen, J.K. Pedersen, N.K. Poulsen,

"A dynamic stability limit of grid-connected induction generators", IASTED International Conference on Power and Energy Systems, Marbella, Spain, September 19-22, 2000, pp.235-244.

[111] IEEE PES Working Group on System Oscillations, "Power System Oscillations," IEEE Special Publication 95-TP-101, 1995.

[112] J. Machowski, J. W. Bialek, and J. R. Bumby, *Power system dynamics and stability*. John Wiley & Sons, Oct. 1997.

[113] P. W. Sauer and M. A. Pai, *Power System Dynamics and Stability*. Prentice Hall, 1st ed., July 1997.

[114] M. Ilic, J. Zaborsky, Dynamics and control of large electric power systems, New York, US, John Wiley & Sons, Inc., 2000.

[115] F. Mei and B. C. Pal, "Modal Analysis of Grid Connected Doubly Fed Induction Generator," *IEEE Transactions on Energy Conversion*. Vol. 22, No. 3, 2007, pp. 728-736.

[116] L. Wang, F. Howell, P. Kundur, C. Y. Chung, and W. Xu, "Atool for small-signal security assessment of power systems," in*22nd IEEE Power Engineering Society International Conference on Power Industry Computer Applications, 2001. PICA 2001. Innovative Computing for Power - Electric Energy Meets the Market*, pp. 246–252, IEEE, 2001.

[117] U. Kerin, T. N. Tuan, E. Lerch, and G. Bizjak, "Small signal security index for contingency classification in dynamic security assessment," in *PowerTech, 2011 IEEE Trondheim*, pp. 1–6, IEEE,June 2011.

[118] S. Yang, F. Liu, D. Zhang, S. Mei, and G. He, "Polynomial approximation of the damping-ratio-based small-signal security region boundaries of power systems," in *2011 IEEE Power and Energy Society General Meeting*, pp. 1–8, IEEE, July 2011.

[119] J. Paserba *et al.*, "Analysis and control of power system oscillation," *CIGRE special publication*, vol. 38, no. 07, 1996.

[120] G. C. Verghese, I. J. Perez-Arriaga, and F. C. Schweppe, "Selective modal analysis with applications to electric power systems, part II: the dynamic stability problem," *IEEE Transactions on Power Apparatus and Systems*, vol. PAS-101, pp. 3126–3134, Sept. 1982.

[121] I. J. Perez-Arriaga, G. C. Verghese, and F. C. Schweppe, "Selective modal analysis with applications to electric power systems, PART i: Heuristic introduction," *IEEE Transactions on Power Apparatus and Systems*, vol. PAS-101, pp. 3117–3125, Sept. 1982.

[122] Marcelo Gustavo Molina and Pedro Enrique Mercado (2011), I. Albahadly (Ed.), "Modelling and Control Design of Pitch-Controlled Variable Speed Wind Turbines," ISBN: 978-953 307-221 -0, *In Tech*.

[123] O. Anaya-Lara, N. Jenkins, J. Ekanayake, P. Cartwright, andM. Hughes, *Wind Energy Generation: Modelling and Control*.Wiley, 1 ed., Sept. 2009.

[124] S.A. Papathanassiou and M.P. Papadopoulos. "Mechanical stresses in fixed-speed wind turbines due to network disturbances". In: *Energy Conversion, IEEE Transactions on* 16.4 (Dec. 2001), pp. 361–367. ISSN: 0885-8969.

[125] J. Ekanayake and N. Jenkins, “Comparison of the response of doubly fed and fixed-speed induction generator wind turbines to changes in network frequency,” *IEEE Transactions on Energy Conversion*, vol. 19, pp. 800– 802, Dec. 2004.

[126] T. Ackermann, *Wind power in power systems*. John Wiley and Sons, Mar. 2005.

[127] Wasynczuk, O., Man, D.T., and Sullivan, J.P., 1981, "Dynamic behaviour of a class of wind turbine generators during random wind fluctuations", *IEEE Trans. on Power Apparatus and Systems*, Vol. 100, No. 6, pp. 2837-2845.

[128] Freris, LL. 1990, "Wind Energy Conversion Systems", Prentice Hall Inc., United King.

[129] Abbas, F. A. R., and Abdulsada, M. A. 2010. Simulation of Wind-Turbine Speed Control by MATLAB. International Journal of Computer and Electrical Engineering. Vol. 2, No. 5, 1793-8163p.

[130] Khajuria, S., and Kaur, J. 2012. Implementation of Pitch Control of Wind Turbine using Simulink (Matlab). International Journal of Advanced Research in computer Engineering and technology (IJARCET), vol1, ISSN: 2278-1323.

[131] E. Hinrichsen and P. Nolan, “Dynamics and stability of wind turbine generators,” *IEEE Transactions on Power Apparatus and Systems*, vol. PAS-101, no. 8, pp. 2640 – 2648, Aug.1982.

[132] T. Burton, *Wind energy: handbook*. John Wiley and Sons, Dec.2001.

[133] S.A. Papathanassiou, M.P. Papadopoulos, “Dynamic behavior of variable speed wind turbines under stochastic wind”, IEEE Transactions on Energy Conversion, v.14, n.4, Dec. 1999, pp.1617-1623.

[134]A. Hansen, P. Sorensen, F. Iov, and F. Blaabjerg, “Control of variable speed wind turbines with doubly-fed induction generators,” *Wind Engineering*, vol. 28, pp. 411–432, June 2004.

[135] J. G. Slootweg, H. Polinder, and W. L. Kling, “Representing wind turbine electrical generating systems in fundamental frequency simulations,” *IEEE Transactions on Energy Conversion*, vol. 18, pp. 516– 524, Dec. 2003.

[136] Peter vas, “Vector control of ac machines”, Oxford university press, 1990.

[137] “World wind energy association, wwea 2014, http://www.wwindea.org.”.

[138] D. Gautam, L. Goel, R. Ayyanar, V. Vittal, and T. Harbour, "Control strategy to mitigate the impact of reduced inertia due to doubly fed induction generators on large power systems," *IEEE Transactions on Power Systems*, vol. 26, pp. 214–224, Feb. 2011.

[139] V. Akhmatov, "Analysis of dynamic behaviour of electric power systems with large amount of wind power" Ph.D. dissertation, Tech. Univ.Denmark, Lyngby, Denmark, 2003.

[140] R. S. Pena, "Vector control strategies for a doubly-fed induction generator driven by a wind turbine" Ph.D. dissertation, Univ. Nottingham, Nottingham, U.K., 1996.

[141] M. V. A. Nunes, J. A. P. Lopes, H. H. Zurn, U. H. Bezerra, and R.G. Almeida, "Influence of the variable-speed wind generators in transient stability margin of the conventional generators integrated in electrical grids," *IEEE Trans. Energ y C onvers.*, vol. 19, no. 4, pp. 692–701, Dec.2004.

[142] J. Morren and S. W. H. de Haan, "Ridethrough of wind turbines with doubly-fed induction generator during a voltage dip," *IEEE Trans. Energ y Convers.*, vol. 20, no. 2, pp. 435–441, Jun. 2005.

[143] F. M. Hughes, O. Anaya-Lara, N. Jenkins, and G. Strbac, "Control of DFIG-based wind generation for power network support," *IEEE Trans. Power Syst.*, vol. 20, no. 4, pp. 1958–1966, Nov. 2005.

[144] Mohammad Hasanuzzaman Shawon, Ahmed Al-Durra, Cedric Caruana and S.M. Muyeen, "Small Signal Stability Analysis of Doubly Fed Induction Generator including SDBR," journal of International Conference on Electrical Machines and Systems Vol. 2, No.1 , pp.31~ 39 , 2013 31 **.** HTTP://DX.DOI.ORG/10.11142/JICEMS.2013.2.1.31

[145] F. Wu, X. P. Zhang, K. Godfrey, and P. Ju, "Small signal stability analysis and optimal control of a wind turbine with doubly fed induction generator," *IET Generation, Transmission & Distribution*, vol. 1, pp. 751–760, Sept. 2007.

[146] Tang .Y, Ju. Ping, He. Haibo, Qin.Ch and Wu.F, '' Optimized Control of DFIG-Based Wind Generation Using Sensitivity Analysis and Particle Swarm Optimization," IEEE Trans. Smart Grid., vol.4, No.1, pp.509~520, March 2013.

[147] J. Wilkie, W. E. Leithead, and C. Anderson, "Modelling of wind turbine by simple models," *Win d En g.*, vol. 14, no. 4, pp. 247–274, Jul. 1990.

[148]S. K. Salman and A. L. J. Teo, "Windmill modeling consideration and factors influencing the stability of a grid-connected wind power based embedded generator," IEEE Trans. Power Syst., vol. 18, No. 2, pp. 793~802, May 2003.

[149] C. Hamon, " Doubly-fed Induction Generator Modeling and Control in DigSilent Power Factory," Master Thesis, *KTH School of Electrical Engineering*, 2010.

[150] Pena, R., Clare, J.C. and Asher, G.M. (1996) A doubly fed induction generator using back-to-back PWM converters supplying an isolated load from a variable speed wind turbine. IEE Proceedings Electric Power Applications, 143(5), 380–387.

[151] A. Petersson, *Analysis, Modeling, and Control of Doubly-Fed Induction Generators for Wind Turbines*. PhD thesis, Department of Energy and Environment Chalmers University of Technology, 2003.

[152] S. Heier, Grid integration of wind energy conversion systems, Chicester, UK: JohnWiley & Sons Ltd., 1998.

[153] Hansen, A. D.: 'Generators and power electronics for wind turbines', in Ackermann, T.(Ed): 'Wind Power in Power systems' (John Wiley&Sons, Ltd, New York, 2005).

[154] MULLER S., DEICKE M., DONCKER R.W.D.: 'Adjustable speed generators for wind turbines based on doubly-fed induction machines and 4-quadrant IGBT converters linked to the rotor'. Proc. IEEE Ind. Appl. Conf., Rome, Italy, October 2000, pp. 2249–2254.

[155] DATTA R., RANGANATHAN V.T.: 'Variable-speed wind power generation using doubly fed wound rotor induction machine – a comparison with alternative schemes', IEEE Trans. Energy Convers., 2002, 17, (3), pp. 414–421

[156] HOLDSWORTH L., WU X.G., EKANAYAKE J.B., JENKINS N.: 'Comparison of fixed speed and doubly-fed induction wind turbines during power system disturbances', IEE Proc. Gener. Transm. Distrib., 2003, 150, (3), pp. 343–352.

[157] RODRIGUEZ J.M., FERNANDEZ J.L., BEATO D., ET AL.: 'Incidence on power system dynamics of high penetration of fixed speed and doubly fed wind energy systems: study of the Spanish case', IEEE Trans. Power Syst., 2002, 17, (4), pp. 1089–1095.

[158] KOCH F.W., ERLICH I., SHEWAREGA F., BACHMANN U.: 'Dynamic interaction of large offshore wind farms with the electric power system'. Proc. Power Tech. Conf., Bologna, Italy, June 2003, pp. 1–7.

[159] Yamamoto, M., and Motoyoshi, O.: 'Active and reactive power control for doubly-fed wound rotor induction generator', IEEE Trans. Power Electron., 1991, 6, (4), pp. 624–629.

[160] T. Thringer. A. Petersson. and. T. Petru. "Grid disturbance response of wind turbines equipped with induction generator and doubly-fed induction generator." In Proc. of IEEE power Eng. Soc. General Meeting vol.3.july 2003.pp.1542-1547.

[161] G. K. Venayagamoorthy, R. G. Harley, and D. C. Wunsch, "Comparison of heuristic dynamic programming and dual heuristic programming adaptive critics for neuro-control of a turbo-generator," *IEEE Trans. Neural Networks*, vol. 13, no. 3, May 2002, pp. 764-773.

[162] M. Lown, E. Swidenbank, B. W. Hogg, "Adaptive fuzzy logic control of a turbine generator system," *IEEE Trans. Energy Conversion*, vol.12, no. 4, Dec. 1997, pp. 394-399.

[163] V. Akhmatov, *Induction Generators for Wind Power*. Brentwood, CA, USA: Multi-science, 2005.

[164] M. Kayikci and J. V. Milanovic, "Assessing transient response of DFIG based wind plants the in fluence of model simpli fications and parameters," *IEEE Trans. Power Syst.*, vol. 23, no. 2, pp. 545–554, May 2008.

[165] S. Seman, J. Niiranen, S. Kanerva, A. Arkkio, and J. Saitz, "Performance study of a doubly fed wind-power induction generator under network disturbances," *IEEE Trans. Energy Convers*, vol. 21, no. 4,pp. 883–890, Dec. 2006.

[166] S. Hu, X. Lin, Y. Kang, and X. Zou, "An improved low-voltage ridethrough control strategy of doubly fed induction generator during grid faults," *IEEE Trans. Power electron.*, vol. 26, no. 12, pp. 3653–3665, Dec. 2011.

[167] D. Xiang, L. Ran, P. J. Tavner, and S. Yang, "Control of a doubly fed induction generator in a wind turbine during grid fault ride-through," *IEEE Trans. Energy Convers.*, vol. 21, no. 3, pp. 652–662, Sep. 2006.

[168] R. G. Almeida, J. A. P. Lopes, and J. A. L. Barreiros, "Improving power system dynamic behavior through doubly fed induction machines controlled by static converter using fuzzy control," *IEEE Trans . Power Syst.*, vol. 19, no. 4, pp. 1942–1950, Nov. 2004.

[169] T. Tang and L. Xu, "A flexible active reactive power control strategy for a variable speed constant frequency generating system," *IEEE Trans. Power Electronics*, vol. 10, no. 4, Jul. 1995, pp. 472-477.

[170] Tapia, G. and Otaegui A. T., *Optimization of the Wind Generation: Comparison between Two Algorithms*, Green Energy Contributions, Book Chapter, Springer Netherlands, ISBN 978-1-4020-2933-2, 2005.

[171] Martins de Carvalho, J. L., *Dynamical Systems and Automatic Control*, Prentice Hall International Series in Systems and Control Engineering, ISBN 0-132217-55-4, 1993.

[172] Ogata, K., *Modern Control Engineering*, Prentice Hall, 3rd Edition, ISBN 0-132273-07-1, 1996.

[173] M. A. Abido, "Robust design of multi machine power system stabilizers using simulated annealing," *IEEE Trans. Energy Conversion*, vol. 15, no. 3, Sept. 2000, pp. 297-304.

[174] M. A. Abido, "A novel approach to conventional power system stabilizer design using tabu search," *Int. Journal Electrical Power and Energy Systems*, vol. 21, no. 6, Aug. 1999, pp. 443-454.

[175] Gaing, Z.-L., *A particle swarm optimization approach for optimum design of PID controller in AVR system*, IEEE Transactions on Energy Conversion, Vol. 19, no. 2, pp. 384-391, June 2004.

[176] D. B. Fogel, Evolutionary Computation: Toward a New Philosophy of Machine Intelligence, New York: IEEE Press, 2000, ISBN 0-7803-5379-X.

[177] S.P. Ghoshal, Optimization of PID gains by particle swarm optimization in fuzzy based automatic generation control, Electr. Power Syst. Res. 72 (2004) 203–212.

[178] M.A. Marra, B.L. Walkott, "Stability and Optimality in Genetic Algorithm Controllers,"

Proceedings IEEE International Symposium on Intelligent Control. Dearborn, MI. September, 15-18, 1996.

[179] G. Wang, M. Zhang, X. Xu, C. Jiang, "Optimization of Controller Parameters Based on the Improved Genetic Algorithms," *Proceedings of the 6th World Congress on Intelligence Control and Automation*, June 21- 23, 2006, Dalian, China.

[180] W. Qiao, G.K. Venayagamoorthy, R.G. Harley, "Design of Optimal Control PI Controllers for Doubly Fed Induction Generators Driven by Wind Turbines Using Particle Swarm Optimization," *Int. Joint Conf. on Neural Network*, Vancouver, BC, Canada, pp. 1982-1987, July, 2006.

[181] Mishra Y, Mishra S, Li. F, Dong. Zh. Y and Bansal R.C, "Small-Signal Stability Analysis of a DFIG-Based Wind Power System under Different Modes of Operation," IEEE Trans. Energy Convers, Vol.24, NO. 4, PP.972~982, Dec 2009.

[182]*Vriois.T.D, Koutiva.X.I and Vovos.N.A, "A Genetic Algorithm-Based Low Voltage Ride-Through Control Strategy for Grid Connected Doubly Fed Induction Wind Generators," IEEE Trans. Power Syst., Vol. 29, NO. 4, pp. 1325–1334, May. 2014.*

[183] Holland J (1975) Adaptation in natural and artificial systems. University of Michigan Press, Ann Arbor.

[184] Farmer JD, Packard N, Perelson A (1986), "The immune system, adaptation and machine learning". Physica 22:187–204.

[185] Kennedy J, Eberhart RC (1995) Particle swarm optimization. Proceedings IEEE International Conference on Neural Networks, Piscataway, 1942–1948.

[186] Storn R, Price K (1997) Differential evolution–a simple and efficient heuristic for global optimization over continuous spaces. J Glob Optim 11:341–359.

[187] Passino KM (2002) Biomimicry of bacterial foraging for distributed optimization and control. IEEE Control Syst Mag 22:52–67.

[188] Eusuff M, Lansey E (2003) Optimization of water distribution network design using the shuffled frog leaping algorithm. J Water Resour Plan Manag ASCE 129:210–225.

[189] Karaboga D (2005) an idea based on honey bee swarm for numerical optimization. Technical Report-TR06, Erciyes University, Engineering Faculty, Computer Engineering Department, Turkey.

[190] Simon D (2008) Biogeography-based optimization. IEEE Trans Evol Comput 12:702–713.

[191] Rashedi E, Nezamabadi-pour H, Saryazdi S (2009) GSA: a gravitational search algorithm. Inf Sci 179:2232–2248.

[192] Ahrari A, Atai A (2010) Grenade Explosion Method-A novel tool for optimization of multimodal functions. Appl Soft Comput 10(4):1132–1140.

[193] Mhetre. S. Punam. Jun, 2012. Genetic Algorithm for Linear and Nonlinear Equation, International Journal of Advanced Engineering Technology, E-ISSN 0976-3945.

[194] McCall, J., "Genetic Algorithms for Modeling and Optimization", Journal of Computational and Applied Mathematics 184, pp. 205 – 222, 2005.

[195] Application of Genetic Algorithm in Solving Linear Equation Systems. Al Dahoud Ali , Ibrahiem M. M. El Emary, Mona M. Abd El-Kareem.

[196] R. Anulmozhiyal and Dr. K. Baskarn, 'Speed Control of Induction Motor Using Fuzzy PI and Optimized Using GA', International Journal of Recent Trends in Engineering, Vol. 2, No. 5, November 2009.

[197] Shady. M. Gadoue, D. Giaous and J. W. Finch, 'Genetic Algorithm Optimized PI and Fuzzy Mode Speed Control for DTC drives', Proceedings of the World Congress on Engineering 2007, Vol. 1, WCE 2007, July 2-4, 2007, London, U.K.

[198] Neenu Thomas, Dr. P. Poongodi, 'Position Control of DC Motor Using Genetic Algorithm-based PID Controller', Proceedings of the World Congress on Engineering 2009, Vol. 2, WCE 2009, July 1 -3, 2009, London, U.K.

[199] R.L. Haupt, S.E. Haupt, "Practical Genetic Algorithms", John Wiley and Sons, New York, 2004.

[200] Wassim. A, Bedwani, and Oussama M. Ismail, 'Genetic Optimization of Variable Structure PID Control Systems', Computer Systems and Applications, ACS/IEEE International conference on 2001.

[201] M. A. poller." Doubly-fed induction machine models for stability assessment of wind farms." In Proc. of Power Tech. Conf. Vol. 3. June 2003. pp 1-6.

[202] V. Akhmatov. "Variable-speed wind turbine with doubly-fed induction generators. Part1: modelling in dynamic simulation tools." Wind Engineering. Vol. 26. No. 2. pp. 85-108. Mar.2002.

[203] A.D. Hansen, P. Sorensen, F. Blaabjerg, "Overall control strategy of variable speed doubly-fed induction generator wind turbine", (in Grid Integration and electrical systems of wind turbines and wind farms [CD-ROM]), Nordic Wind Power Conference 2004 (NWPC 04), Göteborg (SE), 1-2 March 2004.

[204] B.H. Chowdhury, S. Chellapilla, "Double-fed induction generator control for variable speed wind power generation", Electric Power Systems Research, Volume: 76, Issue: 9-10, Pages: 786-800, June 2006.